Role of Pannexin 1 in the modulation of inhibitory synaptic plasticity in mouse hippocampus.

Tesis entregada a

LA UNIVERSIDAD DE VALPARAÍSO

En Cumplimiento Parcial de los requisitos para optar al grado de

Doctora en Ciencias con Mención en Neurociencia

Facultad De Ciencias

Por

Francisca Javiera García Rojas

Marzo, 2022

Dirigida por: Dr. Marco Arturo Fuenzalida Núñez

Co-Dirigida por: Dr. Álvaro Oscar Ardiles Araya

Agradecimientos

Primero que todo, a mi madre, una guerrera. Gracias a su esfuerzo y amor he llegado hasta donde estoy ahora. Agradezco su paciencia y dedicación para siempre decirme que estudiara y que me realizara profesional y personalmente. Agradezco su sabiduría para tomar las decisiones y para aconsejarme ante la adversidad, la cual nos hizo más fuertes.

Segundo, agradezco a mi aquelarre familiar, mi matriarcado, que incluye a mi hermana Fer, mi prima/hermana Isidora, Fabiola mi segunda mamá, Ximena, mi abuelita Elsa y mi tesorito pequeño Luisita, quien llegó a dar luz y amor a nuestras vidas. Todo su amor, apoyo y fuerza siempre estuvo presente en todo este proceso y fue crucial para seguir adelante. Gracias por creer en mí y en mis capacidades. José Miguel, mi monito, también el hombre de la familia, gracias por tu preocupación y la cuota de humor que siempre tuviste.

Tercero, agradezco a mis amig@s, la familia que una escoge. Soy afortunada de contar con la calidad de personas que me han brindado su amistad y cariño en todo este tiempo. Gracias por las innumerables risas, brindis, cafés aventuras, apoyo en cada situación difícil o fácil. Gracias por impulsarme a creer en mí, por darme su confianza y lealtad. Tenerlas (los) en mi vida fue y será siendo fundamental para todo lo que me depara la vida. Uds. saben quiénes son. L@s quiero infinito.

Finalmente, y no por ello menos importante, agradezco a mi querido laboratorio “lechón lab” como nos hacemos llamar coloquialmente. Siempre he sentido que el laboratorio es mi segunda casa y familia. No podría haber llegado a un mejor lugar, en donde siempre me sentí cómoda y feliz, en donde el ambiente laboral fue siempre ameno, en donde nunca faltaron los panoramas para las fechas importantes, ni la comida y en donde siempre hubo apoyo y colaboración. Agradezco a mi tutor Marco, quien estuvo presente en cada etapa de mi tesis, para responder cada pregunta y para siempre contribuir con su retroalimentación y conocimientos. Hago mención honrosa a mis queridas Cami y Odra, quienes hace rato dejaron de ser solo compañeras de laboratorio y hoy son grandes amigas. Gracias totales por su apoyo en todo, por su preocupación constante, por su confianza, por su lealtad y por todos los bajones que nos comimos fuera y dentro del laboratorio. ¡¡Las adoro mis neuroplasticity girls!!.

ÍNDEX

I. List of Figures

Supplementary figures

II. List of Symbols, Abbreviations and Nomenclature

2-AG: 2-arachidonoyl glycerol

10panx: mimetic peptide inhibitor of Panx1 (WRQAAFVDSY)

αpanx1: pannexin-1 antibody

μM: micromolar

μm: micrometer

μL: microliter

A1R: adenosine A1 receptor

ACSF: artificial cerebral spinal fluid

ADO: adenosine

AEA: N-arachidonylethanolamide

AM-251: CB1R antagonist

AMPAR: α-amino-3-hydroxy-5-methyl-4-isoxazolepropionic acid receptor

ATP: adenosine 5' triphosphate

BAPTA: 1,2-bis(o-aminophenoxy) ethane-N,N,N',N'-tetraacetic acid

Ca^{2+}: calcium ion

CA1: cornu ammonis area 1 of the hippocampus

CA3: cornu ammonis area 3 of the hippocampus

cAMP: 3'-5'-cyclic adenosine monophosphate

CCK: cholecystokinin

Cs: cesium

cm: centimeter

CNS: central nervous system

CNQX: cyanquixaline (6-cyano-7-nitroquinoxaline-2,3-dione)

CPZ: capsazepine

αCx43: connexin-43 antibody

D-APV: D-(-)-2-amino-5-phosphonopentanoic acid

DMSO: dimethylsulfoxide

eCB: endocannabinoid

eIPSCs: evoked inhibitory postsynaptic currents

EGTA: ethylene glycol tetraacetic acid

EPSC: excitatory postsynaptic current

FAAH: fatty acid amide hydrolase

GABA: gamma-amino-butyric acid

GDPβS: Guanosine 5′-[β-thio]diphosphate trilithium salt

H89: *N*-[2-[[3-(4-Bromophenyl)-2-propenyl]amino]ethyl]-5-isoquinolinesulfonamide

HEPES: 4-(2-hydroxyethyl)-1-piperazineethanesulfornic acid

Hz: hertz

iLTD: inhibitory Long-Term Depression

IPSC: inhibitory postsynaptic current

K^+: potassium ion

KCl: potassium chloride

kDa: kilodalton

LTD: long-term depression

LTP: long term potentiation

mIPSCs: miniature inhibitory postsynaptic currents

M: molar

MΩ: megaohm

Mg^{2+}: magnesium ion

$MgCl_2$: magnesium chloride

Mg: milligram

mGluR: metabotropic glutamate receptor

mL: millilitre

mm: millimetre

mM: millimolar

ms: millisecond

mV: millivolt

n: sample size

Na^+: sodium ion

nm: nanometer

nM: nanomolar

NMDAR: N-methyl-d-aspartate receptor

P value: significance

P2X7: purinoreceptor 7

pA: picoampere

Panx1: pannexin-1

Panx2: pannexin-2

Panx3: pannexin-3

Panx1 -/-: Panx1 knock out mouse

PKA: protein kinase A

PKC: protein kinase C

PLC: phospholipase C

PPR: paired pulse ratio

PPD: paired-pulse depression

PPF: paired-pulse facilitation

PBN: probenecid

pS: picosiemen

PSD-95: postsynaptic density-95

PV: parvalbumin

PyNs: pyramidal neurons

scPanx: scrambled inactive form of 10panx (FSVYWAQADR)

SEM: standard error of mean

sIPSCs: spontaneous inhibitory postsynaptic currents

TRPV1: transient receptor potential vanilloid 1

TTX: tetrodotoxin

VGCC: voltage-gated calcium channels

WT: wild-type

III. Abstract

The interplay between excitatory and inhibitory activity is essential for neural circuit refinement and learning. A large variety of proteins modulate the efficacy of excitatory glutamatergic circuits. However, only in recent years, has been studied their impact on inhibitory GABAergic circuits. Recently it has been shown that Pannexin 1 (Panx1), a non-selective transmembrane channel that allows the passage of several ions and metabolites such as ATP, can regulate glutamatergic transmission, however, its functional role in GABAergic transmission is unknown. Using the patch-clamp technique, pharmacology, transgenic and wild-type mouse we studied the contribution of Panx1 on the GABAergic synaptic efficacy in CA1 pyramidal neurons (PyNs). Here, we report that blockage of Panx1 reduces the GABAergic synaptic transmission in the hippocampus. Specifically, we observed a decrease in the amplitude of evoked inhibitory postsynaptic currents (eIPSCs), a reduction in the frequency of spontaneous inhibitory postsynaptic currents (sIPSCs), and a decrease in GABA release onto CA1 PyNs. In addition, we show that the depression in GABAergic synaptic transmission induced by Panx1 blockage involves the activation of cannabinoid CB1 receptors which depressed GABA release via a presynaptic Ca^{2+}-dependent downregulation of PKA signaling.

In conclusion, our results indicate that neuronal Panx1 is an important regulator of hippocampal GABAergic transmission suggesting it might play a role in brain functions and cognitive processes.

IV. Introduction

Synaptic transmission

Neuronal communication is essential for brain functioning. This elaborated form of cellular communication, named synaptic transmission, occurs as a biologic process in which a neuron interacts with another neuron through a synapse (Holz et al., 2012). The synapses allow the transference of information between neurons and can be either electrical or chemical. In electrical synapses, the cytoplasm of adjacent neurons is directly connected by a cluster of intercellular channels called gap junctions (Pereda, 2014). In chemical synapses, information is transferred via neurotransmitter release from presynaptic neurons which act on neurotransmitters receptors located at the postsynaptic cells. Chemical synapses can be excitatory or inhibitory. In the adult central nervous system (CNS), the main excitatory and inhibitory neurotransmitters are glutamate and γ-aminobutyric acid (GABA), respectively. The binding of both excitatory and inhibitory neurotransmitters to ionotropic or metabotropic receptors, triggers specific cellular processes in the postsynaptic cells. The activation of ionotropic glutamate receptors produces Na^+, K^+, and Ca^{2+} flux across the postsynaptic membrane producing membrane depolarization and, if the threshold is reached, a postsynaptic action potential. Conversely, GABA activates ionotropic GABA receptors that are permeable to Cl^-, hyperpolarizing the postsynaptic neurons and decreasing the likelihood of occurring a postsynaptic action potential (Purves, 2004).

Synaptic transmission is a plastic process, in which strength or efficacy may vary depending on several factors such as previous synaptic activity, the coincidence of pre and postsynaptic firing, among others. (Heidelberger et al., 2014). Thus, synaptic plasticity is an activity-dependent modification of synaptic transmission at preexisting synapses (Citri & Malenka, 2008). It has been proposed that synaptic plasticity plays a crucial role in the ability of the brain to incorporate learnings and store them as enduring memories (Citri et al., 2008). Synaptic plasticity plays an important role in the balance of the inhibitory and excitatory activity in the brain during learning and memory processes (Zhou & Yu, 2018). In addition, synaptic plasticity dysfunction contributes to several neuropsychiatric disorders (Citri & Malenka, 2008; McCullumsmith et al., 2004).

Hippocampus and GABAergic synaptic plasticity

The hippocampus is a brain structure essential for cognitive processes such as learning and memory. Electrophysiological recordings in animals (Berger et al., 1983), as well as magnetic resonance imaging (MRI) in humans (Henke et al., 1997) (Gabrieli et al., 1997) have provided evidence that the

hippocampal activity is involved in episodic or episodic-like learning and memory (Neves et al., 2008).

The hippocampus, located in the medial temporal lobe, is composed of the *cornus ammonis* (CA, subdivided in CA1, CA2, and CA3), the dentate gyrus, the entorhinal cortex, and the subiculum. The CA1 PyNs receive a major input from CA3 neurons via the Schaffer collaterals and project to the subiculum. In turn, CA1 and the subiculum project back to the deep layers of the entorhinal cortex (Andersen et al., 2007).

In the rodent brain, the hippocampal longitudinal axis is extended in a C-shaped fashion from dorsal (septal)-to ventral (temporal), corresponding to a posterior-to-anterior axis in humans (Strange et al., 2014). The dorsal and ventral regions of the hippocampus have different connectivity with other brain structures and different functions. For instance, the dorsal hippocampus receives visual and spatial information from sensory cortices via the medial entorhinal cortex, meanwhile, the ventral hippocampus is connected with the amygdala, prefrontal cortex, and hypothalamus (Canteras & Swanson, 1992). The differences in the connectivity of the dorsal and ventral hippocampus with other brain regions may have direct implications in their role in different behaviors. For example, the ventral hippocampus is involved in regulating emotional and stress responses, meanwhile, the dorsal hippocampus in involved in cognitive functions such as learning and memory.

The role of the hippocampus in learning and memory has positioned it as the preferred experimental model to study diverse forms of synaptic plasticity that have been proposed as the basis of these cognitive processes. A form of synaptic plasticity was first observed in the hippocampal formation by Bliss and Lomo. They found that repetitive stimulation of the perforant path produced an enhancement in the synaptic transmission in the dentate area that lasted for several hours (Bliss & Lømo, 1973). Different forms of synaptic plasticity, such as the long-term potentiation (LTP) and depression (LTD) (Dudek & Bear, 1992), have emerged as putative cellular and molecular mechanism underlying learning and memory in the CNS (Collingridge et al., 2010; Lynch, 2004). Besides LTP and LTD, there are other forms of synaptic plasticity including EPSP-spike (E-S) potentiation (Abraham et al., 1985), spike-timing-dependent plasticity (STDP) (Buchanan & Mellor, 2010), or depotentiation (Staubli & Lynch, 1990). Currently, the hippocampus is still a crucial experimental model to study diverse mechanisms that modulate synaptic plasticity.

Most of the studies have been dedicated to understanding the different mechanisms that govern the synaptic plasticity in excitatory synapses. However, despite their importance in the excitatory/inhibition balance, the different forms of synaptic plasticity in GABAergic synapses are

poorly known. A major challenge has been identifying the cellular and molecular mechanism responsible for the induction, expression, and maintenance of inhibitory synaptic plasticity. The inhibitory synapses undergo short- and long-term forms of synaptic plasticity (Castillo et al., 2011; Chevaleyre et al., 2006). The activity-dependent changes in the inhibitory transmission are accompanied by changes in the synaptic efficacy, the synapse structure, morphological reorganization of postsynaptic density, and the novo formation and elimination of inhibitory contacts (Bourne & Harris, 2011; Flores & Mendez, 2014; Pizzarelli et al., 2020). The plasticity in inhibitory synaptic transmission depends on changes at the presynaptic level in GABA release or, at the postsynaptic level, in the number, sensitivity, and responsiveness of GABA receptors (Fritschy & Panzanelli, 2014; Kittler & Moss, 2003).

In the hippocampus, the GABAergic local interneurons represent only ~10-15% of the total neuron population (Bezaire & Soltesz, 2013), however, the GABAergic synapses exhibit a wide diversity determined by the several types of GABAergic interneurons (Rozov et al., 2017). Hippocampal GABAergic interneurons have been classified considering their axonal and dendritic connectivity, morphology, electrophysiological properties, molecular markers, and development origins (Pelkey et al., 2017). In the hippocampal CA1 region, the interneurons include parvalbumin-expressing basket cells (14%), neurogliaform cells (9%), cholecystokinin-expressing basket cell (9%), bistratified cells (6%), oriens lacunosum-moleculare (O-LM, ~4-5%), and chandelier cells (4%) (Pelkey et al., 2017). In the hippocampus, the two most well-characterized interneurons are those expressing cholecystokinin (CCK) and parvalbumin (PV). Although both CCK and PV cells are classified as basket cells with perisomatic targeting, they are non-overlapping populations with distinct electrophysiological and functional characteristics (Armstrong & Soltesz, 2012).

Although GABAergic interneurons represent only a small fraction of hippocampal neurons, they have a tremendous capacity to control the activity of glutamatergic principal neurons at different levels and under different states of hippocampal activity (Csicsvari et al., 1999; Klausberger, 2005; Ylinen et al., 1995). The plastic changes in GABAergic transmission directly affect the regulation of neuronal excitability and neural circuit function and therefore, contributes to learning and memory, and neural circuit refinement (Castillo et al., 2011). However, further studies are necessary to understand the role of the plastic changes in GABAergic synapses in the regulation of excitability, dendritic integration, precise timing of the neuronal firing, and generation of brain oscillations.

Pannexin 1 channels: properties and role in synaptic transmission

Pannexin channels (Panx) were first identified through a BLAST search of GenBank for vertebrate homologs of invertebrate gap junction forming innexin proteins (Panchin et al., 2000).

Despite the limited sequence homology between innexins, connexins (vertebrate gap junction proteins), and pannexins, they share several common structural features. Panx channels are composed of 6 subunits with four transmembrane domains, two extracellular loops, and intracellularly oriented N- and C-terminal domains (Figure 1). Currently, three members of the Panx family have been identified Panx1, Panx2, and Panx3 (Figure 2). Panx1 and Panx2 are expressed in the CNS (Bruzzone et al., 2003), but the most well-characterized is the Panx1. The study of Panx2 has been challenged because is predominantly localized within intracellular compartments (Le Vasseur et al., 2019) (Boassa et al., 2015). Panx1 is broadly expressed in the cortex, hippocampus, striatum, thalamus, cerebellum, and olfactory bulb (Bruzzone et al., 2003; Ray et al., 2005). In the hippocampus, Panx1 expression at both mRNA and protein level is enriched in the pyramidal and granular cell layers, indicating a robust expression in the principal excitatory neurons (Ray et al., 2005; Zoidl et al., 2007). Nevertheless, Panx1 also has been detected in GABAergic interneurons within *stratum oriens*, *radiatum* and *lacunosum moleculare* (Vogt et al., 2005; Zoidl et al., 2007). Besides Panx1 expression in neurons, it is also expressed in glial cells, including astrocytes and microglia (Iglesias et al., 2009).

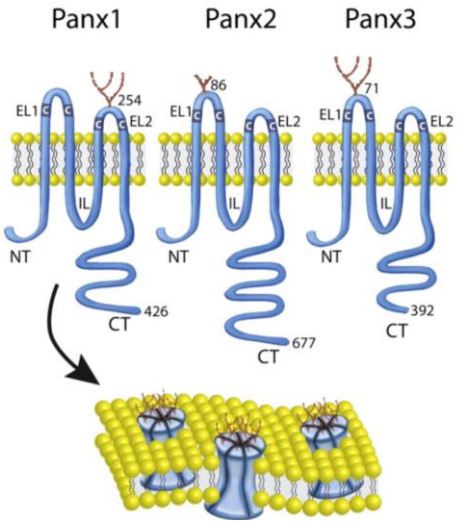

Figure 1: **Schematic representation of the three pannexin family members.** Panx1 (426), Panx2 (677) and Panx3 (392) of varying amino acid lengths are all tetra-spanning integral membrane proteins with N-glycosylation sites at amino-acid 254 (Panx1), 86 (Panx2, predicted), and 71 (Panx3). Panx1 has been shown to oligomerize into a hexamer to form single-membrane channels at the cell surface of many mammalian cells. EL1, EL2 (extracellular loops 1 and 2), IL (intracellular loop), CT (carboxy-terminus) and NT (amino-terminus). (Penuela et al., 2013).

Panx1 is a membrane integral protein that forms non-selective channels whose opening allows ion flux and the release of metabolites such as ATP (Bao et al., 2004). Panx1 affects diverse cell functions including the regulation of cells' electrical properties when it acts as an ion channel. Noticeably, Panx1 permeability varies in an activity-dependent mode. Constitutively, Panx1 exhibits low conductance (~50-80 pS) and it primarily permeates chloride (Ma et al., 2012). However, different stimuli can produce a change in Panx1 conductance towards a high conductance state (~100-500 pS) allowing the flux of cations leading to a membrane depolarization (Bao et al., 2004; Dahl, 2018; Pelegrin & Surprenant, 2006; Thompson et al., 2008). Panx1 can be directly activated by diverse stimuli such as elevated extracellular potassium levels (Silverman et al., 2009), mechanical stimulation (Bao et al., 2004), or caspase cleavage (Chekeni et al., 2010). In addition, Panx1 can also be indirectly activated in response to activation of NMDA glutamate receptors (NMDARs) (Thompson et al., 2008; Weilinger et al., 2016), ATP-gated P2X7 receptors (Pelegrin & Surprenant, 2006), or α1-adrenergic receptors (Billaud et al., 2015).

Although the physiological role of Panx1 is poorly understood, it is known it contributes to diverse processes from neurodevelopment, synaptic plasticity, up to learning and memory (Figure X) (Yeung et al., 2020). Furthermore, Panx1 also participates in several physiopathological processes such as ischaemic stroke (Weilinger et al., 2016), epilepsy (Dossi et al., 2018; Santiago et al., 2011), and cortical spreading depression (Ni et al., 2018). Indeed, the Panx1-mediated Ca^{2+} influx and ATP release has been linked the disturbance of ion homeostasis, neuronal death during ischemic events (Chekeni et al., 2010), inflammasome activation (Silverman et al., 2009), and macrophage migration and chemotaxis in chronic pain (Hanstein et al., 2016).

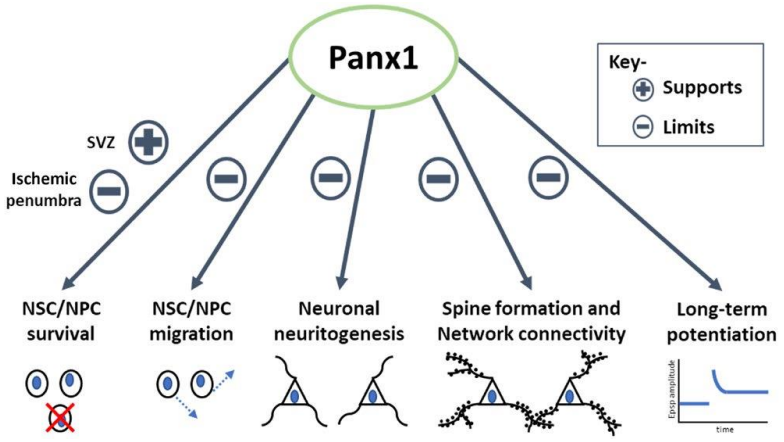

Figure 3: Panx1 in neuronal maturation and network activity Panx1 plays a critical role in supporting the maintenance of neural stem cell / neural progenitor cells (NSC / NPCs) in the subventricular zone (SVZ) of the

adult brain. Conversely, Panx1 activity limits NSC / NPC survival in the ischemic penumbra during stroke. Panx1 inhibits the migration of NSC / NPCs and neuritogenesis in developing neurons. In mature neurons, Panx1 negatively regulates dendritic spine formation and network connectivity. Panx1 activity can also modulate synaptic plasticity by attenuating long-term potentiation (LTP), instead favoring long-term depression (LTD) (Yeung et al., 2020).

The involvement of Panx1 in synaptic plasticity was discovered with loss-of-function approaches using transgenic Panx1-/- mouse. At the hippocampal circuit level, the Panx1-/- mouse show increased neuronal excitability, enhanced long-term potentiation (LTP), and an attenuated long-term depression (LTD) (Prochnow et al., 2012) (Ardiles et al., 2014). At the behavioral level, Panx1 -/- mouse show a deficit in novel object recognition and spatial reversal learning on Morris water maze tests (Gajardo et al., 2018, Prochnow et al., 2012). The cellular and molecular mechanisms responsible for the contribution of Panx1 to synaptic plasticity in the hippocampus are complex. Using Panx1-/- mouse, it was shown that in the CA1 hippocampal area, Panx1 contributes to synaptic strength by modifying the induction threshold for LTP (Ardiles et al., 2014). The role of Panx1 in hippocampal synaptic plasticity was corroborated with the pharmacological inhibition of Panx1 with probenecid (PBN) in wild-type mouse (Ardiles et al., 2014). At the synaptic plasticity field, it has been showed that the loss of Panx1 increased neuronal excitability and induced a long and persistent LTP over time (Prochnow et al., 2012). This phenomenon was observed in the CA1 region of hippocampal slices from Panx1 -/- adult mouse (knock out of Panx1). Phenotypically, Panx1 -/- mouse showed deficit in the novel object recognition test as well as spatial reversal learning on Morris water maze (Gajardo et al., 2018, Prochnow et al., 2012). Consistently, in 2014, another research showed that Panx1 contributed to the synaptic strength, modifying the induction threshold for excitatory synaptic plasticity in hippocampal CA1 of adult mouse. Ardiles et al., showed that Panx1 -/- mouse or pharmacological inhibition of Panx1 with probenecid (PBN) lead to increased LTP, attenuated LTD and reduced threshold for the induction of LTP (Ardiles et al., 2014).

The contribution of Panx1 to hippocampal synaptic plasticity may be mediated by the ATP released through the channel pore. At the synapse, ATP can modulate the synaptic transmission due to its action on presynaptic or postsynaptic ATP receptors which are known as P type (P2XRs, P2YRs). In addition, once in the extracellular space, ATP is rapidly hydrolyzed into adenosine (ADO), which also can modulate synaptic plasticity through of activation of ADO receptors (Dias et al., 2013). Therefore, it has been proposed that the disturbance in the ATP and ADO levels causes the alterations in hippocampal synaptic plasticity observed in the Panx1 -/- mouse. Interestingly, the knock-out of Panx1 modifies the expression of NMDARs in a subtype-specific manner (GluN2). This finding

suggests that the Panx1 loss-of-function may affect LTP and LTD by affecting the contribution of GluN2 receptors to the glutamatergic-dependent synaptic plasticity (Gajardo et al., 2018).

Finally, it was recently reported that NMDARs signal regulate the Panx1 function through Src kinase to facilitate AEA uptake from brain tissue, which can regulate glutamate release in CA1 PyNs following Schaffer collateral stimulation via presynaptic TRPV1 channels (Bialecki et al., 2020). Together this evidence supports to the role of Panx1 channels as an important modulator of synaptic plasticity in adult mouse hippocampus, but the most studies have focused on Panx1 role in glutamatergic transmission. Despite the crucial role of inhibitory transmission in synaptic plasticity, it is unknown the role of Panx1 in GABAergic synaptic plasticity.

Because of the versatility of Panx1 functions, it could contribute to GABAergic synaptic plasticity directly by its role as an ion channel or indirectly via the release of ATP, ADO, and AEA. Although it has not been demonstrated the association with Panx1-mediated release (only in uptake), it is known that AEA is involved in the modulation in GABAergic neurotransmission (Kim & Alger, 2010). Specifically, reduced AEA extracellular levels are associated with increased GABA release that results in activity-deprived hippocampus (Kim & Alger, 2010). Moreover, AEA exogenously applied in rat hippocampal slices increases a specific type of GABAergic synaptic plasticity known as paired-pulse depression (Al-Hayani et al., 2001). However, there is no evidence about the role of Panx-mediated release of AEA in GABAergic transmission or GABAergic synaptic plasticity in the hippocampus.

In summary, Panx1 contributes to synaptic plasticity in the hippocampus by mechanisms involving the Panx1-mediated changes in Glu2 NMDA receptors and, putatively, the changes in Panx1-mediated control in ATP, ADO, and AEA levels. However, it remains unexplored the contribution of Panx1 to hippocampal plasticity by acting on GABAergic transmission, which is also regulated by AEA. Then, we hypothesize that Panx1 contributes to hippocampal synaptic plasticity by affecting both glutamatergic and GABAergic transmission.

Because the Panx1 role in glutamatergic synaptic plasticity has been previously examined, but the Panx1 role in GABAergic synaptic plasticity is unknown, then, the proposed research question is:

Can Panx1 channels modulate GABAergic transmission efficacy in the CA1 hippocampus?

To address our research question, we will use as experimental model brain slices from adult mouse containing the CA1 hippocampal and we will examine the synaptic plasticity occurring at the PyNs.

V. Hypothesis

Pannexin 1 modulates the efficacy of the GABAergic synaptic transmission onto CA1 pyramidal neurons in the mouse hippocampus

Aims

General aim

Evaluate the role of Panx1 in the efficacy of the inhibitory synaptic transmission onto CA1 pyramidal neurons in the mouse hippocampus.

Specific aims

1.1) Study if Panx1 knock-out and Panx1 blockage changes the efficacy of the GABAergic synaptic transmission onto CA1 PyNs of the mouse hippocampus.

1.2) Determine whether Panx1 as a source of adenosine regulate GABAergic transmission onto the CA1 region of mouse hippocampus.

1.3) Determine the molecular mechanisms involved in the changes induced with the Panx1 knock-out and Panx blockage in the GABAergic transmission.

VI. Methodology

Animals

The animal care procedures and slices preparation followed the Animal care standards outlined in the National Institute of Health (United States) guidelines and were approved by the Institutional Animal Ethics Committee of the Universidad de Valparaíso. This study used adult male and female WT mouse (C57BL/6J) and Panx1 KO mouse (Anselmi et al., 2008; Ardiles et al., 2014). Animals were housed on a 12 h light/dark cycle and maintained in a temperature- and humidity-controlled environment with ad libitum access to food and water.

Slice preparation

We used isoflurane to anesthetize the mouse, which was decapitated, and the brain was removed and submerged in cold (~1°C) artificial cerebrospinal fluid (ACSF, in mM: 124.00 NaCl, 2.70 KCl, 1.25 KH2PO4, 1.30 MgSO4, 26.00 NaHCO3, 10.00 Glucose, 2.50 CaCl2). The pH of ACSF was stabilized at ~7.4 by bubbling with a mixture of oxygen 95% and CO2 5%. Under these conditions, coronal slices of the dorsal hippocampus (300µM) were cut with a vibratome (Campden Instruments, model MA752) with bubbled ACSF. Next, we transferred the hippocampal slices to the incubation chamber with bubbled ACSF and were maintained at room temperature (20-22 °C) until electrophysiological recordings (~1 hour after slice collection).

Electrophysiology

After 1-h incubation, brain slices were transferred to a 1 ml recording chamber in the patch-clamp setup. The recording chamber was coupled with a magnifying glass to obtain blind patch-clamp recordings. Slices were perfused with ACSF through a circulation system at room temperature and with a constant flow (~1ml/min). The recording setup was installed on an antivibration table to allow stable recordings by preventing vibrations from the environment. In addition, electrophysiological recordings were realized into a Faraday cage to diminish the electric noise from external electric devices.

We used the patch-clamp technique for whole-cell recordings from the soma of CA1 PyNs. The voltage-clamp configuration was used to record evoked and spontaneous inhibitory postsynaptic currents (eIPSCs and sIPSCs, respectively). The holding potential was adjusted at the reversal potential of glutamatergic currents (0mV) to obtain only inhibitory postsynaptic currents. For the recordings, a chlorinated silver wire electrode (Ag/AgCl) was contained into a borosilicate glass micropipette with a tip resistance of 4-6 MΩ. Recording pipettes were made in a pipette puller (Sutter

Instrument Co., P-97) and were filled with an internal solution containing in mM: 131 Cesium-Gluconate (Cs-Gluc), 10 HEPES, 10 EGTA, 2 Glucose, 1 CaCl2, 8 NaCl, 4 Mg2ATP, 0.4 Na3GTP buffered to pH 7.2 – 7.3 with CsOH.

The electrode into the recording pipette was connected to an EPC-7 patch-clamp amplifier for voltage-clamp recording (HEKA, Instruments, MA, United States). Moreover, we compensated the capacitive currents to 70%, and neurons were accepted only when the seal resistance was > 1 GΩ, and the access resistance (Ra; 7- 14 MΩ) did not change by > 20% during the experiment. Data were low-passed, filtered at 3.0 kHz, and sampled at rates between 6.0 and 10.0 kHz using an A/D converter (ITC-16, InstruTech) and acquired with the Pulse Fit software (Heka Instruments). Data were analyzed with the pClampfit 10.7.0.3 software (Molecular Devices, LLC). As the reference electrode, we used an epoxy electrode filled with KCl and a resistance of 2.7 KΩ (World Precision Instruments, Inc). The stimulation electrode consisted of a septate pipette filled with ACSF previously mentioned and two silver wires coupled to a stimulation source (Isoflex).

The experimental design consisted in recording postsynaptic inhibitory currents onto PyNs of CA1 area in adult mouse in the voltage-clamp mode. The evoked IPSC (eIPSCs) were obtained by recording and stimulating GABAergic fibers in stratum pyramidal of CA1 area. The stimulation electrode was positioned in the pyramidal layer at ~40-50 µm from the recording pipette. In all the experiments, a baseline of the inhibitory currents was recorded for 10-15 minutes. Next, different drugs were applied in the bath, and the inhibitory current was continuously recorded.

In some experiments, the intracellular solution contained either the G-protein coupled receptor (GPCR) inhibitor guanosine 5'-O-(2-thiodiphosphate) (GDPβS, 2mM), the fast calcium chelator, 1,2-bis (o-amino phenoxy) ethane-N,N,N', N′-tetraacetic acid (BAPTA, 40mM), the membrane-impermeable PKA inhibitor, PKI6-22 peptide (2.5 mM) or the C-terminal anti-Panx1 polyclonal antibody (α-panx1; 0.25 ng/µl).

The recording solutions used in this study had a composition in mM as follows:

1) Cs-Gluc: 131 Cs-Gluconate, 10 HEPES, 10 EGTA, 2 Glucose, 1 CaCl2, 8 NaCl, 4 Mg2ATP, 0.4 Na3GTP.
2) Cs-Gluc + GDPβS: 131 Cs-Gluconate, 2 GDPβS, 10 HEPES, 10 EGTA, 2 Glucose, 1 CaCl2, 8 NaCl, 4 Mg2ATP, 0.4 Na3GTP.
3) Cs-Gluc + BAPTA: 111 Cs-Gluconate, 20 BAPTA, 10 HEPES, 2 Glucose, 8 NaCl, 4 Mg2ATP, 0.4 Na3GTP.

4) Cs-Gluc + PKI_{6-22}: 131 Cs-Gluconate, 0,0025 PKI_{6-22}, 10 HEPES, 10 EGTA, 2 Glucose, 1 CaCl2, 8 NaCl, 4 Mg2ATP, 0.4 Na3GTP.

All the recording solutions were buffered to pH 7.2 – 7.3 with CsOH and the osmolarity was between 280-290 mOsm.

Paired pulse protocol

To determine the effect of Panx1 blockage on GABA release, we used the paired-pulse protocol (PPP). This protocol consists of stimulating the inhibitory fibers with 2 electrical pulses separated by 100ms. GABAergic synapses have a high release probability, then PPP induces short-term plasticity in which the second eIPSC has a lower amplitude relative to the first eIPSC. This type of synaptic plasticity is known as paired pulse depression (PPD). The PPP provides the paired-pulse ratio (PPR), which was calculated as (R2/R1), where R1 and R2 are the peak amplitudes of the first and second eIPSC.

Coefficient of variation

The analyses of the coefficient of variation (CV) were implemented to elucidate whether the changes in the inhibitory synaptic transmission are at the pre or postsynaptic level. This analysis is sensitive to changes in the probability of release (Pr) and the number of release sites. CV was estimated as the standard deviation (SD) of the eIPSC amplitude divided by the mean eIPSC amplitude (Brock et al., 2020; Andersen et al., 2007).

* Both PPR and CV were measured before (10 min) and after (15 min) bath application of the Panx1 blocker 10panx (100µM).

Recording of inhibitory postsynaptic currents in miniature (mIPSCs)

To determine whether if Panx1-induced effects depended on network excitability, the synaptic transmission was studied in the absence of action potential firing. The miniature IPSCs (mIPSCs) were recorded in the presence of the voltage-gated sodium channel blocker tetrodotoxin (TTX, 500nM). mIPSCs were recorded before and after bath application of the Panx1 blockers 10panx and PBN.

Chemicals and reagents

All the salts were purchased from Sigma-Aldrich Chemistry (St. Louis, MO, United States), Tocris (Bioscience, Pittsburg, PA, United States, Merck Millipore, and Cayman Chemical (Sarasota, FL, United States). 10panx (WRQAAFVDSY) and sc10panx (FSVYWAQADR) were synthesized by

Beijing SBS Genetech Co., Ltd (Beijing, China). The C-terminal anti Panx1 polyclonal antibody (α-panx1; 0.25 ng/µl) (Bialecki et al., 2020; Weilinger et al., 2012, 2016) was purchased from Invitrogen (catalog #488100, rabbit polyclonal).

The 2-amino-5-phosphonopentanoic acid (D-AP5; 50 mM), 7-nitro-2,3-dioxo-1,4-dihydro quinoxaline-6-carbonitrile (CNQX; 20 µM), and DAMGO (3 µM) were dissolved in water and added to the ACSF as needed. Dihydrochloride (H89, 10mM) was dissolved in DMSO and added to the ASCF as needed.

Analysis

Data analyses were made with the Clampfit program software (10.7.0.3; pCLAMP 10.7; Molecular Device, Chicago, IL. USA). For statistical analyses and graphics construction, the computational software GraphPad Prism 8.0.1 for Windows was used. The data normal distribution was verified using the Shapiro Wilk test (SW). To determine differences before and after the tested drug, the data with a normal distribution were analyzed with the Student's two-tailed t-test. Nonparametric data were analyzed with the Wilcoxon matched-pairs signed-rank test for paired data. Unpaired student t-test was used for comparison between two groups. Results are reported as mean ± sem (n = number of cells). eIPSCs are presented as percentage. Differences were considered statistically significant at $P < 0.05$ (*), $P < 0,01$ (**) $P < 0.001$ (***), $P < 0.0001$ (****).

VII. Results

Specific aim 1.1: Study if Panx1 knock-out and Panx1 blockage changes the efficacy of the GABAergic synaptic transmission onto CA1 PyNs of the mouse hippocampus.

Panx1 can regulate excitatory synaptic plasticity, increase neuronal excitability, and promote behavioral and cognitive changes (Prochnow et al., 2012; Gajardo et al 2018). Although Panx-1 is also expressed in GABAergic interneurons, whether Panx-1 regulates GABAergic transmission is unknown. To evaluate the role of Panx1 in spontaneous and evoked GABAergic synaptic transmission, we selectively inhibited Panx1 with 10panx (100µM). We voltage-clamped CA1 pyramidal neurons (PyNs) at 0mV (reversal potential to glutamatergic transmission) and recorded the spontaneous and evoked IPSCs. We recorded a baseline of evoked inhibitory postsynaptic currents (eIPSCs) during 10 min. Next, we tested the effects of bath application of 10panx (100µM) in eIPSC. We observed that 10panx reduced the eIPSCs amplitude (baseline: 100.22 ± 1.55%, 10panx: 73.33 ± 6.86%; p = 0.0055; n = 10 per condition, Fig. 3C) but it did not affect the kinetics of those currents (Fig. S1). The effect of 10panx was not associated with any change in the access resistance throughout the experiment (Fig. 3B). The 10panx-induced depression in eIPSCs amplitude was accompanied by an increase in the paired-pulse ratio (PPR) (ACSF: 0.55 ± 0.03, 10panx 0.66 ± 0.05; p = 0.0048; n = 10 per condition, 3D), suggesting a decrease in the probability of GABA release onto PyNs of CA1 of hippocampus. However, the CV remained unchanged under these conditions (ACSF: 0.245 ± 0.040, 10panx: 0.272 ± 0.051; p = 0.2681, n = 10; Fig. 3D).

To corroborate the specificity of the 10panx effects, we evaluated the effects of sc 10panx (100 µM), an scrambled mimetic peptide of 10panx (Bialecki et al., 2020), onto inhibitory transmission. Bath application of sc 10panx did not modify neither the amplitude of eIPSCs (ACSF: 98.90 ± 1.98%, sc 10panx: 93.90 ± 10.47%; p = 0,6613; n = 7 per condition, Fig. 3E-F) nor the PPR (ACSF: 0.61 ± 0.02, sc 10panx: 0.64 ± 0.02; p = 0.3171; n = 7 per condition, Fig. 3F).

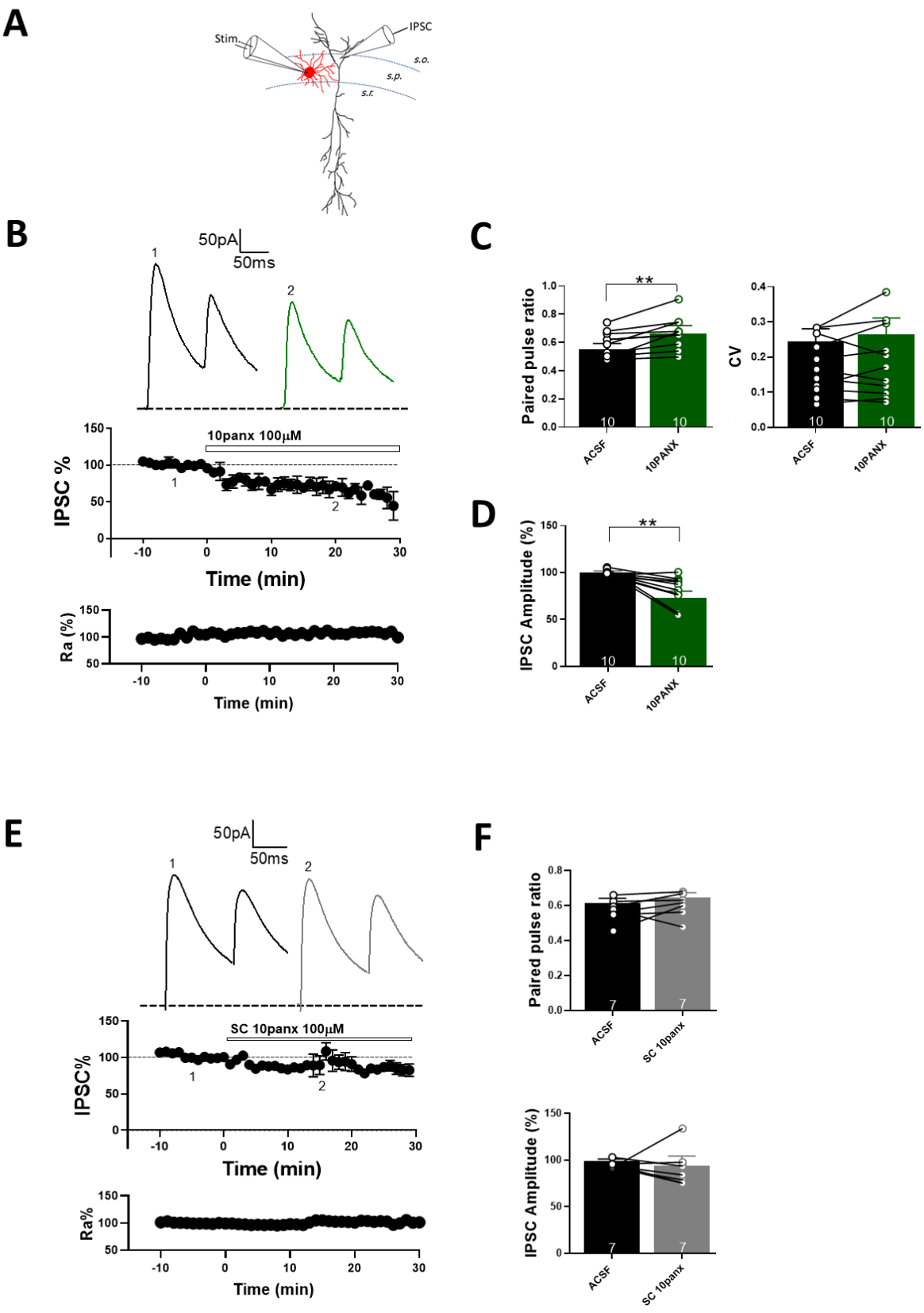
A
Stim
IPSC
s.o.
s.p.
s.r.
B
50pA
50ms
1
2
10panx 100μM
IPSC %
Time (min)
Ra (%)
Time (min)
C
Paired pulse ratio
**
ACSF
10PANX
CV
ACSF
10PANX
D
IPSC Amplitude (%)
**
ACSF
10PANX
E
50pA
50ms
SC 10panx 100μM
IPSC%
Time (min)
Ra%
Time (min)
F
Paired pulse ratio
ACSF
SC 10panx
IPSC Amplitude (%)
ACSF
SC 10panx

Figure 3: Block of Panx1 with 10panx decreases evoked IPSC onto CA1 pyramidal neurons of mouse hippocampus. A) Schematic diagram showing the CA1 pyramidal neurons and localization of the stimulation and recording electrodes. In red, GABAergic interneuron and in black pyramidal neuron. **B)** Traces of evoked IPSCs and PPR in the absence and the presence of 10panx (top). Temporal course showing the changes in the eIPSC amplitude before, during and after 10panx (100µM) application (middle). Temporal course showing Ra% throughout the experiment (bottom). **C)** Average (± SEM) of the eIPSC amplitude in the absence (ACSF) or following bath application of 10panx. **D)** Average (± SEM) of the PPR at 100 ms intervals (left) and CV (right) in the absence (ACSF) or following bath application of 10panx. **E)** Traces from a representative experiment before and after sc10panx application (top). IPSC% vs time plot before and after sc10panx application (middle). Temporal course showing Ra% throughout the experiment (bottom). **F)** Average (± SEM) of the PPR (top) or IPSC amplitude (bottom) in the absence (ACSF) or following bath application of sc 10panx. Significance was determined using Student's t-test, *p<0.05. The number of recorded cells is indicated within bars.

To investigate the role of Panx1 in the inhibitory synaptic transmission, we inhibited Panx1 channels in single PyNs of CA1 area by inclusion in the recording pipette of a specific antibody against Panx1 (α-panx1 0.25ng/µl) (Bialecki et al., 2020; Weilinger et al., 2012, 2016). To corroborate the specificity of α-panx1 on GABAergic transmission, we also tested the effects of a polyclonal antibody against α-Cx43 (0.3 ng/µl) (Bialecki et al., 2020, Weilinger et al., 2012). Thus, we recorded eIPSCs and compared the effect of intracellular α-panx1 or α- Cx43 in the inhibitory transmission. In the presence of α-panx1, the PPR value significantly increases compared with the PPR in the presence of α-Cx43 (Fig. 4C). Next, we recorded eIPSCs in the presence of intracellular α-panx1 and then we applied 10panx (100µM). The effect of 10panx in the GABAergic transmission was abolished in the presence of α-panx1. The bath application of 10panx did not change neither the eIPSCs amplitude (ACSF with α-panx1: 100.79 ± 1.39%, α-panx1 + 10panx: 93.67 ± 7.53%; p = 0.4543, n = 6 per condition, Fig. 4A-B) nor the PPR (ACSF with α-panx1: 0.72 ± 0.052, α-panx1 + 10panx: 0.70 ± 0.050; p = 0.4929, n = 6 per condition, Fig. 4B, top). These results suggest that blocking postsynaptic Panx1 is sufficient to decrease the GABAergic transmission efficacy. These data indicate that α-panx1 specifically blocks Panx1 and corroborate that blocking Panx1 located in postsynaptic CA1 PyNs depresses the GABAergic transmission.

To further examine the specificity of 10panx on GABAergic transmission, we evaluated its effects in hippocampal slices from Panx1 knock-out (KO) mouse. 10panx did not affect neither the eIPSC amplitude (ACSF: 99.82 ± 1.25%, 10panx: 99.34 ± 10.93%; p = 0.9825; n = 5 per condition, Fig.4D-E) nor the PPR (ACSF: 0.61 ± 0.05, 10panx: 0.58 ± 0.06; p = 0.5320, n = 5 per condition, Fig. 4E) of GABAergic transmission onto PyNs from Panx1 KO mouse. These results indicate that 10panx decreases the GABAergic transmission efficacy due to its specific effect on postsynaptic Panx1.

To evaluate the effects of Panx1 knock-out in the basal GABAergic transmission, we measured the inhibitory efficacy onto CA1 PyNs from Panx1 KO mouse. In CA1 PyNs, the Panx1 knock-out did not change the eIPSCs amplitude, which was evaluated using input-output curves (Fig. 4F). Consistently, the PPR did not change in PyNs from Panx1 KO compared with the wild-type mouse (WT: 0.3805 ± 0.03; n = 15, Panx1 KO: 0.453 ± 0.06; n = 10; p = 0.2918; Fig. 4F). These results suggest that Panx1 knock-out does not affect the basal GABAergic transmission onto PyNs.

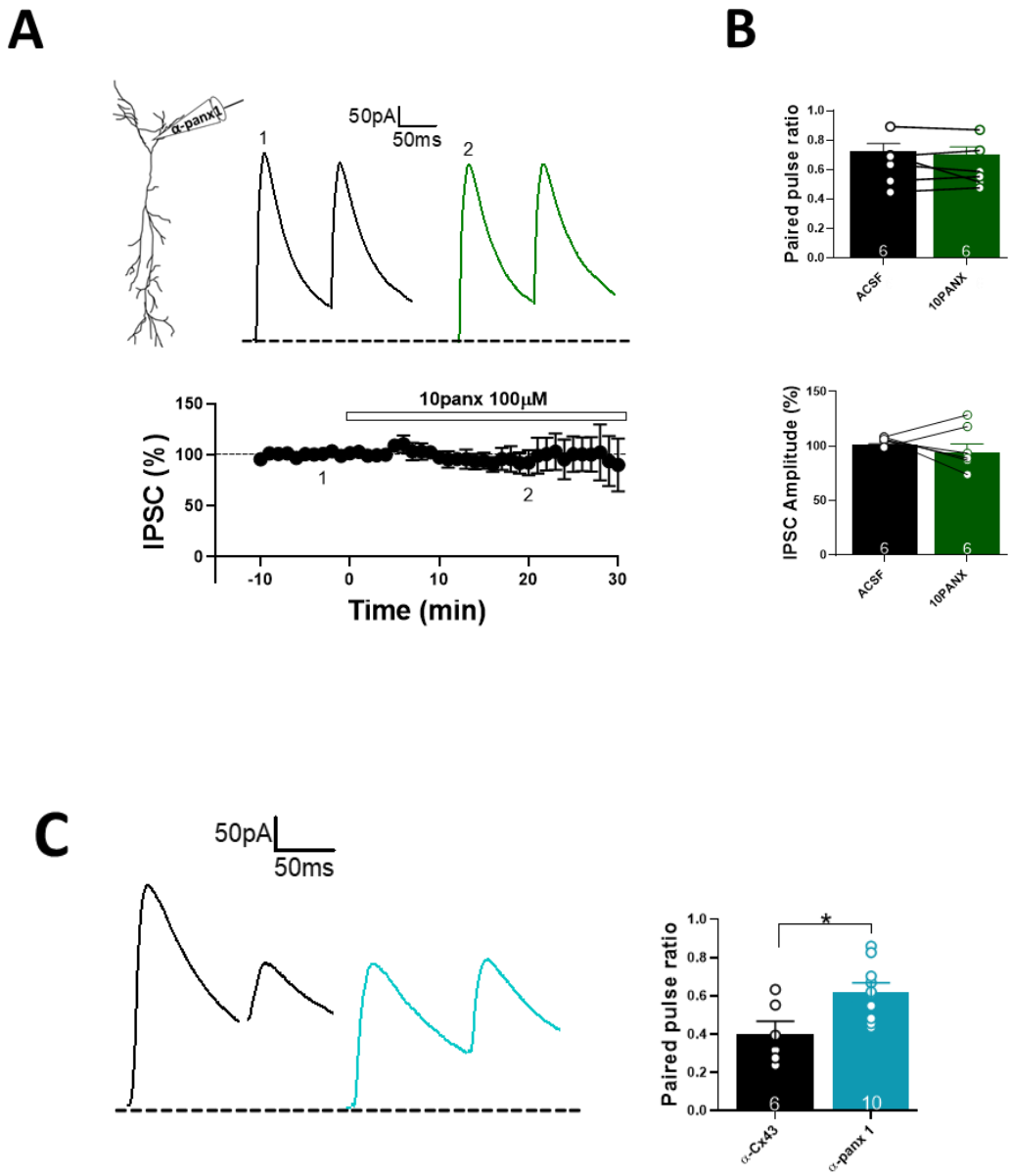

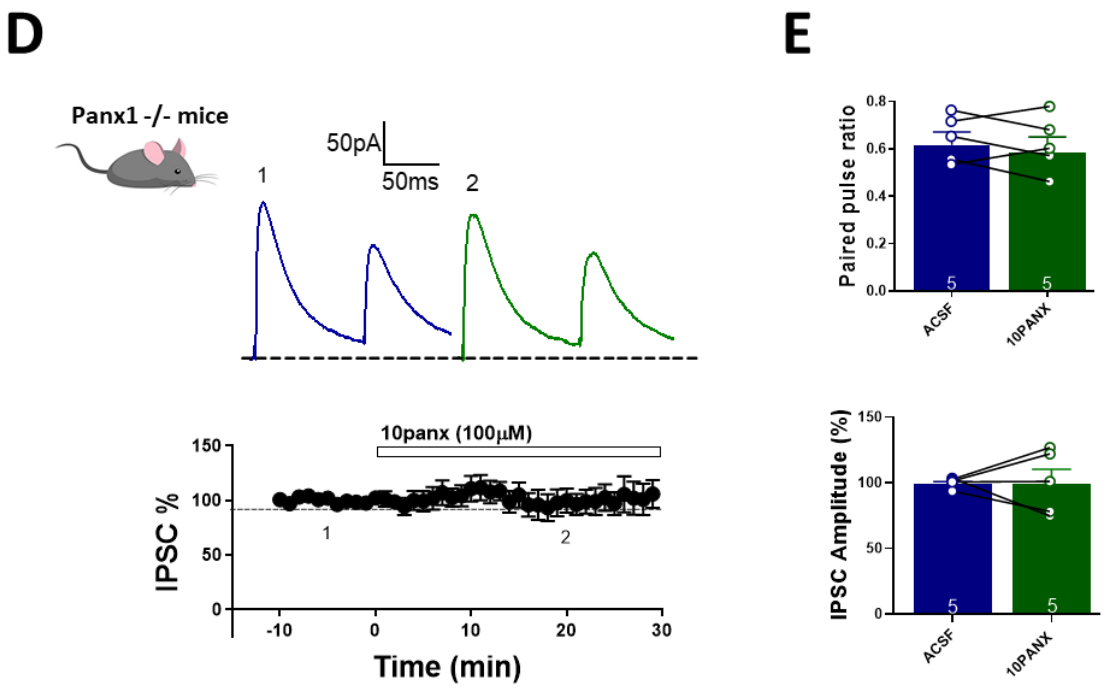
D
Panx1 -/- mice
50pA
50ms
1
2
10panx (100μM)
IPSC %
150
100
50
0
-10
0
10
20
30
Time (min)
E
Paired pulse ratio
0.8
0.6
0.4
0.2
0.0
5
5
ACSF
10PANX
IPSC Amplitude (%)
150
100
50
0
5
5
ACSF
10PANX

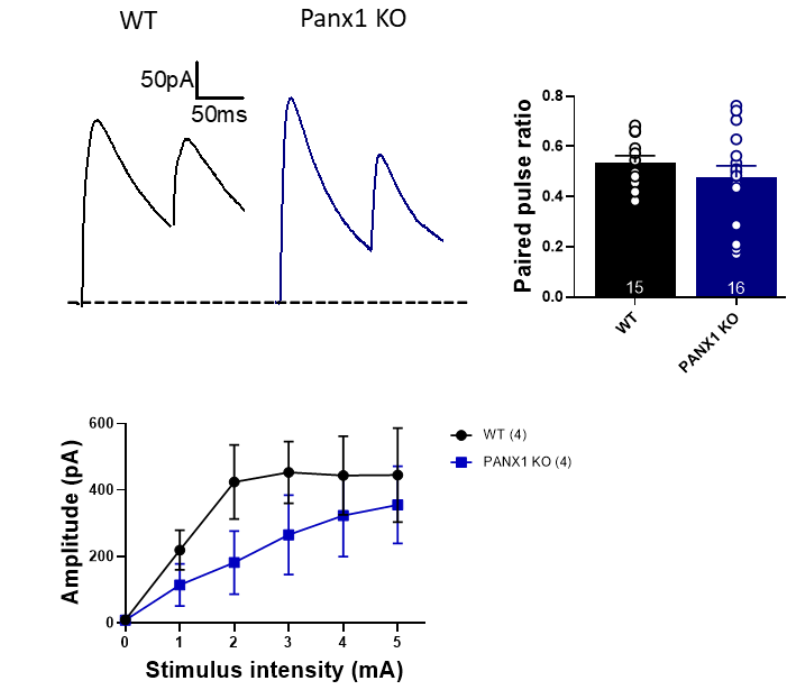
F
WT
Panx1 KO
50pA
50ms
Paired pulse ratio
0.8
0.6
0.4
0.2
0.0
15
16
WT
PANX1 KO
Amplitude (pA)
600
400
200
0
0
1
2
3
4
5
Stimulus intensity (mA)
WT (4)
PANX1 KO (4)

Figure 4: Block of postsynaptic Panx1 is sufficient to decrease the basal GABAergic efficacy. A) Representative traces of evoked IPSC by using α-panx1 (0.25ng/µl) in the patch pipette before and after 10panx application (top). Temporal course showing IPSC% from cells recorded with α-panx1, before, during, and after 10panx application (bottom). **B)** Bath application of 10panx had no effects in the PPR (top) and IPSC amplitude (bottom) in cells recorded with α-panx1 in the patch pipette**. C)** Samples traces of evoked IPSCs from CA1 neuron recorded with α-Cx43 (black) and α-panx1 (light blue)(left). Block of Panx1 with α-panx1 in the pipette augmented PPR (middle) and decreased IPSC amplitude (right) compared with its respective control, α-Cx43 (0.3ng/µl). **D)** Representative traces of evoked IPSCs for each condition in hippocampal slices from Panx1 KO mouse (top). IPSC% vs time plot before and after 10panx addition in pyramidal neurons from Panx1 KO mouse (bottom). **E)** Bath application of 10panx did not affect PPR (top) and IPSC amplitude (bottom) in hippocampal slices from Panx1 KO mouse. **F)** Samples traces from evoked IPSC and PPR for pyramidal neurons were recorded from wt mouse (black) and Panx1 KO mouse (blue)(left). The PPR (middle) and eIPSC from input-output curves (right) were not different between groups. Data are performed as mean ± SEM . *$p<0.05$. The number or recorded cells is indicated within bars.

Next, we examined the effects of blocking Panx1 on spontaneous IPSCs (sIPSCs). Blocking Panx1 with 10panx significantly decreased the sIPSC frequency (ACSF: 3.86 ± 0.33 Hz, 10panx: 2.83 ± 0.32 Hz; $p = 0.0078$; n = 8, Fig. 5A), but it did not affect the sIPSC amplitude (ACSF: 38.28 ± 4.72 pA, 10panx: 32.65 ± 3.23 pA; $p = 0.1511$; n = 8, Fig. 5A).

Several reports suggest that Panx1 blockage affects hippocampal excitability (Prochnow et al., 2012; Ardiles et al., 2014, Bialecki et al., 2020). To discard whether the 10panx effect on sIPSC frequency is dependent on action potential-evoked presynaptic GABA release, we blocked the action potential generation with tetrodotoxin (TTX, 500nM) and we recorded the miniature IPSCs (mIPSC) before and after 10panx application. In these conditions 10panx significantly reduced the frequency of mIPSCs (ACSF: 1.97 ± 0.33 Hz, 10panx: 1.36 ± 0.27 Hz; $p = 0.0010$; n = 8 per condition, Fig. 5B), but it did not affect the mIPSCs amplitude (ACSF: 15.36 ± 0.73 pA, 10panx: 14.96 ± 1.18 pA; $p = 0.5136$, n = 8 per condition, Fig. 5B). Next, we examine the effect of intracellular α-Panx1 in sIPSCs onto PyNs. We found that in cells with α-Panx1, the frequency of sIPSCs was significantly lower than those with α-Cx43 (α-Cx43: 4.48 ± 0.53 Hz, α-Panx1: 2.58 ± 0.43 Hz, $p = 0.0197$, n = 6 per condition, Fig. 5C), while sIPSCs amplitude remained unaffected (α-Cx43: 28.42 ± 3.57 pA, α-Panx1: 24.22 ± 3.74 pA; $p = 0.4368$, n = 6 per condition, Fig. 5C). A change in mIPSCs frequency has been attributed to presynaptic changes in neurotransmitter release probability. Then, these results suggest that the Panx1-induced decrease in spontaneous GABAergic activity occurs at presynaptic level.

Finally, we quantified the inhibitory spontaneous transmission in hippocampal slices from Panx1 KO mouse. In CA1 PyNs, neither sIPSCs frequency (WT: 3.86 ± 0.33 Hz, Panx1 KO: 4.30 ± 0.45 Hz; $p = 0.4444$; n = 8 per condition; Fig. 5D) nor amplitudes (WT: 38.28 ± 4.71 pA, Panx1 KO: 41.94 ± 2.67 pA; $p = 0.5105$; n = 8 per condition; Fig. 5D) showed differences in Panx1 KO neurons compared

with control mouse. Similarly, the mIPSC frequency (WT: 1.97 ± 0.33 Hz; n = 8, Panx1 KO: 2.06 ± 0.27 Hz; n = 6; p = 0.8417; Fig. 5E) and amplitudes (WT: 15.36 ± 0.73 pA; n = 8, Panx1 KO: 16.71 ± 1.07 pA; n = 6; p = 0.3044; Fig. 5E) from CA1 PyNs from Panx1 KO was comparable to their wild-type counterparts . These results suggest that Panx1 knock-out does not affect the basal inhibitory GABAergic synaptic transmission in the hippocampus.

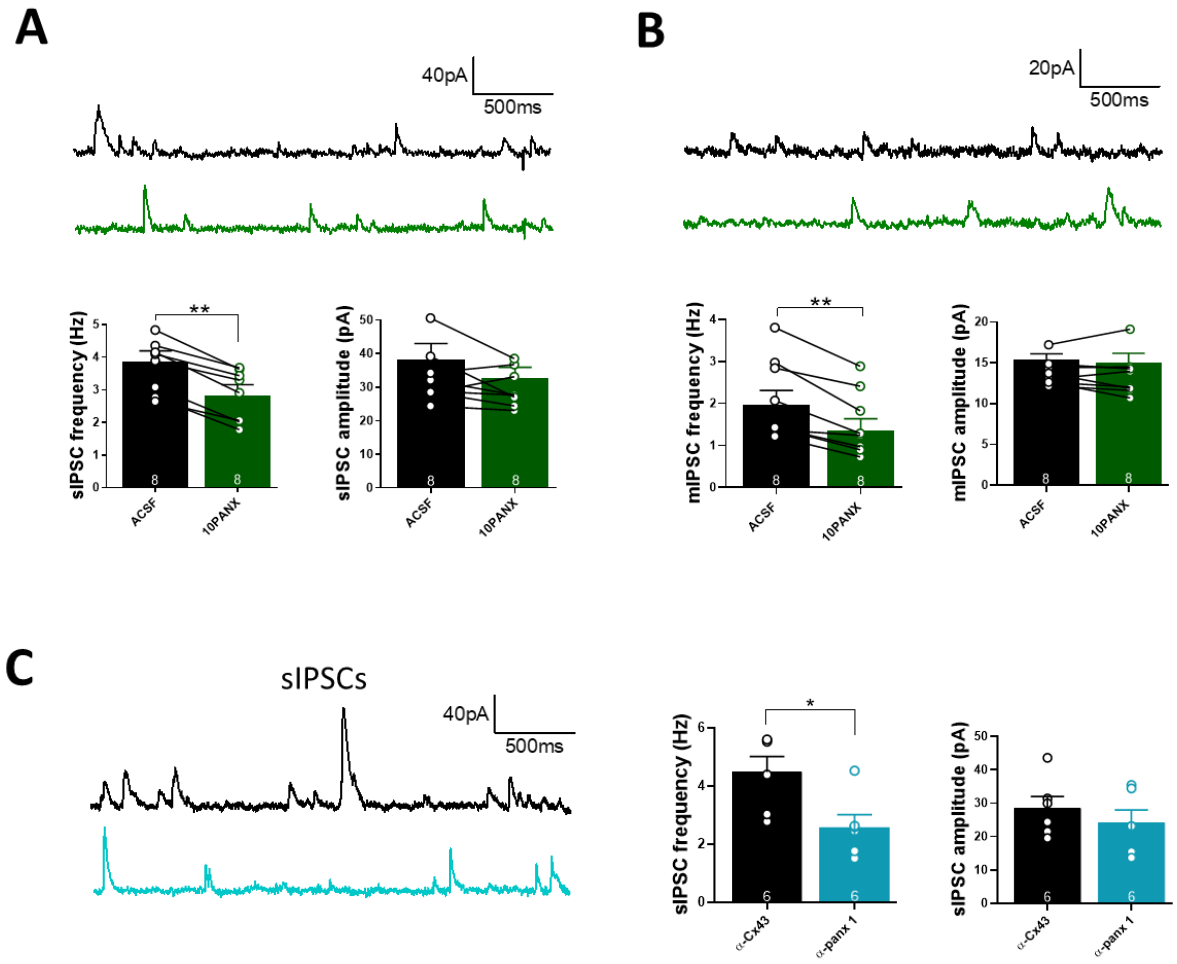

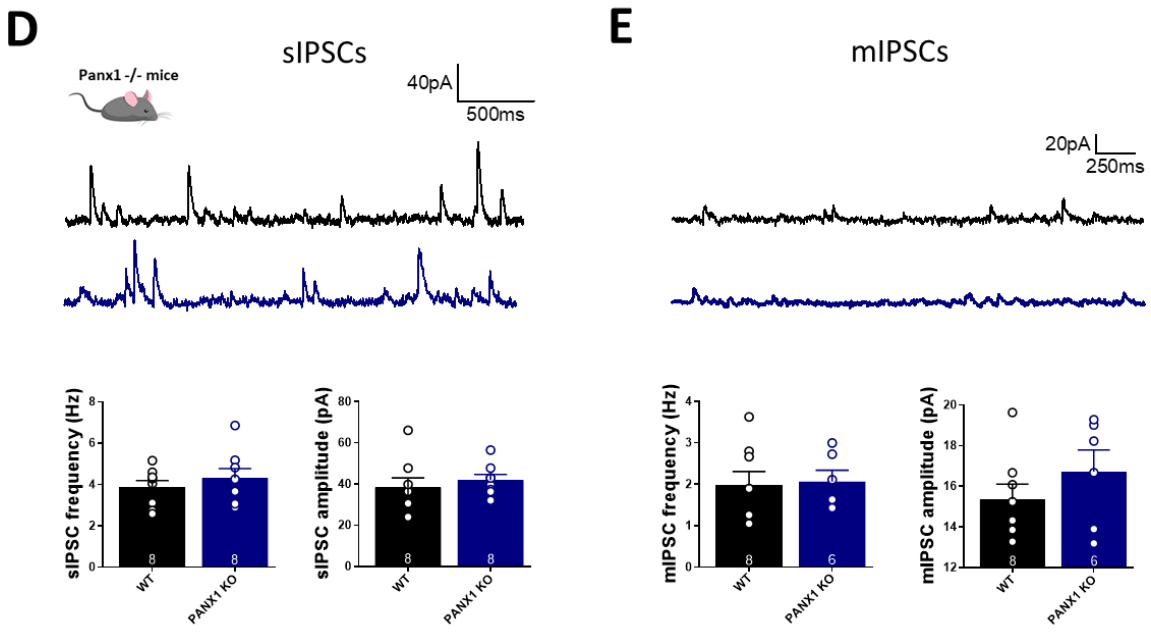

Figure 5: Block of Panx1 with 10panx decreases spontaneous GABAergic transmission onto pyramidal cells of mouse hippocampus. A) Samples traces of sIPSCs from pyramidal cells before (black) and after (green) 10panx application (top). Block of Panx1 decreased sIPSC frequency (left), while sIPSC amplitude was unchanged (right). **B)** Representative sample traces showing mIPSCs recorded before and after bath application of 10panx (top). 10panx decreased mIPSC frequency compared with basal condition (left). **C)** Samples traces of sIPSCs obtained from pyramidal cells recorded with α-Cx43 (black) and α-panx1 (light blue) in the patch pipette (left). The frequency of sIPSCs was reduced in the presence of α-panx1 compared with its control condition, α-Cx43 (middle), while sIPSCs amplitude remained unaffected (right). **D)** Quantitative analyses of sIPSC frequency (left) and amplitude (right) did not show significant differences between control and Panx1 KO mouse. **E)** Absence of Panx1 did not affect neither mIPSC frequency (left) and mIPSC amplitude (right) compared with WT mouse. No significant changes were observed in mIPSCs amplitude in the presence of 10panx (right). Data are performed as mean ± SEM . *p<0.05, ** p<0.01. Number or recorded cells is indicated within bars.

Block of Panx1 with probenecid decreased GABAergic efficacy onto PyNs of mouse hippocampus.

A great variety of drugs and chemicals have been identified as inhibitors of Panx1 channels, thus in addition to the inhibitory peptide 10panx, we tested probenecid (PBN), which has been previously used to block Panx1 channels in glutamatergic neurons (Ardiles et al., 2014). Bath application of PBN (200µM) induced a fast a long-lasting depression in the eIPSCs amplitude compared with baseline (ACSF: 99.49 ± 1.35%, PBN: 53.40 ± 4.62%; $p < 0.0001$; n = 11 per condition, Fig. 6A-B). This depression was accompanied by a significant increase in the PPR (ACSF: 0.38 ± 0.03, PBN: 0.48 ± 0.04; $p < 0.0001$; n = 15 per condition, Fig. 6B), suggesting that PBN decreases the GABA release. In addition, we recorded spontaneous inhibitory activity. We found that PBN significantly decreased

both sIPSC frequency (ACSF: 3.96 ± 0.33 Hz, PBN: 2.11 ± 0.29 Hz; p = 0.0028; n = 8 per condition, Fig. 6C) and amplitude (ACSF: 33.27 ± 2.48 pA, PBN: 24.49 ± 1.61 pA, p = 0.0064, n = 8 per condition, Fig. 6C) compared with basal condition.

To rule out that PBN disturbs the presynaptic excitability and to confirm PBN impacts the inhibitory synaptic efficacy via its effects on release probability, we recorded mIPSCs. We observed that PBN induced a significant decrease in mIPSCs frequency compared with basal condition (ACSF: 1.86 ± 0.29 Hz, PBN: 0.92 ± 0.11 Hz; p = 0.0129; n = 5 per condition, Fig. 6D). However, mIPSCs amplitude did not change with the bath application of PBN (ACSF: 18.45 ± 2.91 pA, PBN: 16.77 ± 2.58 pA; p = 0.1256; n = 5 per condition, Fig. 6D). As previously observed with 10panx and α-Panx1, blocking Panx1 with PBN affected the PPR and mIPSCs frequency, suggesting that the decrease in GABAergic efficacy occurs at the presynaptic level. However, the finding that PBN decreased the IPSC amplitude, suggests that another mechanism at the postsynaptic level might be involved in the Panx1blockage-induced effects in the hippocampal GABAergic transmission.

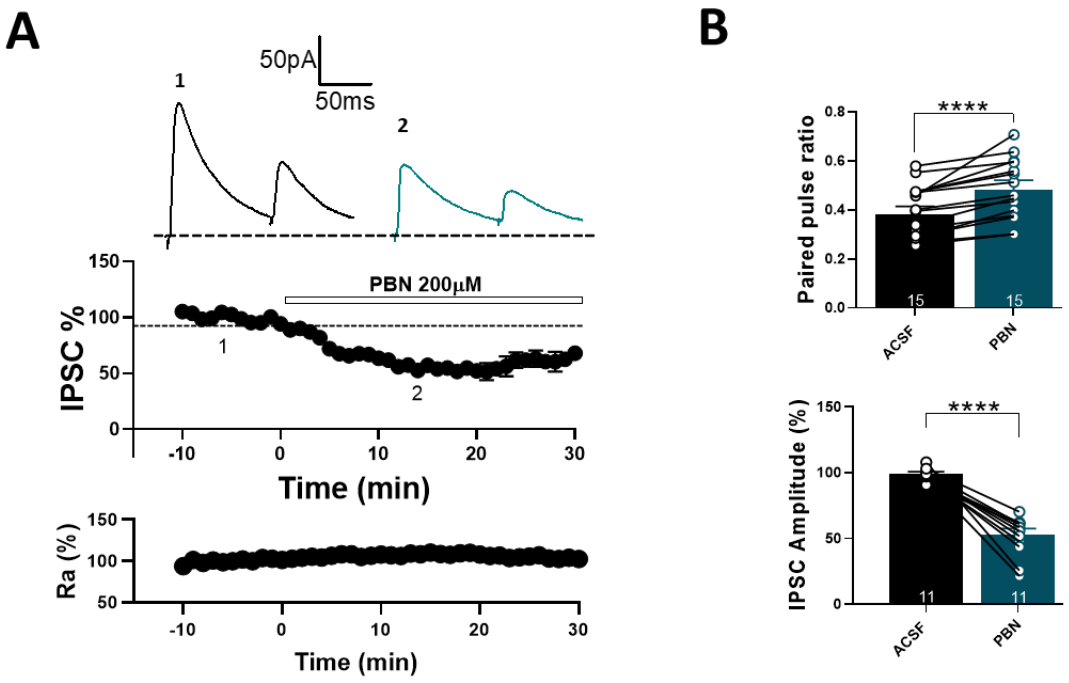

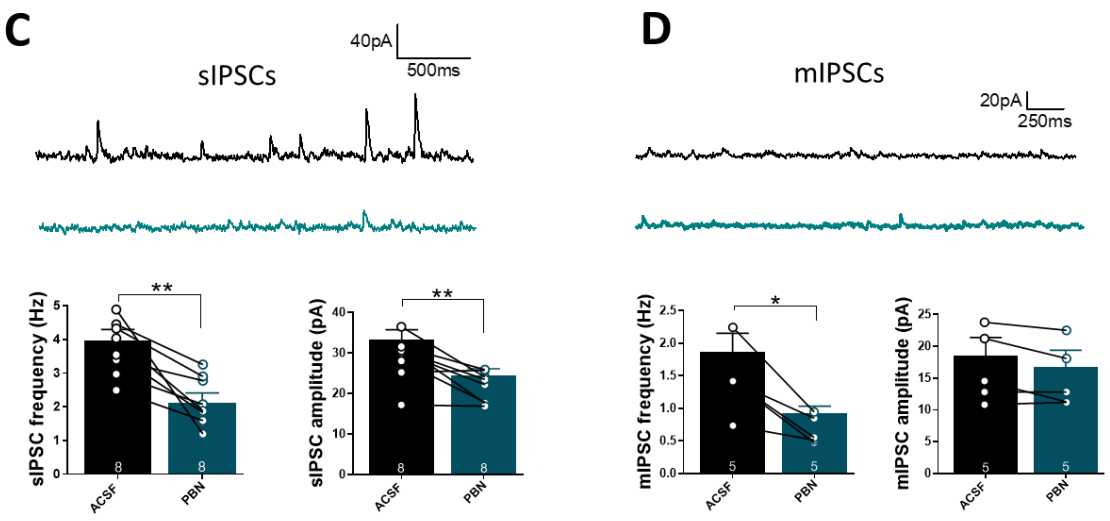

Figure 6: Block of Panx1 with PBN decreases evoked and spontaneous GABAergic efficacy onto pyramidal cells of mouse hippocampus. A) Samples traces from evoked IPSCs and PPR for each condition (top). Temporal course showing the changes in the IPSC amplitude before, during and after PBN (200µM) application (middle). Temporal course showing Ra% along the experiment (bottom). **B)** Application of PBN showed an increase of PPR at 100 ms intervals compared to the ACSF group (top). IPSC amplitude was significantly decreased with bath application of PBN (bottom). **C)** Representative sample traces showing sIPSCs recorded before and after bath application of PBN (top). PBN decreased significantly the sIPSC frequency (left) and sIPSC amplitude (right) compared with basal condition. **D)** Samples traces from mIPSCs before and after PBN application (top). Quantitative analyses showed that PBN induced a significant decrease in the frequency of mIPSCs (left), while mIPSCs amplitude remained unchanged (right). Data are performed as mean ± SEM . *p<0.05. Number or recorded cells is indicated within bars.

Specific aim 1.2: Determine whether Panx1 as a source of adenosine reduce GABAergic transmission in CA1 region of mouse hippocampus.

Adenosine (ADO) can regulate the GABAergic transmission in several brain areas included hippocampus (Jeong et al., 2003; Rombo et al., 2015, 2016). ADO exerts specific action in hippocampal interneurons controlling for example GABA release from PV interneurons (Rombo et al., 2015) or acting onto extrasynaptic $GABA_AR$ (Rombo et al., 2016) and therefore providing a fine control of network excitability in the hippocampus. Given that ADO is generated largely by the hydrolysis of ATP and Panx1 channels contribute to elevate the ATP levels in the extracellular space, we postulated that depression in inhibitory transmission mediated by Panx1 blockers, could be occurring due to a reduction or unbalance in extracellular levels of ADO. Thus, we evaluated whether ADO application (100 µM) could revert the PBN-mediated depression in GABAergic synaptic efficacy. According to our previous results, application of PBN (200µM) induced a significant

decrease in eIPSCs amplitude compared with basal condition (ACSF: 100.47 ± 1.66 %, PBN: 62.32 ± 5.73 %, p value= 0.0002; n = 7 per condition. Fig. 7A-B). However, in the presence of PBN, bath application of ADO was unable to induce changes in the eIPSCs amplitude (PBN: 62.32 ± 5.73 %, PBN + ADO: 61.32 ± 3.56 %; p value= 0.8845, n = 7 per condition, Fig. 7A-B). The PBN-mediated depression in eIPSCs was accompanied by an increase in PPR (ACSF: 0.487 ± 0.07; PBN: 0,555 ± 0.06, p value= 0.0179, n = 7 per condition. Fig. 7B). Nevertheless, ADO application did not change the PPR value induced by previous application of PBN (PBN: 0,555 ± 0.061, PBN + ADO: 0.540 ± 0.058; p value= 0.726, n = 7 per condition, Fig. 7B).

Next, we examined the effect of ADO in spontaneous GABAergic activity when Panx1 was blocked. According to our previous results PBN caused a significant decrease in sIPSC frequency compared with basal condition (ACSF: 4.065 ± 0.415 Hz, PBN: 2.16 ± 0.424 Hz; p value= 0.041, n = 5 per condition. Fig. 7D). However, we observed that sIPSCs frequency was significantly lower when ADO was applied in the presence of PBN (PBN: 2.16 ± 0.424 Hz, PBN + ADO: 1.425 ± 0.287 Hz; p value= 0.024, n = 5 per condition, Fig. 7D). The amplitude of sIPSC was decreased in the presence of PBN compared with basal condition (ACSF: 34.75 ± 2.27 pA, PBN: 25.654 ± 1.627 pA; p value= 0.027, n = 5 per condition, Fig. 7D), but remains unchanged when ADO was applied (PBN: 25.654 ± 1.627 pA, PBN + ADO: 23.95 ± 1.156 pA; p value= 0.061, n = 5, Fig. 7D).

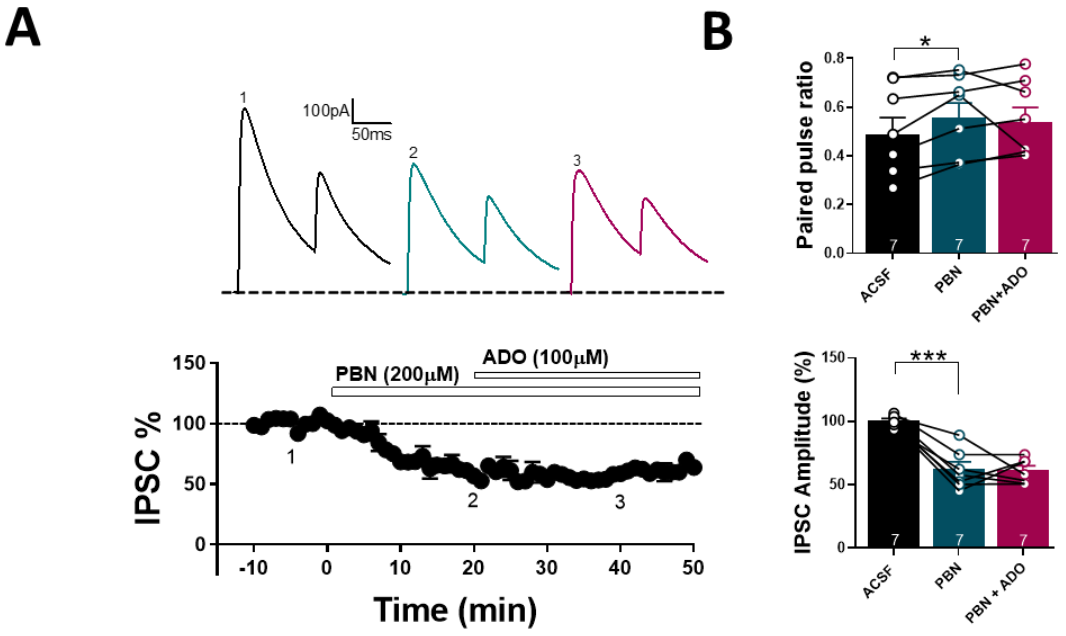

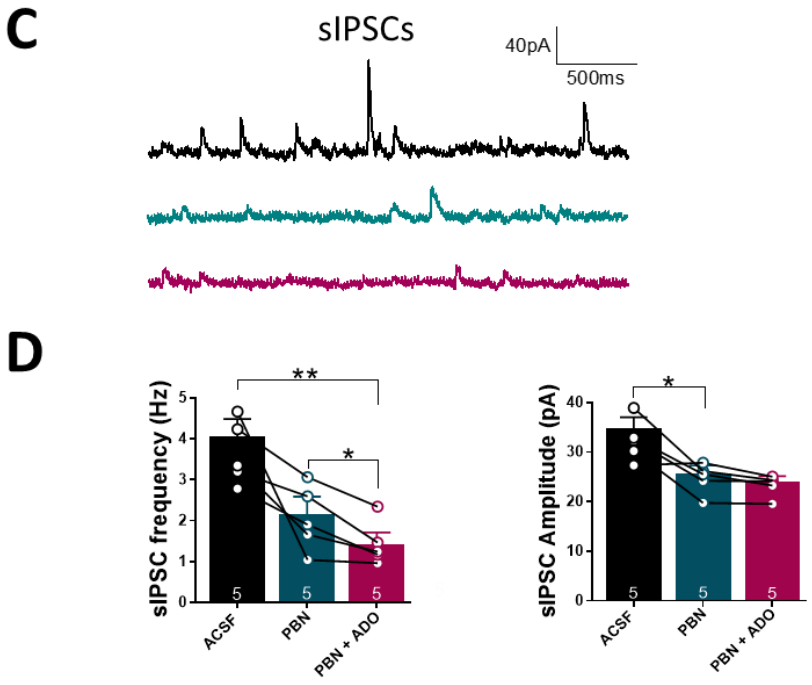

Figure 7: Adenosine application cannot revert PBN-mediated depression in GABAergic efficacy on pyramidal neurons in mouse hippocampus. A) Samples traces from evoked IPSCs and PPR for each condition (top). Temporal course showing the changes in the IPSC amplitude before, during and after PBN (200µM) and ADO (100µM) application (bottom). **B)** Application of PBN showed an increase of PPR at 100 ms intervals compared to the ACSF group. In the presence of PBN, bath application of ADO also induced an increase in the PPR compared with PBN and ACSF condition (top). IPSC amplitude was significantly decreased with bath application of PBN (bottom). ADO application in the presence of PBN had no effect in the IPSC amplitude, compared with PBN condition (bottom). **C)** Representative sample traces showing sIPSCs recorded for ACSF, PBN and PBN+ADO conditions. **D)** Quantitative analyses showed that PBN induced a significant decrease in the frequency of sIPSCs (left) and sIPSCs amplitude (right). In the presence of PBN, application of ADO decreased the frequency of sIPSCs (left), but the amplitude of sIPSCs was unchanged (right). Data are performed as mean ± SEM . *p<0.05. Number of recorded cells is indicated within bars**.**

We next explored whether ADO could prevent the PBN-mediated depression in GABAergic efficacy. To address this, we applied 100 µM ADO for 20 minutes. We observed that ADO did not affect the eIPSCs amplitude compared with baseline (ACSF: 100.42 ± 2.589 %, ADO: 102.43 ± 10.32 %; p value = 0.8190, n = 5 per condition, Fig. 8A-B). After that, we applied PBN, but IPSCs amplitude was unchanged by PBN in presence of ADO (ADO: 102.43 ± 10.32 %, ADO + PBN: 91.705 ± 14.504 %; p value= 0.257, n = 5 per each condition, Fig. 8A-B). Moreover, we found that ADO application increased significantly the PPR respect to control group (ACSF: 0.617 ± 0.047, ADO: 0.699 ± 0.040; p value= 0.0009, n = 6 per condition, Fig. 8B). Under these conditions, PBN application was unable

to modify the PPR value (ADO: 0.699 ± 0,040, ADO + PBN: 0.689 ± 0.043; p value= 0.8536, n = 6, Fig. 8B). Because data have been pointing to a predominant and direct effect of ADO on excitatory transmission (Rombo et al., 2016; Yoon et al., 1991; Lambert et al., 1991), we also study the effect of ADO application on excitatory postsynaptic currents eEPSCs. We found that ADO decreased the amplitude of eEPSCs compared with baseline (ACSF: 99.75 ± 1.27%, ADO: 30.70 ± 17.00%; p = 0.0513, n = 3; Fig. 8C), which was accompanied with an increase in the PPR (ACSF: 0.96 ± 0.23, ADO: 1.57 ± 0.21; p = 0.0759, n = 3; Fig. 8D).

Taken together, these results suggest that changes in probability of GABA release induced by PBN, and ADO could be occluding each other.

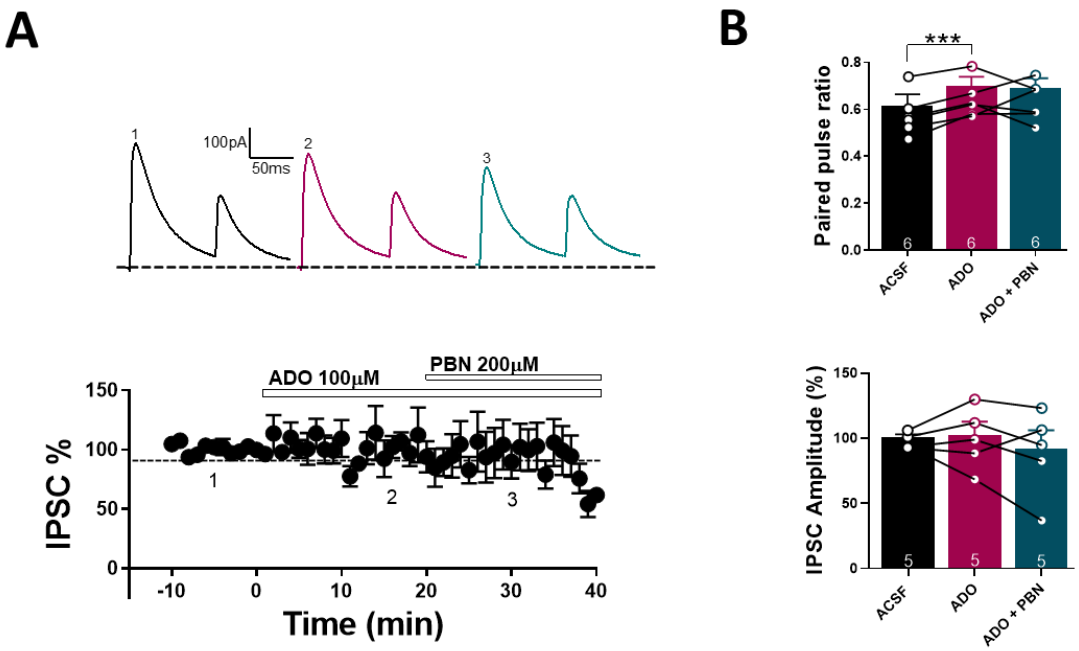

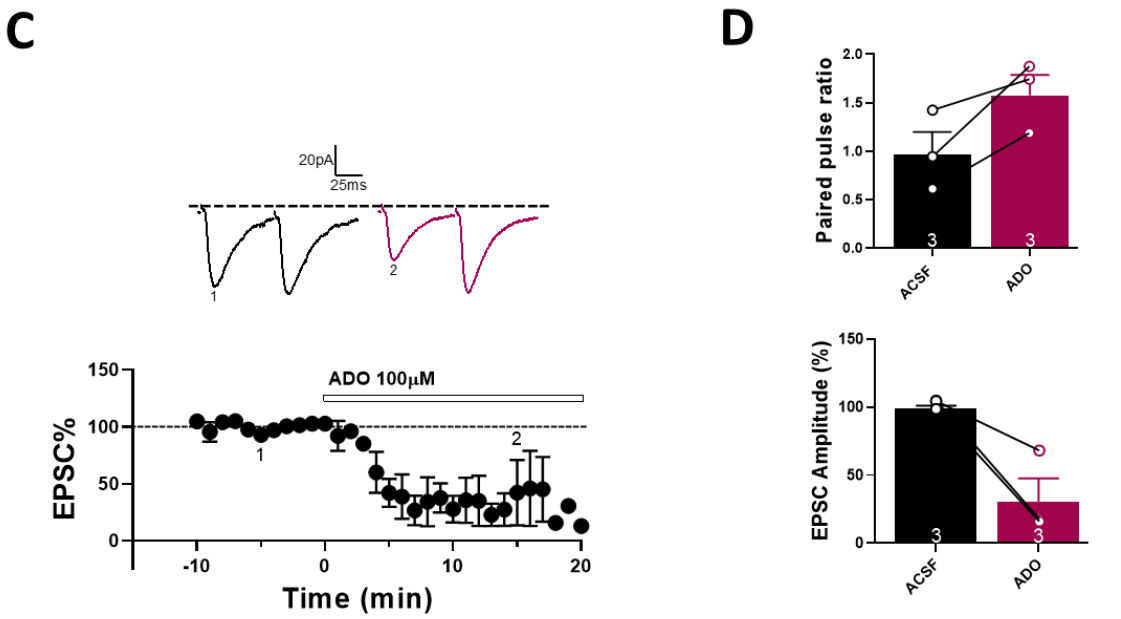

Figure 8: Previous application of adenosine occludes PBN-mediated depression in GABAergic efficacy onto pyramidal neurons of mouse hippocampus. A) Samples traces from evoked IPSCs and PPR for each condition (top). Temporal course showing the changes in the IPSC amplitude before, during and after ADO (100µM) and PBN (200µM) application (bottom). **B)** Application of ADO showed a significant increase of PPR at 100 ms intervals compared to the ACSF group. In the presence of ADO, bath application of PBN had no effect in the PPR compared with ADO and ACSF condition (top). IPSC amplitude was unaffected by ADO and PBN application compared with basal condition (bottom). **C)** Temporal course showing the changes in the EPSC amplitude before and after ADO (100µM) application. **D)** Application of ADO showed a decrease in EPSC amplitude compared with basal condition (bottom), while PPR was increased in the presence of ADO (top). Data are performed as mean ± SEM . *p<0.05. Number of recorded cells is indicated within bars.

The most studied metabolite released across the Panx1 channels is ATP (Bao et al., 2004), which can then act at the synapses and modulate synaptic transmission through their activity on purinergic receptors located pre- or post-synaptically (Kato et al., 2004). Thus, we investigate whether ATP-related signaling could be involved in the PBN-induced depression of GABAergic efficacy. In accordance with our previous results, PBN application caused a significant decrease in eIPSCs (ACSF: 100.01 ± 0.16 %, PBN: 68.36 ± 5.25 %, p value= 0.00; n = 6 per condition. Fig. 9C) and an increase in the PPR (ACSF: 0.581 ± 0.038, PBN: 0.654 ± 0.031; p value= 0.011, n = 6 per condition, Fig. 9B) compared with basal condition. In the presence of PBN, we applied ATP (250µM) directly on the hippocampal slice and we analyzed only short-term synaptic plasticity, because ATP is rapidly hydrolyzed into adenosine. The PPR remained unchanged when we applied ATP in the presence of PBN (PBN: 0.654 ± 0.031, PBN + ATP: 0.668 ± 0.058; p value= 0.7160, n = 6 for each condition, Fig. 9B). We also analyzed the PPR post ATP application, however it was still unaltered (PBN: 0.654

± 0.031, post ATP: 0.642 ± 0.037; p value= 0.5123, n = 6 per condition, Fig. 9B). All together these data indicate that PBN-mediated depression in GABAergic efficacy does not involve ATP/Adenosine signaling.

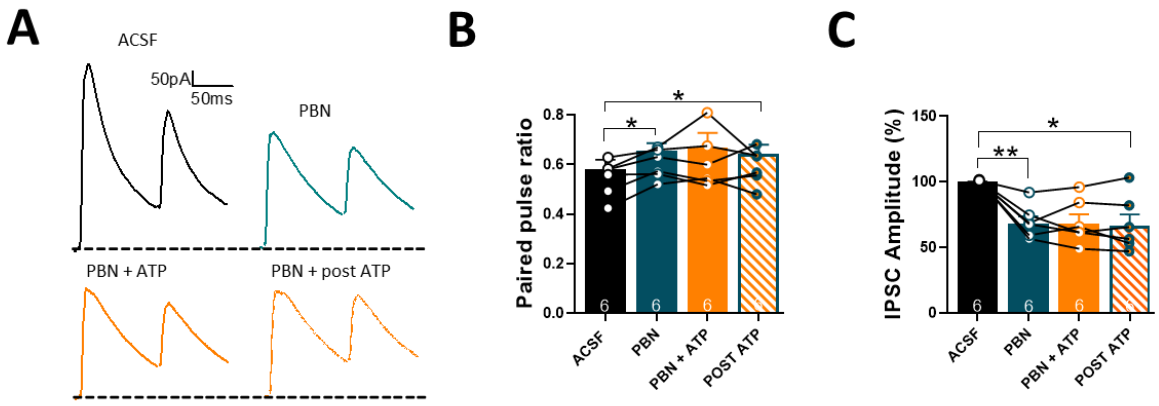

Figure 9: ATP application cannot revert PBN-mediated depression in GABAergic efficacy onto pyramidal neurons. A) Samples traces from evoked IPSCs and PPR for each condition (left). **B)** Application of PBN showed an increase of PPR at 100 ms intervals compared to the ACSF group (turquoise bar). In the presence of PBN, direct application of ATP 500nM on the hippocampal slice, had no effect in the PPR compared with PBN condition (orange bar). The PPR remains unchanged after ATP application in the presence of PBN. **C)** IPSC amplitude was significantly decreased with bath application of PBN (turquoise bar). Direct application of ATP on the slice had no effect in the IPSC amplitude, compared with ACSF and PBN condition. Data are performed as mean ± SEM . *p<0.05. Number of recorded cells is indicated within bars.

1.3) Determine the mechanism involved in changes of inhibitory transmission during Panx1 blockade.

The data presented in this work show that block of Panx1 decreases GABAergic efficacy onto CA1 PyNs in mouse hippocampus. This form of synaptic plasticity occurs at the pre- and postsynaptic level. At presynaptic compartment is expressed by modifications in probability of GABA release, while postsynaptically is expressed by changes due to long-lasting depression in amplitude of eIPSCs. Now, we want to determine the signaling pathways and mechanism involved in the block of Panx1-mediated depression of inhibitory transmission.

The blockade of Panx1-mediated depression of inhibitory transmission requires the activation of CB1 receptor and presynaptic cAMP/PKA pathway.

Because population of GABAergic interneurons in hippocampus is widely heterogeneous, we focused to study with pharmacological approach the two major perisomatic-targeting interneurons in CA1

PyNs, Parvalbumin (PV)- or Cholecystokinin (CCK)- containing interneurons, to elucidate whether 10panx-induced depression in GABAergic efficacy onto PyNs is interneuron specific.

PV+ basket cells interneurons also called fast-spiking basket cells, play a key role in regulating the hippocampus and prefrontal cortex activity by controlling output of pyramidal cells (Armstrong & Soltesz, 2012; Udakis et al., 2020). PV+ cells express presynaptic μ-opiate receptors (MOR), which is Gi-protein coupled and thus contribute to hyperpolarizing GABAergic interneurons (Svoboda & Lupica, 1998; Wimpey & Chavkin, 1991). It has been reported that MOR activation disinhibits principal cells by decreasing GABA release onto CA1 PyNs (Cohen et al., 1992; Shao et al., 2020). Therefore, we investigated whether GABA release from PV interneurons is implicated in the effect of 10panx. To address this, we added a specific MOR agonist, DAMGO (3μM) and 15 minutes later we applied 10panx. We previously evaluated the effect of DAMGO in basal GABAergic transmission. We found that DAMGO application significantly decreased GABAergic efficacy, because a significant decrease in eIPSCs amplitude (ACSF: 97.13 ± 1.37%, DAMGO: 57.96 ± 3.37%; $p = 0.028$, $n = 4$, Fig. S1) and in probability of GABA release were observed (ACSF: 0.43 ± 0.08, DAMGO: 0.60 ± 0.11; $p = 0.0206$, $n = 4$, Fig. S1). On the other hand, in the presence of DAMGO application of the inhibitor peptide of Panx1, 10panx (100μM) had no effect on PPR (ACSF+DAMGO: 0.68 ± 0.07, DAMGO+10panx: 0.69 ± 0.06; $p = 0.95$; $n = 7$ per condition, Fig. 10B). Also, in the presence of DAMGO, eIPSC amplitude was unaffected by 10panx (ACSF+DAMGO: 103.59 ± 4.49%, DAMGO+10panx: 94.92 ± 13.68%; $p = 0.51$, $n = 6$ per condition, Fig. 10A-B). These results suggest that 10panx-mediated depression in inhibitory efficacy could be involve GABA release from PV+ interneurons, but a specific experimental approach will be required to confirm this idea.

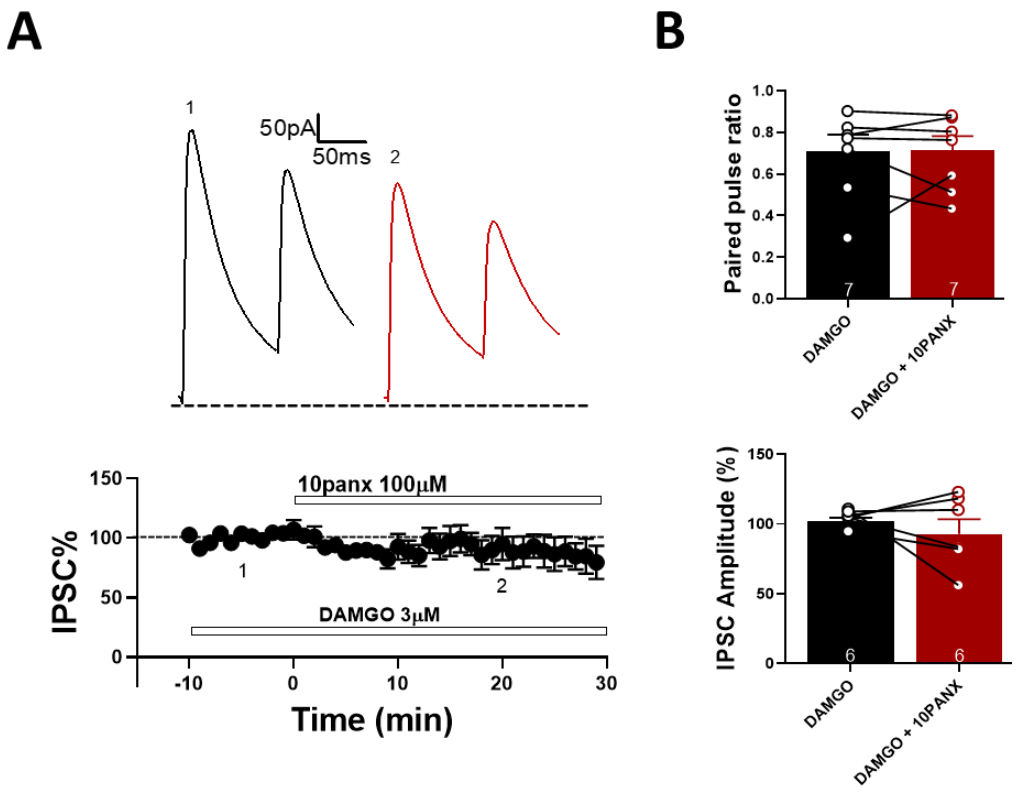

Figure 10: 10panx-induced depression involves µ-opiod receptors signaling. A) Representative samples traces from evoked IPSCs and PPR for each condition (top). IPSC% vs time plot before and after 10panx addition in the presence of agonist of µ-opiod receptors, DAMGO 3µM (bottom). **B)** PPR was not changed with DAMGO preincubation and after 10panx application (top). Slices pretreated with DAMGO did not show changes in the IPSC amplitude with 10panx application (bottom). Data are performed as mean ± SEM . *p<0.05. Number of recorded cells is indicated within bars.

On the other hand, we also studied the participation of CCK-containing interneurons in the depression of GABA transmission by Panx1 blockage. CCK basket cells are also called regular-spiking basket cells, which express cannabinoid receptors (CB1Rs) and thus respond to eCBs. Increasing evidence supports that eCBs act as mediators of synaptic plasticity (Chevaleyre et al., 2006; Chevaleyre & Castillo, 2003). One of the clearest examples of presynaptically form of LTD in the brain is mediated by eCBs, where postsynaptic activity releases eCBs, which travel toward presynaptic terminal to activate CB1R, a Gi/o protein coupled, thereby suppressing neurotransmitter release (Castillo, 2012; Chevaleyre et al., 2006).

The decreased frequency of spontaneous activity and in GABA release induced by 10panx, raised the question of whether CB1Rs could be involved in the effect of block Panx1 in GABAergic transmission. To evaluate eCBs signaling we first recorded inhibitory currents in the presence of

AM251 (5μM), an inverse agonist of CB1Rs. We found that AM251 had no effect in basal GABAergic efficacy, because both eIPSC amplitude (ACSF:102.85 ± 0.75%, AM251: 100.14 ± 8.71%; p = 0.7669, n = 5 per condition. Fig. 11A-B) and PPR (ACSF: 0.68 ± 0.05, AM251: 0.67 ± 0.04; p = 0.6466, n = 5; Fig. 11B) remained unchanged compared with baseline. Next, under this condition we applied 10panx (100μM). In pretreated slice with AM251 (5 μM), bath application of 10panx failed to change both the eIPSC amplitude (AM251: 100.70 ± 1.22%; AM251+10panx: 103.44 ± 13.41%; p = 0.8503, n = 6 per condition. Fig.11A-B) and PPR (AM251: 0.644 ± 0.04, AM251+10panx: 0.66 ± 0.06; p = 0.6610, n = 6. Fig. 11B).

In addition, we also tested AM251 at 20μM. Under this concentration, bath application of 10panx also was unable to change eIPSCs amplitude (AM251: 99.031 ± 1.109%, AM251+ 10panx: 91.64 ± 7.91%; p = 0.4087; n = 7 per condition, Fig. S3). The PPR also remained unaffected with application of 10panx in the presence of AM251 20μM (AM251: 0.536 ± 0.07, AM251+ 10panx: 0.517 ± 0.07; p = 0.2641; n = 7 for each condition, Fig. S3).

Because the activation of presynaptic CB1R inhibit the GABA release in CA1 inhibitory synapses, we reasoned that if CB1R activation is required to induce the Panx1 blockage-dependent inhibitory depression, this effect should be occluded by the exogenous cannabimimetic and CB1R agonist, WIN 55,212,2 (WIN). GABAergic efficacy was decreased after WIN (5μM) application compared with basal condition (eIPSC amplitude: ACSF: 99.64 ± 0.99%, WIN: 79.89 ± 4.87%; p = 0.0035, n = 9. Fig. S3/ PPR ACSF: 0.54 ± 0.03, WIN: 0.66 ± 0.05; p = 0.0106, n = 9. Fig. S3).

We observe that pretreated slice with WIN (5μM) completely occluded the 10panx-mediated GABAergic depression. In the presence of WIN, bath application of 10panx had no effect in both eIPSCs amplitude (WIN: 99.283 ± 1.787%, WIN ± 10panx: 103.983 ± 13.76%; p = 0.742; n = 6 for each condition, Fig. 11C-D) and PPR (WIN: 0.722 ± 0.08, WIN + 10panx: 0.692 ± 0.04; p = 0.621; n = 6 for each condition, Fig. 11D).

These results indicate that CB1R-expressing interneurons (CCK+ interneurons) also are involved in the 10panx-mediated depression of GABAergic efficacy onto PyNs.

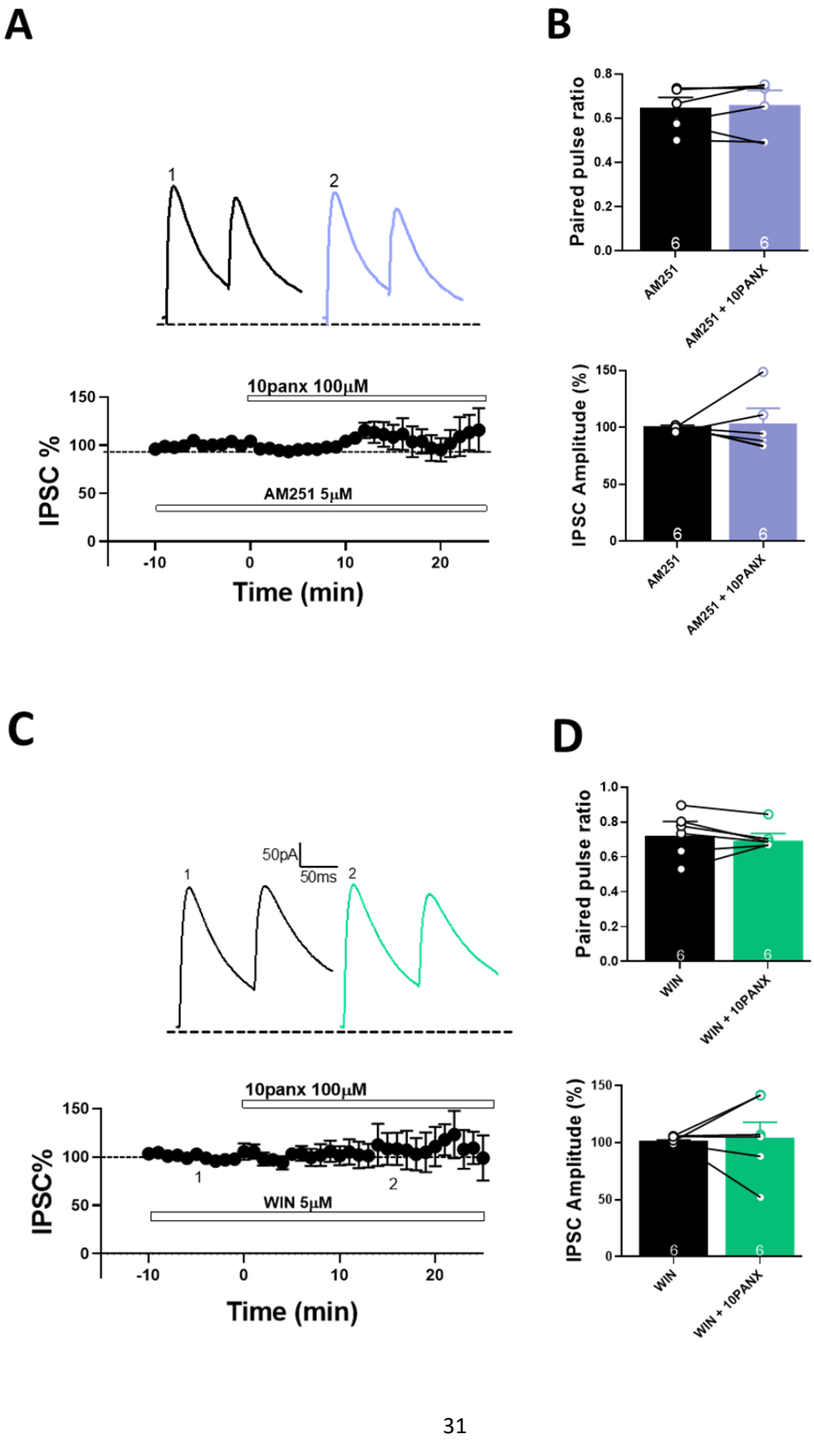
A
B
1
2
10panx 100μM
AM251 5μM
IPSC %
Time (min)
Paired pulse ratio
AM251
AM251 + 10PANX
IPSC Amplitude (%)
C
D
50pA
50ms
WIN 5μM
IPSC%
WIN
WIN + 10PANX

Figure 11: The blockage Panx1-dependent depression of inhibitory transmission requires the activation of CB1 receptors. A) Samples traces from evoked IPSCs and PPR for each condition (top). Temporal course showing IPSC% before and after 10panx application, in the presence of AM251 (bottom). **B)** Bath application of 10panx had no effect neither in the PPR (top) or in the IPSCs amplitude (bottom) when the slice was pretreated with AM251. **C)** Representative experiment for evoked IPSCs recorded for each condition (top). IPSC% vs time plot showing the changes in the IPSC% before, during and after 10panx application in the presence of WIN (bottom). **D)** Preapplication of WIN occluded the 10panx-mediated depression in the GABA release (top) and IPSC amplitude (bottom). Data are performed as mean ± SEM . *p<0.05. Number of recorded cells is indicated within bars.

The cAMP-PKA signaling pathway has been implicated in the regulation of synaptic plasticity in many brain regions. At hippocampal synapses have been demonstrated that activation of PKA potentiates inhibitory synaptic transmission and causes a presynaptic facilitation by directly increasing the probability of exocytosis (Capogna et al., 1995; Trudeau et al., 1996). On the other hand, it has been reported that eCB-mediated depression of GABAergic transmission involves downregulation of the cAMP/PKA/RIM1α pathway, which finally leads to a long-term decrease in GABA release (Chevaleyre et al., 2008). In accordance with our previous results that involved eCB signaling in the 10panx-caused decrease of GABAergic efficacy, we also evaluated whether cAMP/PKA pathway could be involved in this form of GABAergic synaptic plasticity.

We tested the participation of PKA in the GABAergic depression by perfusing the cell permeable protein kinase A inhibitor, H89 (10μM) and recording a baseline of eIPSCs and PPR. Bath application of H89 did not show a significant effect in the eIPSC amplitude (ACSF: 100.49 ± 1.49%, H89: 93.93 ± 10.05%; p = 0.5766, n = 5. Fig. S4), while a significant increase in the PPR compared with baseline was observed (ACSF: 0.50 ± 0.04, H89: 0.69 ± 0.04; p = 0.0370, n = 5. Fig. S4).

Afterthat, we added 10panx. In the presence of H89, 10panx had no effect in both eIPSCs (H89: 97.38 ± 1.36%, H89 +10panx: 80.09 ± 7.95%; p = 0.0806; n = 6 per condition, Fig. 12A-B) and PPR (H89: 0.69 ± 0.03, H89 +10panx: 0.70 ± 0.04; p = 0.5922; n = 6 per condition, Fig. 12B).

Due to H89 is a cell-permeant PKA inhibitor, its effect occurs in the pre and postsynaptic compartment. To study specifically a postsynaptic role of PKA in the effect of Panx1 blockage on GABA probability of release, we included a membrane-impermeable PKA inhibitor, PKI6-22 peptide (2,5 μM) in the internal recording solution, and then we applied 10panx in the bath. We found that blocking postsynaptic PKA did not affect the decrease of GABA release induced by the blockage of Panx1 (ACSF: 0.47 ± 0.04, 10panx: 0.56 ± 0.05; p = 0.049; n = 6 per condition, Fig. 12D). Nevertheless, the effect of 10panx in eIPSCs amplitude was blocked in the presence of PKI6-22 (ACSF: 98.76 ± 2.47%, 10panx: 102.16 ± 5.16%, p = 0.499, n = 6 per condition, Fig. 12C-D). Taken together, these results indicate that block of Panx1 with 10panx reduce GABAergic transmission,

which involved the activation of CB1R, a downregulation of presynaptic cAMP/PKA pathway, and postsynaptic PKA activity due to lack effect of 10panx in amplitude of eIPSCs in the presence of PKI6-22.

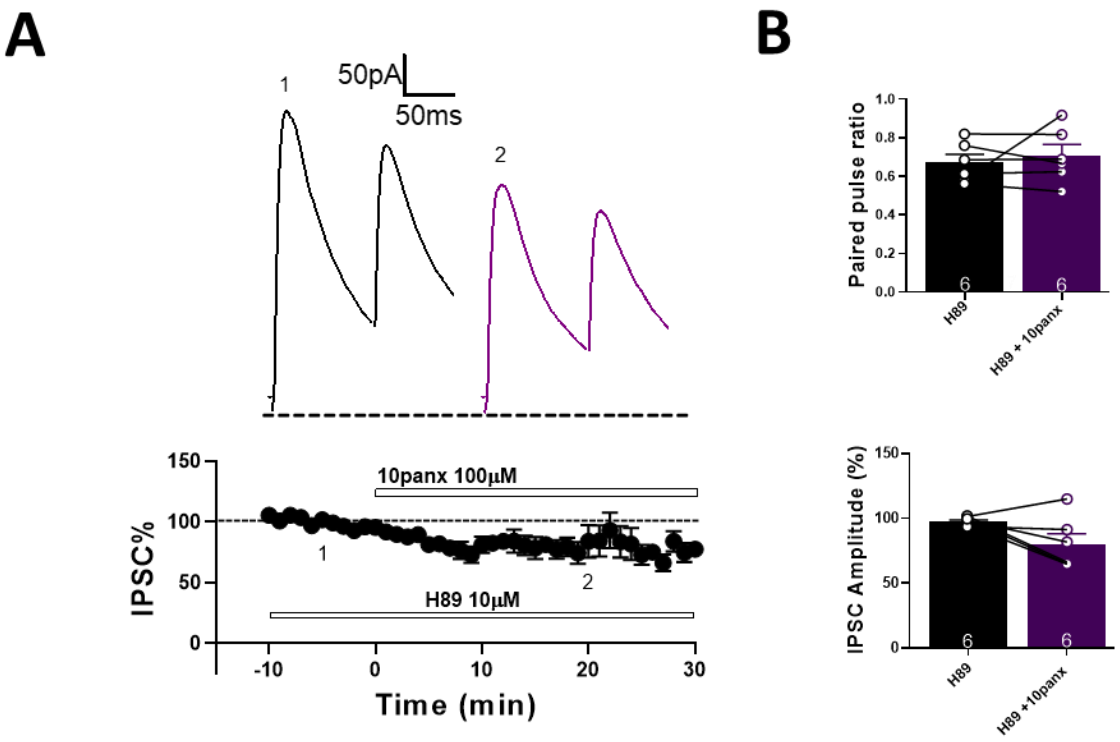

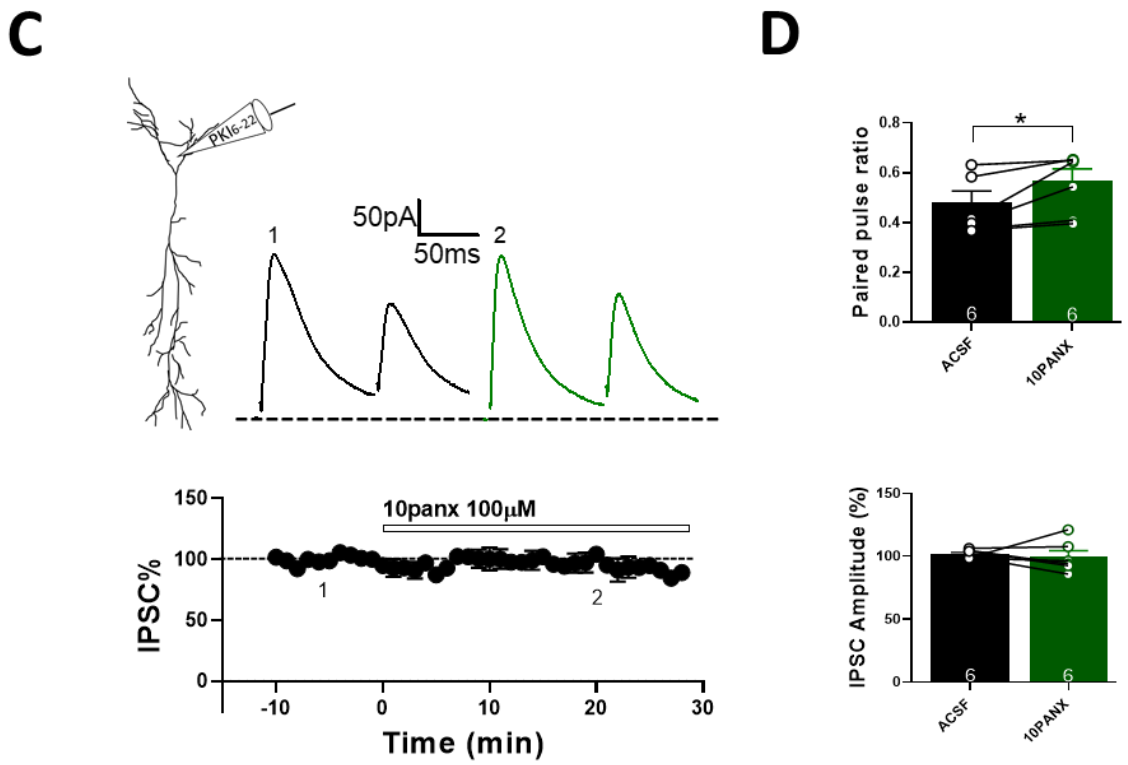

Figure 12: 10panx-mediated depression in GABA release requires presynaptic cAMP/PKA signaling. A) Samples traces from evoked IPSC and PPR for each condition (top). Temporal course showing the changes in the IPSC amplitude before, during and after 10panx (100µM) application with the presence of PKA inhibitor H89 (10µM) (bottom). **B)** H89 pre incubation blocked the10panx-induced increase in PPR (top) and had no significant effect in IPSC amplitude in the presence of 10panx (bottom). **C)** Representative traces from evoked IPSC and PPR for each condition with PKI_{6-22} peptide (2,5 µM)) loaded in the recording pipette. On the bottom is showed IPSC% vs time plot before and after 10panx addition with PKI_{6-22} peptide. **D)** Loading PKI_{6-22} peptide failed to block the 10panx-mediated increase in paired pulse ratio (top). 10panx had no effect in the IPSC amplitude in cells recorded with PKI_{6-22} peptide in the recording pipette (bottom). Data are performed as mean ± SEM . *p<0.05. Number of recorded cells is indicated within bars.

10panx-mediated depression of GABAergic efficacy requires a rise in postsynaptic Ca^{2+}

The release of eCBs occur mainly through two mechanisms: activation of G-protein coupled receptors or increase of intracellular Ca^{2+} (Chevaleyre & Castillo, 2003; Varma et al., 2001). To test whether postsynaptic G-protein activation was required for the 10panx-mediated depression in GABA release and eIPSCs, we included the irreversible G protein inhibitor GDP-βS (2 mM) in the recording pipette and then we applied 10panx. We found that after 10panx application the PPR was significantly increased (ACSF: 0.56 ± 0.02, 10panx: 0.64 ± 0,03; p = 0.0082; n = 6, Fig. 13B). This reduction in

GABA release was accompanied with a significant decrease in the eIPSCs amplitude in the presence of 10panx compared with basal condition (ACSF: 96.29 ± 0.97%, 10panx: 53.33 ± 6.29%; p = 0.0015, n = 6 per condition, Fig. 13A-B).

As described above, postsynaptic Ca^{2+} increase plays a main role in eCB signaling and eCB-dependent synaptic plasticity in the hippocampus (Ohno-Shosaku et al., 2001; Wilson & Nicoll, 2001). Therefore, we determine whether the postsynaptic calcium increase contributed to GABA depression when Panx1 was blocked. To address this, we added the calcium chelator, BAPTA (20mM) in the intracellular recording solution and under this condition we blocked Panx1. We found that 10panx application had no effect in the PPR in the presence of BAPTA compared with baseline (ACSF: 0.60 ± 0.01, 10panx: 0.68 ± 0.05; p = 0.1281; n = 7 per condition, Fig. 13D). eIPSCs amplitude also remained unchanged after bath application of 10panx (ACSF: 99.46 ± 1.22%, 10panx: 105.09 ± 10.25%; p = 0.5777; n = 7 per condition, Fig. 13C-D).

Together, these results suggest that 10panx-mediated GABAergic depression not involved postsynaptic G-protein but an increase of postsynaptic Ca^{2+} levels was required for the induction of GABAergic depression.

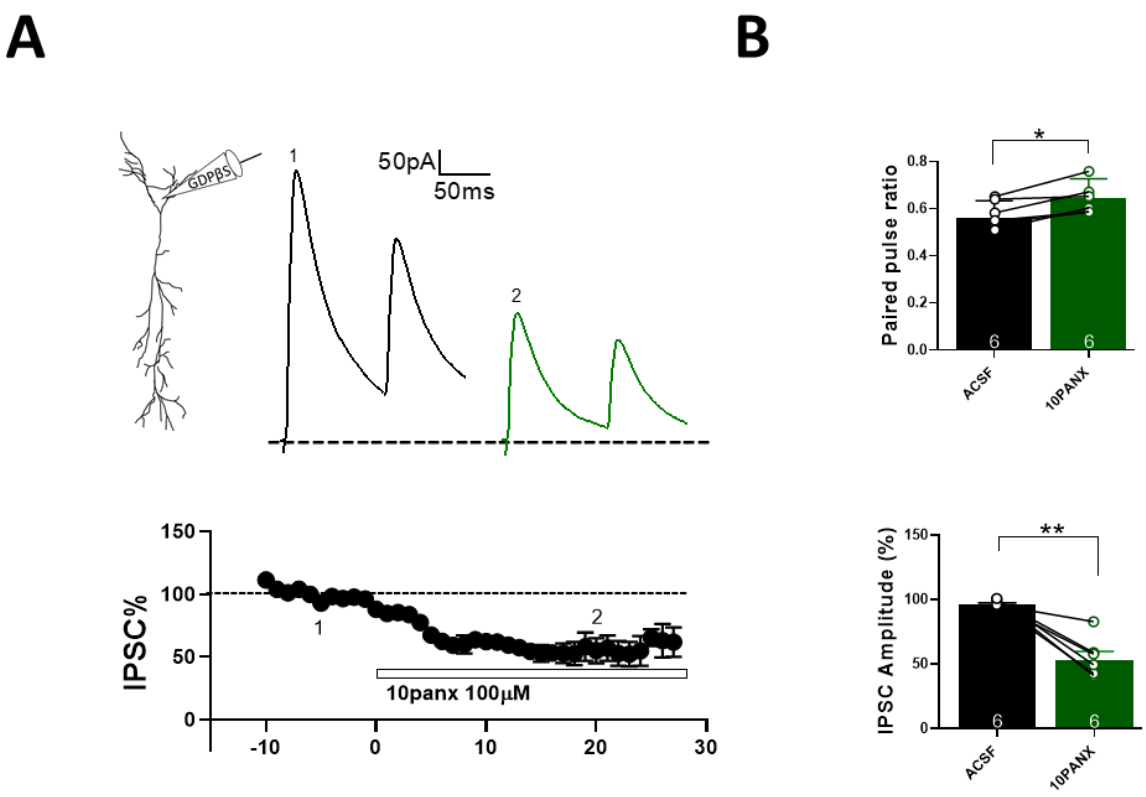

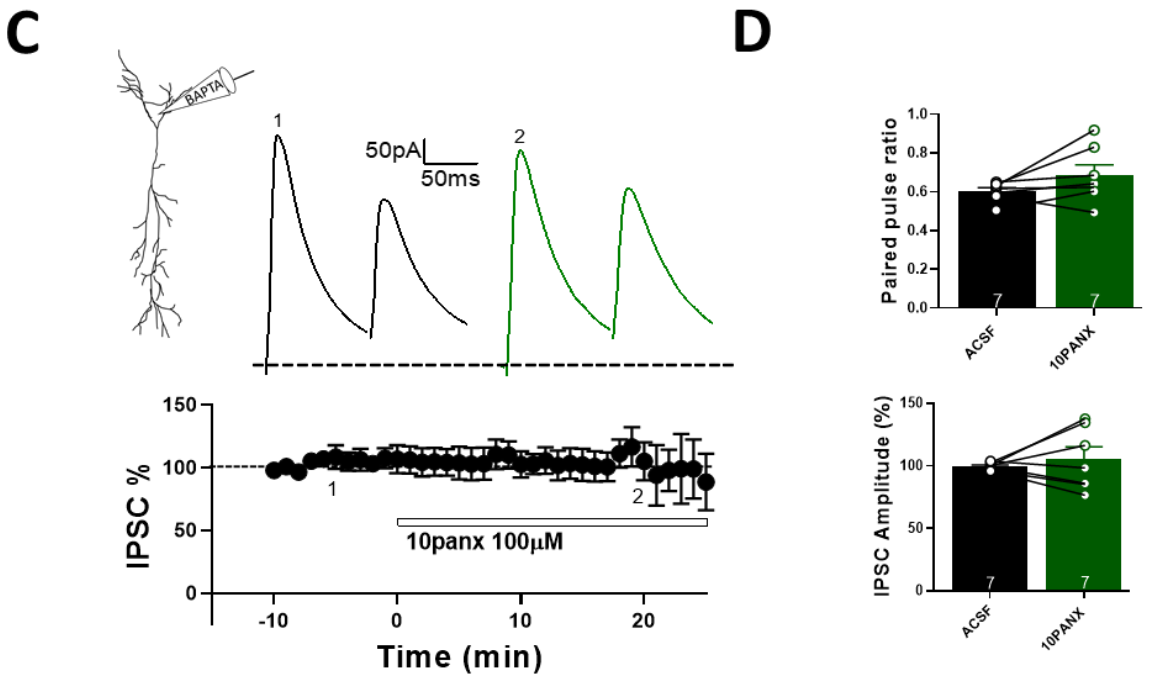

Figure 13: 10panx-induced depression requires postsynaptic Ca^{2+} levels, but not postsynaptic G-protein-coupled receptors activity. A) Samples traces from evoked IPSC and PPR for each condition (top). Temporal course showing IPSC% before, during and after 10panx with G-protein inhibitor GDP-βS (2mM) in the recording pipette (bottom). **B)** With GDP-βS, bath application of 10panx significantly increased PPR (top) and decreased IPSC amplitude (bottom). **C)** Samples traces from a CA1 neuron recorded with BAPTA in the recording pipette for each condition (top). Temporal course showing IPSC% before, during and after 10panx application in the presence of 20mM BAPTA in the patch pipette (bottom). **D)** 10panx application increased PPR in cells recorded with 20mM BAPTA in the recording pipette (top). 10panx-induced depression in the IPSC amplitude was blocked by 20mM BAPTA (bottom). Data are performed as mean ± SEM . *p<0.05. Number of recorded cells is indicated within bars.

We next focused to determine the Ca^{2+} source involved in the decrease of inhibitory efficacy due to Panx1 blockage. It is known that ischemia and prolongated NMDA exposure activate Panx1 channels (Weilinger et al., 2012). This form of Panx1 activation occurs downstream of metabotropic NMDAR activation and is mediated by sarcoma (Src) kinases (Weilinger et al., 2016). Due to the functional interaction between NMDAR and Panx1, we asked whether ionotropic glutamate receptors could be involved in the Panx1-dependent depression of GABAergic synaptic efficacy. Thus, we next investigated the effect of 10panx in the presence of NMDA and AMPA-receptor antagonists, D-AP5 (20µM) and CNQX (20µM) respectively. In the presence of D-AP5 and CNQX, bath application of 10panx induced a significant increase in the PPR (APV/CNQX: 0.50 ± 0.03, APV/CNQX+10panx: 0.62 ± 0.02; p = 0.0134; n = 7 per condition, Fig. 14B), which was accompanied by a robust decrease

in eIPSCs amplitude (APV/CNQX: 99.52 ± 0.99%, APV/CNQX+10panx: 76.37 ± 4.13%; p = 0.0024; n = 7 per condition, Fig. 14A-B). These results indicate that 10panx depresses GABAergic transmission in an independent form of NMDA and AMPA-receptors activation and postsynaptic Ca^{2+} required to this effect comes from another source.

It has been reported that L-type voltage-gated calcium channels (VGCC) play a main role in depolarization-mediated Ca^{2+} influx in CA1 PyNs (Raymond & Redman, 2006). Thus, we investigated if the Ca^{2+} rise that is required for the 10panx effect in GABAergic efficacy, occurs by Ca^{2+} influx through the L-type VGCC. We blocked L-type VGCC by bath application of nimodipine (NMD, 10 µM), which increased basal PPR of GABAergic transmission but had no effects in the amplitude of eIPSC (Fig. S6). Bath application of NMD prevented the induction of Panx1 block-mediated depression in inhibitory efficacy. We observed that PPR was unaffected by 10panx in the pretreated slice with NMD 10µM (NMD: 0.64 ± 0.06, NMD + 10panx: 0.62 ± 0.05; p = 0.3203, n = 6 for each condition, Fig. 14D) and eIPSCs amplitude also remained unchanged (NMD: 98.67 ± 1.07%, NMD + 10panx: 98.17 ± 11.78%; p = 0.9695; n = 6 per condition, Fig. 14C-D). These data indicate that the induction of 10panx-mediated depression in GABAergic efficacy requires a rise in postsynaptic intracellular Ca^{2+}, which is mediated mainly by influx through the L-type VGCCs.

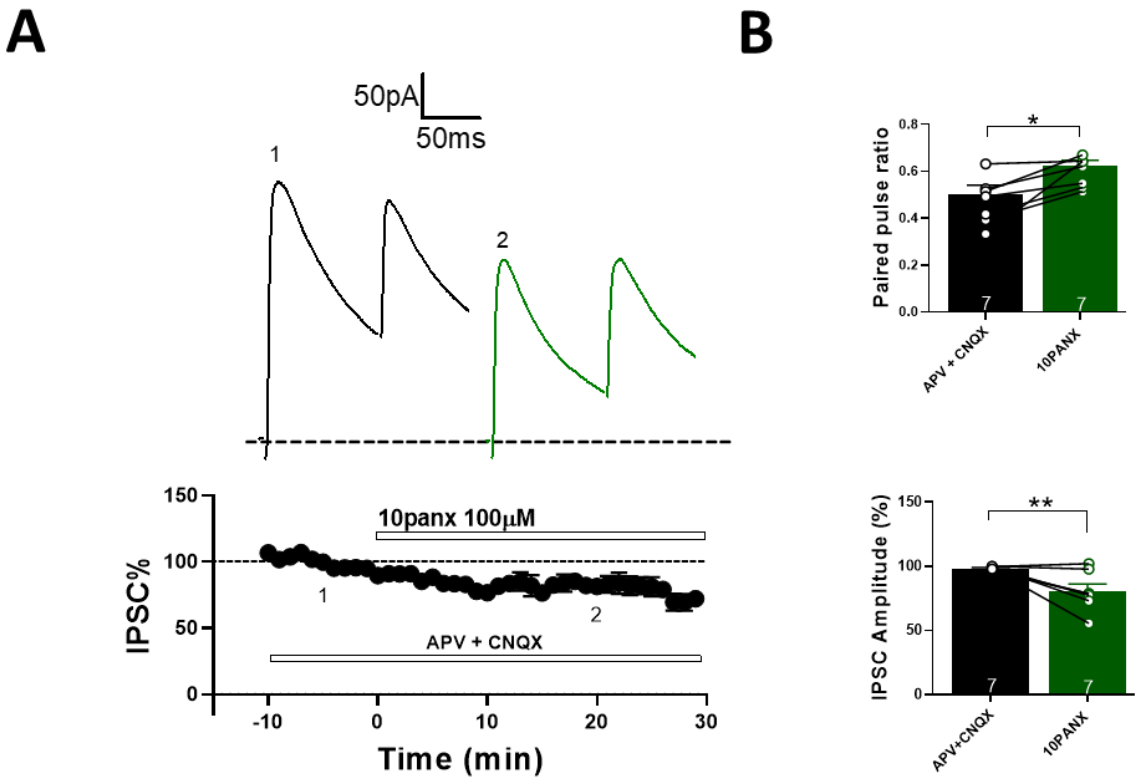

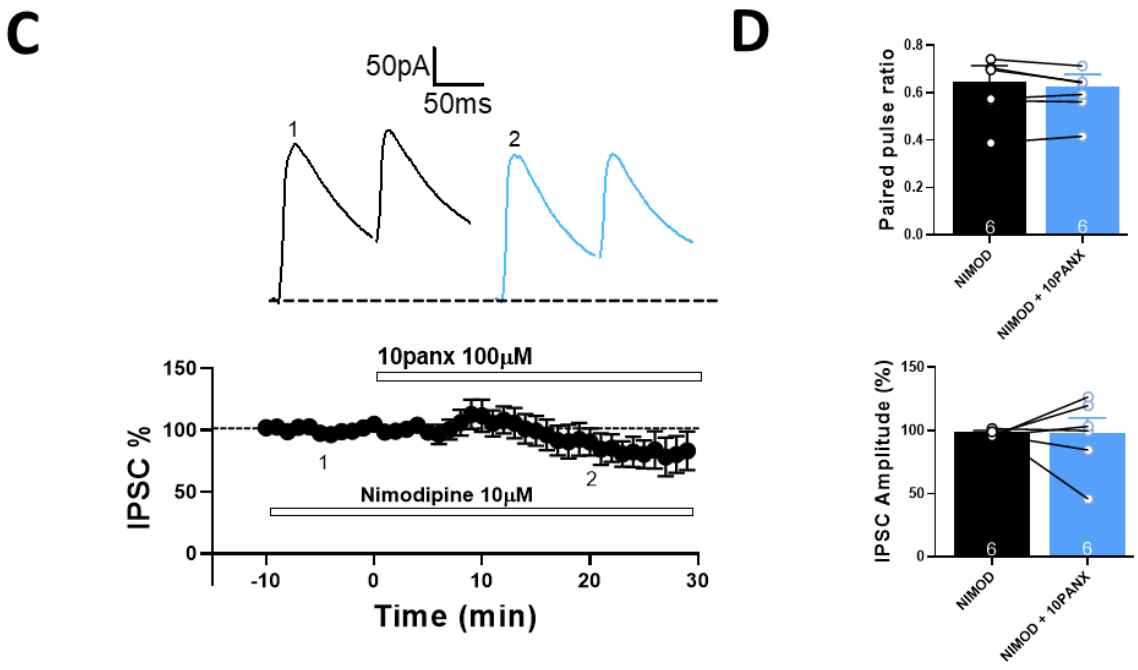

Figure 14: 10panx depressed GABAergic efficacy in an independent form of NMDA and AMPA-receptors activation but requires L-type VGCC activation as source of postsynaptic calcium. A) Samples traces from evoked IPSC and PPR for each condition (top). Temporal course showing the changes in the IPSC amplitude before, during and after 10panx (100µM) application in the presence of D-AP5 (20µM) and CNQX (20µM) (bottom). **B)** Application of 10panx showed a significant increase of paired pulse ratio (top) in the presence of APV and CNQX and it was accompanied of significant decrease in IPSC amplitude (bottom). **C)** Representative experiment of evoked IPSCs from CA1 neurons pretreated with Nimodipine 10µM (black) and after 10panx application (light blue)(top). IPSC% vs time plot showing the changes in the IPSC% before, during and after 10panx application in the presence of Nimodipine (bottom). **D)** Preapplication of Nimodipine occluded the 10panx-mediated depression in GABAergic efficacy because PPR (top) and IPSC amplitude were unchanged (bottom). Data are performed as mean ± SEM. * $p<0.05$. Number of recorded cells is indicated within bars.

The Panx1 blockage regulated the E/I ratio and threshold of synaptic plasticity in CA1 PyNs

The balance between excitation and inhibition is essential in the regulation of brain activity (Sohal & Rubenstein, 2019). Synaptic plasticity at both excitatory and inhibitory synapses is suggested to play a central role in balancing the excitatory and inhibitory inputs to a target cell during the learning process (Froemke, 2015; Rubin et al., 2017). As previously reported (Bialecki., et al. 2020), blocking Panx1 in single postsynaptic CA1 neurons produced an increase in glutamate release, which modify network excitability. In this work we have shown that Panx1 blockade induces depression of inhibitory transmission (see above), suggesting that Panx1 could be important for the appropriate E/I balance. To determine the effect of block of Panx1 in the E/I balance, we tested bath application of

10panx on paired compound AMPA-mediated EPSC and GABA-mediated IPSC, elicited by stimulation in stratum radiatum area and recorded in CA1 PyNs at -40mV in the presence of 20 µM APV, as previously reported (Nanou et al., 2018). This approach considers the synaptic input to the CA1 pyramidal neuron by the direct excitatory pathway and the indirect inhibitory pathway through interneurons activity to obtain the E/I ratio.

We found that in the presence of 10panx the E/I ratio was changed, showing an increase when Panx1 is blocked (Fig. 15). For basal condition, E/I ratio was 0.60 ± 0.15, while with 10panx its value was 1.43 ± 0.52 (p value= 0.0891, n = 7, Fig. 15A). The block of Panx1 considerably altered the E/I ratio in favor of excitation, but inhibitory component also was strongly decreased with 10panx, suggesting that Panx1 channels could be important to maintain an appropriate E/I balance in the hippocampal network.

Finally, we studied excitatory synaptic transmission when Panx1 was blocked. Excitatory postsynaptic currents (eEPSCs) were measured at -65mV. Bath application of 10panx (100µM) caused a significant increase in eEPSC amplitude compared with basal condition (ACSF: 104.33 ± 1.61%, 10panx: 193.25 ± 24.89%; p = 0.0196, n = 5 per condition, Fig. 15B-C). The CV value was significantly reduced in the presence of 10panx (ACSF: 0.26 ± 0.04, 10panx: 0.18 ± 0.02; p = 0.0432, n = 5; Fig. 15D), while PPR was no changed (ACSF: 1.61 ± 0.08, 10panx: 1.44 ± 0.08; p = 0.2891, n= 5 per condition, Fig. 15D).

Taken together all results strongly suggest that Panx1 is an important neuromodulator of hippocampal GABAergic transmission and network excitability, supporting an important role in brain plasticity and cognitive processes.

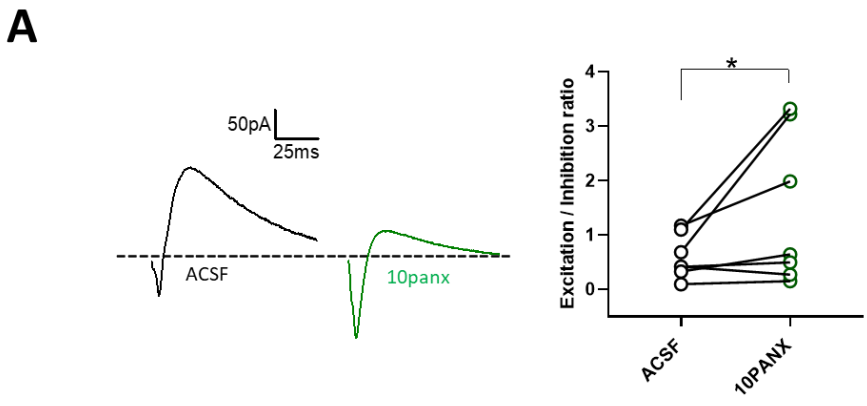

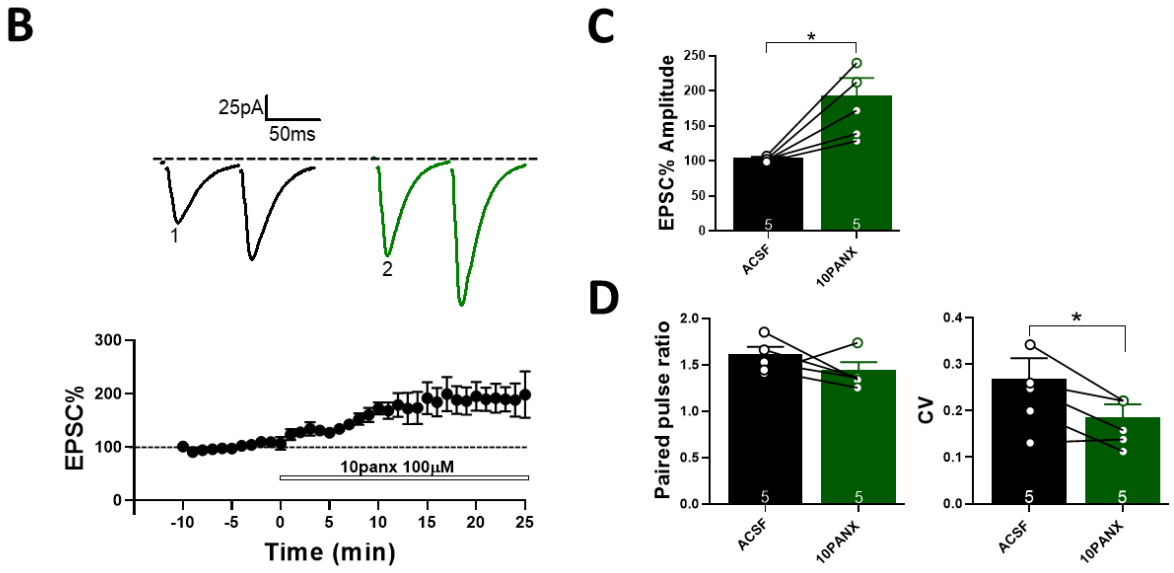

Figure 15: Block of Panx1 increases the excitation to inhibition ratio in CA1 pyramidal neurons of mouse hippocampus. A) Representative samples traces of recorded PSCs paired at -40mV, before and after 10panx application (left). E/I ratio calculated from peak amplitude either for GABAergic and glutamatergic component was increased in the presence of 100µM 10panx (right). **B)** Representative experiment of recorded eEPSCs for each condition (top). Temporal course showing changes in the eEPSCs amplitude before and after 10panx application (bottom). **C)** Bath application of 10panx (100µM) induced a significant increse in the eEPSCs amplitude. **D)** 10panx had no effect in the PPR value (left), but CV showed a significant decrease (right). Data are performed as mean of E/I ratio before and after 10panx addition. *p < 0.05. Number of cells is indicated within graph.

Future directions

In addition to this neuronal expression, Panx1 is also expressed in glial cells, including astrocytes. Astrocyte processes exhibit localized and temporal increases in intracellular calcium levels in response to adjacent synaptic activity (Bazargani & Attwell, 2016). In consequence astrocytes can regulate excitability and plasticity through the release of glutamate, ATP, and D-serine (gliotransmitters). It has been reported that Panx1 are important for channel-mediated gliotransmitter release. In particular, Panx1 channels in complex with P2X7 receptor has been involved to facilitate the release of D-serine in response to ATP (Pan et al., 2015). Astrocyte Panx1-dependent ATP release has been shown to act on peri-synaptic P2X receptors, which leads to their migration to the postsynaptic density and their subsequent down-regulation of NMDARs (Lalo et al., 2016).

Given that astrocytes modulate synaptic transmission and due to astrocytic Panx1 is involved in gliotransmitter release, we studied whether astrocytic signaling could be involved in the depression of GABAergic efficacy induced by PBN. First, we used a transgenic mouse knock out for IP3R2 in astrocytes (IP3R2 -/-), which shows a weakened Ca^{2+} signaling in astrocytes (Mederos et al., 2019; Sherwood et al., 2017; Srinivasan et al., 2015). Under this condition, we blocked Panx1 with PBN (200µM). Bath application of PBN caused a significant decrease in eIPSCs amplitude in hippocampal slices from IP3R2 -/- mouse (ACSF: 96.21 ± 2.38%, PBN: 69.54 ± 9.19%; p = 0.0240; n = 11 per condition, Fig. 16A-B), which is comparable with its effect in WT mouse (Fig.). Conversely, PPR value remained unchanged in the presence of PBN (ACSF: 0.827 ± 0.02, PBN: 0.824 ± 0.03; p value= 0.905, n = 11 per condition, Fig. 16B), which suggest that astrocytic activity could be involved in the effect of PBN in GABA release.

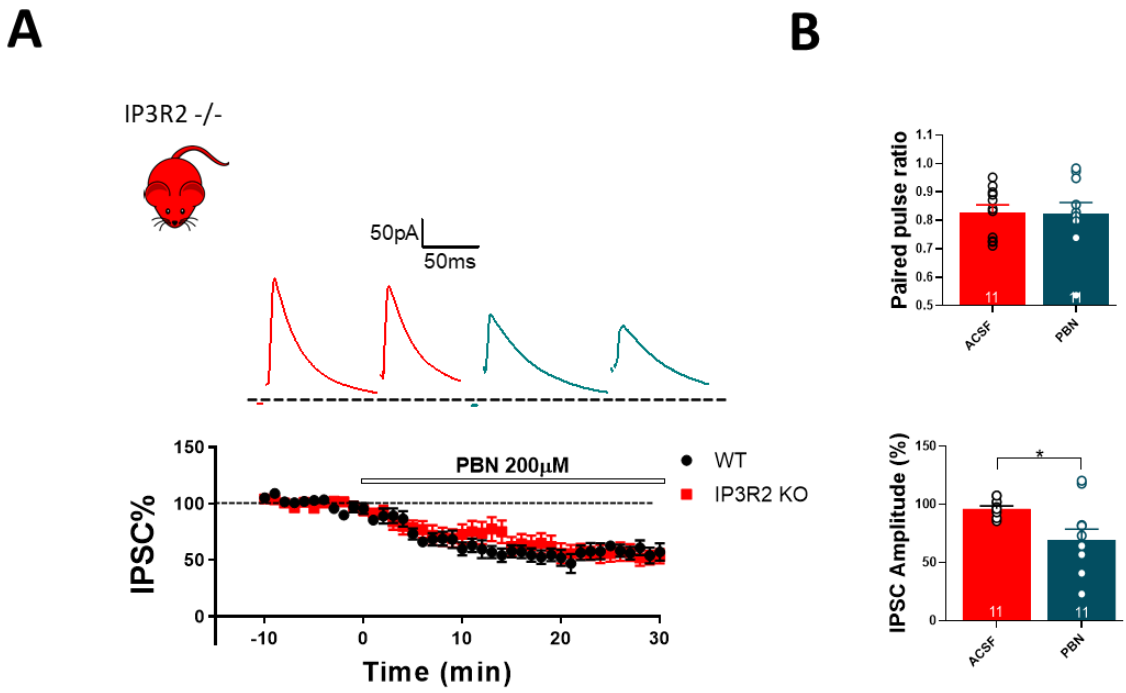

Figure 16: Block of Panx1 with PBN decreases amplitude of GABAergic currents onto pyramidal cells from hippocampal slices of IP3R2 -/- mouse. A) Samples traces from evoked IPSCs and PPR for each condition (top). Temporal course showing the changes in the IPSC amplitude before, during and after PBN (200µM) application in hippocampal slice of wt mouse (black) and IP3R2 -/- mouse (red). **B)** Application of PBN had no effect in the PPR at 100 ms intervals compared to the ACSF condition (top) in pyramidal neurons from IP3R2 -/- mouse. While eIPSCs amplitude was significantly decreased with bath application of PBN (bottom) in hippocampal slice of IP3R2 -/- mouse. Data are performed as mean ± SEM . *p<0.05. Number or recorded cells is indicated within bars.

On the other hand, by using an optogenetic approach we precisely stimulated Ca^{2+} signaling in astrocytes (Mederos et al., 2019). It was achieved by selective expression of melanopsin in hippocampal astrocytes as previously reported Mederos et al 2019. Melanopsin is a photopigment which couples to Gαq-11 to activate PLCβ, leading to the IP3 signaling and the elevation of intracellular Ca^{2+} levels (Panda et al., 2005). Mederos group showed that after ≥5s blue light (473nm) stimulation was observed a transient increase of synaptic strength of CA1 PyNs, therefore, we used this approach in our experiments. We targeted the rAAV5/GFAP104-melanopsin-mcherry virus to the astrocytes of CA1 area in hippocampus of adult mouse. After two weeks, we obtained hippocampal slices and we recorded eIPSCs. After baseline of eIPSCs, we stimulate melanopsin with blue light by 5s, at intervals of 10seg during 1min. We observed that optostimulation of astrocytes had no significant effect in both, the amplitude of eIPSCs (ACSF: 99.50 ± 2.82%, Opto. stim: 104.67 ± 16.47%; p = 0.7855, n = 6 for each condition, Fig. 17B-C) and PPR value (ASCF: 0.911 ± 0.03, Opto. stim: 1.051 ± 0.07; p = 0.0656, n = 6 per condition, Fig. 17C).

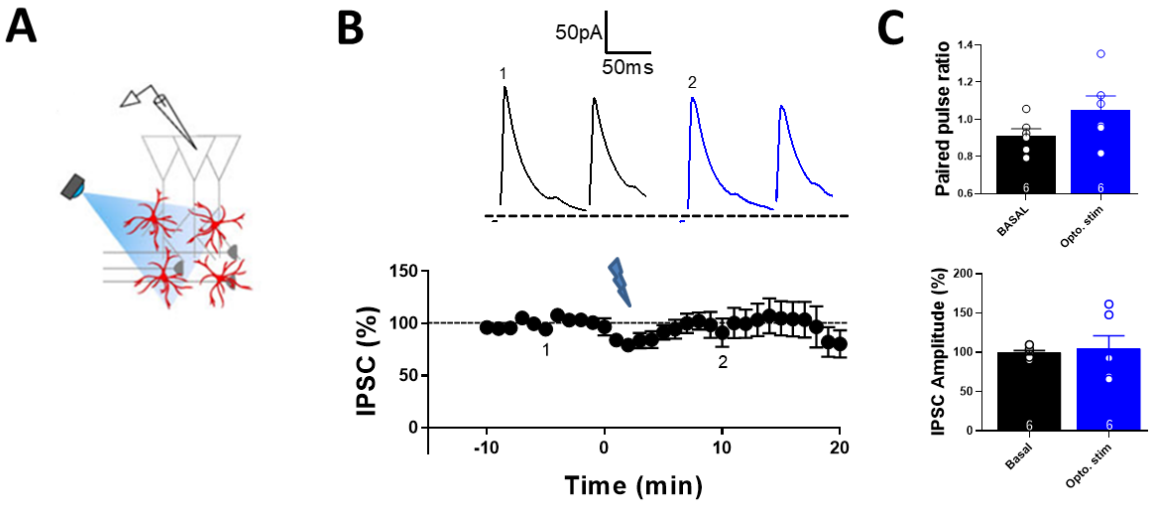

Figure 17: Selective activation of astrocytes did no change evoked GABAergic postsynaptic currents onto pyramidal neurons of mouse hippocampus. A) Schematic diagram showing both CA1 pyramidal neurons recording and optostimulation of astrocytes in hippocampal slice (modificado de Mederos et al., 2019). **B)** Samples traces from evoked IPSCs and PPR for each condition (top). Temporal course showing the changes in the eIPSCs amplitude onto PyNs before and after opto stimulation of hippocampal astrocytes in WT mouse. **C)** Light stimulation of astrocytes did not affect neither PPR (top) or eIPSCs amplitude onto PyNs in mouse hippocampus. Data are performed as mean ± SEM . *p<0.05. Number or recorded cells is indicated within bars.

Next, we evaluated whether astrocytes signaling activation could be involved in PBN-mediated depression of GABAergic efficacy onto PyNs. To address this, we recorded eIPSCs from PyNs in the

presence of PBN (200µM) and then we optostimulated astrocytes as described above. Our preliminary data showed that astrocytes stimulation was unable to change the amplitude of eIPSCs in the presence of PBN (PBN: 98.50 ± 2.10%, PBN + Opto. stim: 76.33 ± 20.14%; p = 0.3410, n = 5 for each condition, Fig. 18A-B), despite a decreasing trend. PPR value also remained unchanged after optostimulation of astrocytes in the presence of PBN (PBN: 0.861 ± 0.03, PBN + Opto. stim: 0.866 ± 0.03; p = 0.7677, n = 5 per condition, Fig. 18B).

All together these preliminary data suggest that astrocytic signaling could be implicated in block of Panx1-mediated GABAergic depression and open new questions about the role of Panx1 in modulation of synaptic transmission, now involving astrocytes activity but in a physiological context.

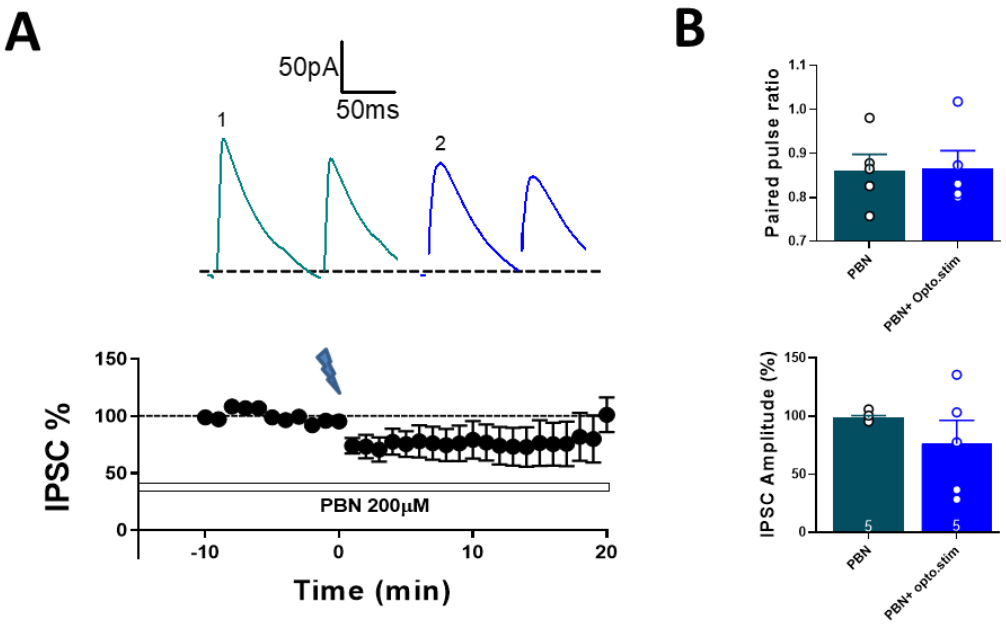

Figure 18: Selective activation of astrocytes signaling does not change GABAergic transmission in the presence of Panx1 blocker PBN. A). Representative experiment showing eIPSCs for each condition (top). Temporal course showing the changes in the eIPSCs amplitude onto PyNs before and after astrocytes activation in the presence of PBN (200µM) (bottom). **B)** Optostimulation of astrocytes did not affect neither PPR (top) or eIPSCs amplitude (bottom) onto PyNs in the presence of PBN (200µM) in mouse hippocampus. Data are performed as mean ± SEM . *p<0.05. Number or recorded cells is indicated within bars.

VIII. Discussion

Information processing within neuronal networks is established by a dynamic interaction between excitatory and local inhibitory interneurons. Like excitatory synapses, inhibitory synapses are also plastic, exhibiting changes in the strength of connectivity throughout the brain. Because of the crucial role of inhibitory synapses on regulating both excitability and timing of neuronal firing, changes in GABAergic efficacy can have important functional consequences. Despite the importance of modulation of the inhibitory transmission for normal network functioning, the precise involvement of mechanisms and neuromodulators that regulate inhibitory plasticity requires further studies.

In this report we demonstrate by the first time that neuronal Panx1 is an important modulator of hippocampal GABAergic synaptic transmission. We found that specific block of Panx1 with mimetic peptide, 10panx, decrease the GABAergic efficacy onto CA1 PyNs of mouse hippocampus. This form of synaptic depression involved a decrease in the probability of GABA release and in the amplitude of IPSCs, which suggests that 10panx-mediated reduction of the inhibitory synaptic transmission has a pre- and postsynaptic locus of expression.

In addition to its role in regulating neurite extension and synapse formation (Wicki-Stordeur & Swayne, 2013) several studies have linked Panx1 function to synaptic plasticity. Prochnow et al., (2012) showed that mouse lacking Panx1 (Panx1-/-) had enhanced excitability, persistent LTP responses and impaired spatial learning (Prochnow et al., 2012). Also, it has observed that eliminating or blocking Panx1 enhances LTP and prevents LTD induction in adult mouse (Ardiles et al., 2014) suggesting the involvement of Panx1 in modulating excitatory synaptic transmission. Given that excitability in the brain is highly dependent on the level of inhibition, it is reasonable to study GABAergic neurotransmission in lacking Panx1 mouse, considering the alterations in glutamatergic transmission in these mouse. Surprisingly, we did not observe significant changes in GABAergic transmission in Panx1 -/- mouse (Fig. 4F). In contrast to the other research of Panx1 -/- mouse in synaptic plasticity, we studied only short-term GABAergic transmission. Additional experiments involving long-term GABAergic plasticity protocols, or recording of eIPSCs by a long time, could be useful to study the effect of Panx1 absence on GABAergic neurotransmission. Currently, a better approach to study the lack of Panx1 is the conditional Panx1 KO mouse (Panx1fl/fl-wfs1-Cre), which allows to delete Panx1 channels at the required age for the experimenter (Bialecki et al., 2020, Weilinger et al., 2012) and rule out the possible compensatory effects in the mouse lacking Panx1 from birth.

Previous studies have shown that Panx1 is widely expressed in the postsynaptic density of hippocampal and cortical synapses but not at the presynaptic membrane (Zoidl et al., 2007). However, our recent preprint article showed that Panx1 also could be present in the presynaptic compartment. This observation was verified by isolating hippocampal synaptosomes and subsequent separation into PSD-enriched fractions and synaptic membranes avoided of PSD (SM), in which the presence of Panx1 was detected in both fractions, suggesting an expression at both presynaptic and postsynaptic levels (Flores-Muñoz C, García-Rojas F, and colls. 2022. Manuscript in revision). These findings contribute to explain our results, in which we found that the block of Panx1 reduces the GABA release probability and the amplitude of eIPSCs (Fig. 3), indicating changes at pre- and postsynaptic level.

In this line, by adding α-panx1 in the patch pipette, we demonstrate that inhibition of postsynaptic Panx1 is the key factor responsible to decrease in GABAergic synaptic activity, because while postsynaptic Panx1 was blocked, bath application of 10panx failed to change GABAergic efficacy. Moreover, α-panx1 by itself decreased GABAergic efficacy, compared with its negative control, α-Cx43 a member of the gap junction superfamily that is not expressed in neurons (Bialecki et al., 2020; Dermietzel et al., 1989). Altogether these results lead us to the questions: What changes take place at the pre and postsynaptic compartment after the block of Panx1? How these changes lead to a decrease of GABA release and in IPSCs amplitude?

In contrast to the characteristic paired-pulse facilitation of EPSCs, in the hippocampus the most of IPSCs show a robust paired-pulse depression (PPD) (Davis et al., 1990; Jiang et al., 2000). It has been demonstrated that basal release probability can affect the subsequent occurrence of PPF or PPD. The possible mechanisms underlying basal PPD of inhibitory synapses are that decreased amplitude of the second IPSC is due to a decrease in the quantal content (m), resulting from depletion of the readily releasable vesicle pool by the first stimulus (Debanne et al., 1996), or due to postsynaptic mechanism such as desensitization of GABAa receptors (Alger et al., 1991) that might explain the decrease in the second pulse-induced currents.

In our results the inhibitory synapses showed a basal PPD, which was increased when we applied 10panx, suggesting a decrease in GABA release probability (Fig. 3), which was also supported with a decrease in the frequency of sIPSCs and mIPSCs (Fig. 5). However, additional analyses by using CV parameter had no differences (Fig. 3). This method is a general standardized measure of dispersion of a probability or noise (Brock et al., 2020). Since the majority of the noise at a synapse is due to the stochastic nature of quantal neurotransmitter release (Otmakhov et al., 1993), modifications in noise as indicated by variations in the CV suggest a presynaptic locus of that change, for instance due to a change in release probability. However, this method involves several

assumptions and conditions, for instance that the quantal size q, should be uniform across all n release sites, which is difficult for inhibitory synapses, in which their synaptic contacts are distributed in the dendritic arbor, axon and at the perisomatic level (Pelkey et al., 2017). The assumptions in the use of CV to determine the locus of synaptic plasticity are more related with the characteristic of excitatory synapse. It is consistent with our results showing a significative decrease in the CV value of eEPSCs after application of 10panx (Fig. 15), which was accompanied with a decrease in PPR, whilst in eIPSCs we found an increase in PPR, but no change was found in CV. Because CV and PPR are indirect methods to evaluate changes in release probability (Faber et al., 1991; Brock et al., 2020), other protocols such as minimal stimulation (Jiang et al., 2000) could be complement the present findings.

A postsynaptic alteration that generates changes in short term plasticity as the probability of release, can also involve changes in the properties of postsynaptic receptors that contribute to short-term plasticity, such as saturation, desensitization or kinetic. We analyzed the kinetic in the inhibitory currents, specifically the time constant at both rise and decay phase (Tau rise and Tau decay respectively) of eIPSCs before and after 10panx application. We did not observe significative changes in rise (ACSF: 6.24 ± 0.96 ms, 10panx: 6.72 ± 0.74 ms; $p = 0.5299$, $n = 10$. Fig. S1) and decay time (ACSF: 92.84 ± 23.07 ms, 10panx: 105.65 ± 30.67 ms; $p = 0.4526$, $n = 10$. Fig. S1) of IPSC, which is related with deactivation and desensitization of postsynaptic receptor (Dawe et al., 2003). Receptor saturation can lead to a decrease in synaptic response amplitude (Foster et al., 2002; Blitz et al., 2004). It has been reported in the climbing fiber to Purkinje cell synapse, which is characterized by a high release probability, that the postsynaptic receptor saturation can acts jointly with presynaptic mechanism to produce highly reliable synapse. In addition, the authors reported that the postsynaptic receptor saturation was dependent of extracellular Ca^{2+} levels and that saturation level influences the PPR and the amplitude of postsynaptic currents (Foster et al., 2002). Since that by changing extracellular concentrations of Ca^{2+} also can modify the basal release probability (Thanawala et al., 2013; Jiang et al., 2000; Wilcox et al., 1994), and considering that our recorded synapses show an initial high release probability, future experiments in which we can modify extracellular Ca^{2+} could be useful to determine whether the increase in PPR induced by 10panx and α-panx1 occurred due to saturation of postsynaptic receptors or by blocking of Panx1.

It has been reported that presynaptic forms of inhibitory plasticity can require a postsynaptic step for their induction, which in many cases involves some form of retrograde communication from the postsynaptic to the presynaptic neuron (Regehr et al., 2009). One of the best characterized form of synaptic plasticity that involve retrograde messengers is a group of lipophilic molecules called

endocannabinoids (eCBs). N-arachidonoylethanolamide (anandamide, AEA) and 2-arachidonoylglycerol are two of the best studied eCBs (Chevaleyre et al., 2006; Devane et al., 1992; Stella et al., 1997). As consequence of specific neuronal activity, eCBs are released from the postsynaptic neuron and travel backward to activate the presynaptic type 1 cannabinoid receptor (CB1Rs) or TRPV1 receptors. CB1Rs are Gi/o-coupled receptors, whose activation result in a suppression of neurotransmitter release at both glutamatergic and GABAergic synapses (Chevaleyre et al., 2006; Ohno-Shosaku et al., 2001, Wilson et al., 2001). At the adult hippocampus, CB1Rs are mainly localized at presynaptic terminals of GABAergic interneurons (Irving et al., 2000; Katona et al., 1999).

Our results proposed that decrease in GABAergic transmission induced by the block of Panx1 involves eCBs signaling, because the blockage of CB1R with AM251, completely blocked the 10panx-mediated decrease in GABAergic transmission onto PyNs. In addition, we observed that the application of CB1R agonist, WIN, occluded the effect of 10panx, which suggest that both eCBs and 10panx exert their effects through a common cellular target to regulate inhibitory transmission.

In our study, the effect of blocking Panx1 in inhibitory synaptic plasticity is expressed by reduction in probability of GABA release and in the IPSCs amplitude. Changes in the probability of release are determined by several factors, but the most studied involve variations in presynaptic action potential-induced Ca^{2+} influx and/or the release machinery (Castillo et al., 2012). However, presynaptic signaling cascades show a high degree of crosstalk, because several kinases that are activated by presynaptic signal transduction cascade also affect the ability of Ca^{2+}-channels to open, close or inactivate in the terminal (Catterall & Few, 2008; de Jong & Verhage, 2009). The main Ca^{2+}-channels, enhance Ca^{2+}-influx and thereby increase the release probability (de Jong et al., 2009).

Previous studies have demonstrated that CB1Rs can target the neurotransmitter release machinery and control GABA release in a PKA-and RIM1α-dependent manner (Chevaleyre et al, 2008). Because we showed that CB1Rs are involved in 10panx-mediated depression of GABAergic transmission, we conducted our research to study if PKA signaling is involved in this form of GABAergic plasticity. Modulation of transmitter release by PKA protein can occur because of the phosphorylation of several presynaptic proteins involved in exocytosis. For example, it has been reported that synapsin I, a synaptic vesicle-associated phosphoprotein is phosphorylated by PKA, which promotes dissociation of synapsin I from synaptic vesicles, thereby enhancing the rate of exocytosis (Menegon et al., 2006). Another presynaptic targets of PKA are vesicular trafficking proteins and they include rabphilin-3A, SNAP-25, and α-SNAP (Fykse et al., 1995; Hirling & Scheller, 1996; Nguyen & Woo, 2003).

Our findings are consistent with the key role of PKA in this form of inhibitory synaptic plasticity, because 10panx-mediated depression was blocked in the presence of PKA inhibitor, H89. Also, we showed that decrease in GABA release probability was still observed in the presence of postsynaptic PKA inhibitor, PKI6-22 peptide, which was included in the internal recording solution. These findings confirm that block of Panx1 through CB1Rs and presynaptic PKA signaling can modulate GABA release onto PyNs in mouse hippocampus.

RIM1α a large multidomain protein that forms a scaffold at the presynaptic active zone can interact with multiple presynaptic proteins and it has been shown to be necessary for several cAMP/PKA-dependent forms of presynaptic plasticity including, inhibitory eCB-LTD in the hippocampus (Chevaleyre et al., 2007, Castillo et al., 2012). Because CB1Rs are involved in the Panx1-dependent changes in inhibitory transmission, it is possible that cAMP/PKA/RIM1α could be underlying the changes in GABA release mediated by the block of Panx1. However, in this research we do not address the downstream target of PKA activation. Future studies should identify which of these molecular targets underlie the reduction in GABA release when Panx1 is blocked.

It is known that eCBs can be released mainly via two separate postsynaptic mechanisms: activation of Gq-protein coupled metabotropic receptors and depolarization-induced Ca^{2+} influx via VGCCs (Chevaleyre et al., 2006). First, we demonstrated that block of Panx1-mediated depression in inhibitory efficacy is independent of signaling that involves G protein-coupled receptors, because the inclusion of irreversible G protein inhibitor GDP-βS in the recording pipette did not affect the 10panx-dependent depression of GABAergic efficacy. Importantly, our data showed that blockage of Panx1-dependent eCBs release is triggered by postsynaptic Ca^{2+} increase, because 10panx-mediated depression was occluded by including the calcium chelator BAPTA in the recording pipette, suggesting that calcium-mediated signaling in the postsynaptic neuron is required for the induction of 10panx-mediated depression in GABAergic synaptic transmission.

Panx1 channels are permeable to ions and neuroactive molecules such as ATP as well as large metabolites (<1 kDa) (Bao et al., 2004), thus it is possible that it may regulate the transport of other molecules that can modulate neurotransmission.

Recently it has been showed a novel role for Panx1 channels to facilitating transport for the signaling lipid, anandamide (AEA) (Bialecki et al., 2020). In this report it was demonstrated that the blockage of Panx1, increased the tissue concentrations of AEA. Also, the authors showed that Capsazepine (CPZ), a TRPV1 antagonist did not modify AEA levels, suggesting that Panx1 channels but no TRPV1 facilitates removal of AEA from the synapse. This function could be presumably by

preventing access of AEA to the intracellular enzyme, FAAH, which degrades it, because the inhibition of FAAH had a similar effect to blocking Panx1 in glutamatergic efficacy. Given that AEA is a ligand of TRPV1, Bialecki and cols., proposed that presynaptic TRPV1 channels mediates the facilitated glutamate release, which is supported with the result that shows no alterations in sEPSCs frequency in TRPV1 -/- mouse (Bialecki et al., 2020).

Although our results show that GABAergic depression mediated by Panx1 blockade requires CB1R activation, we still do not know the type of eCBs involved, 2-AG or AEA. Considering that AEA also acts as a partial agonist of CB1Rs (Luk et al., 2004), we hypothesized that AEA could be the endogenous cannabinoid involved in the 10panx-mediated depression of inhibitory efficacy onto PyNs.

Supporting our hypothesis, it has been described in CA1 region of the hippocampus that AEA signaling can modulate GABAergic neurotransmission (Kim and Alger et al., 2010). Notably a decrease in AEA tone, resulting from AEA degradation, was responsible for increase of GABA release from CB1R-positive interneurons in the activity-deprived hippocampus (Kim and Alger., 2010). This regulatory mechanism permits a selective and local tuning of inhibitory synapses in hippocampal circuit. Currently, we are study if AEA and/or 2AG is/are the eCBs implicated in the depression of GABAergic transmission when Panx1 is blocked.

As described above, the induction of inhibitory depression mediated by the block of Panx1 requires postsynaptic Ca^{2+} signaling. It is known that as a consequence of coincident glutamate binding and membrane depolarization open the NMDA receptors (NMDARs) increases intracellular Ca^{2+}, which activate the intracellular signaling cascades that ultimately are responsible for the changes in synaptic efficacy (Luscher & Malenka, 2012). As in glutamatergic synapses, NMDARs have been involved in inhibitory synaptic plasticity (iLTP/D) of many areas of the brain, including hippocampus (Moreau & Kullmann, 2013). The activation of NMDARs can modulate surface expression of dendritic GABAARs through the translocation of the NMDA-activated CaMKIIα at inhibitory synapses (K. Marsden et al., 2010; K. C. Marsden et al., 2007). Also, the activation of postsynaptic NMDARs can facilitate eCBs release and transiently suppress presynaptic GABA release via retrograde eCBs action (Ohno-Shosaku et al., 2001). Recently it has demonstrated that NMDAR-Panx1 signaling in the postsynapse is involved in the homeostatic regulatory mechanism that buffers AEA accumulation at the synapse (Bialecki et al., 2020). Despite these results, our data show that both NMDAR and AMPAR are not required for Panx1-dependent depression of inhibitory transmission, which indicates that postsynaptic calcium required for this form of inhibitory depression requires calcium from another source.

Several neuronal functions such as neurotransmitter release, gene expression and synaptic plasticity are regulated by voltage-gated Ca^{2+} channels (VGCC)(Catterall & Few, 2008). In hippocampus, five types of Ca^{2+} channels have been described based on their physiological characteristics: T-type channels, and Ca^{2+} channel types N, P, Q and L. L-type VGCCs require strong depolarization to opening and in PyNs are predominantly expressed on soma and proximal dendrites, where they generate somatic Ca^{2+} responses (Westenbroek et al., 1990). In hippocampus it has been observed that repetitive increase in somatic Ca^{2+} via L-VGCC can induce LTP and triggers the gene transcription underlying the maintenance of LTP (Hardingham et al., 1999; Impey et al., 1996; Raymond & Redman, 2006). On the other hand, at GABAergic synapses was reported that BDNF released retrogradely, can trigger a long-lasting potentiation of GABAergic transmission in the newborn rat hippocampus (Kuczewski et al., 2008), which required the activation of L-type VGCCs. Our results showed that depression of inhibitory transmission mediated by the block of Panx1, was independent of activation of NMDARs, but require the activation of L-type Ca^{2+} channels. Although we have shown that L-type calcium channels are required for this form of inhibitory plasticity, it is possible that other sources of intracellular calcium spiking are involved in this form of plasticity. Future research is required to study if another type of VGCCs or Ca^{2+} release of intracellular stores contribute to this form of GABA synaptic plasticity.

Our findings revealed that block of Panx1 is also expressed as postsynaptic change because the amplitude of eIPSCs is decreased in the presence of 10panx. Several forms of inhibitory plasticity occur as consequence of postsynaptic changes in GABAergic transmission, which are manifested through several mechanisms (Kittler & Moss, 2003; Nusser et al., 1998). For example, increases or decreases in channel function can occur as a result of GABAAR phosphorylation by multiple kinases, including PKA, CaMKII, Src and PKA (Kittler et al., 2003). It has been reported that exist a differential modulation of GABAAR subtypes by PKA activity, dependent upon β subunit identity. While PKA modulate negatively at GABAAR that incorporate the β1 subunit, the other ones that contain β3 subunit enhanced their activity by PKA phosphorylation (McDonald et al., 1998).

It was recently postulated that the activity of Panx1 channels induced by mechanical stretch can be reduced by adenosine via a PKA-dependent pathway (López et al., 2020). In this research were identified two PKA target sites (T302 and S328) that modulate the activity of Panx1 channels. The proposed model of adenosine-dependent inhibition of mechanically stretched Panx1 channels involve the activation of adenosine receptors coupled to Gαs subunit (A2A and A2B), which by activation of AC increases the cAMP concentration. The increase in cAMP levels activate PKA, which through the phosphorylation inhibit Panx1 channel activity. Our results showed that in the presence of

postsynaptic PKI6-22, 10panx was ineffective to reduce eIPSC amplitude (Fig. 12), which suggest that postsynaptic PKA is involved in the 10panx-mediated depression of GABAergic efficacy. However, it is possible that interaction between Panx1 and PKA may involve a mechanism other than adenosine, because in the presence of irreversible G protein inhibitor (GDP-βS), the 10panx-mediated depression of GABAergic efficacy was still induced (Fig.13).

It is also described that inhibitory strength is dependent on the cellular gradient which is controlled by the function of chloride transporters. In accordance with Panx1 permeability, it is important to consider that Panx1 constitutively resides in a small pore state, which behaves as a low conductance, primarily chloride-permeable channel (~50–80 pS) (Ma et al., 2012). Therefore, the effect of block Panx1 in the postsynaptic expression of GABAergic efficacy, also could be involving changes in the cellular gradient of chloride.

Adenosine/ATP and hippocampal GABAergic transmission

Evidence of modulation of GABAergic transmission by ADO has been found in several brain areas relevant for fine control of movement, drug addiction or sleep (Sebastião et al., 2015). At the hippocampus, evidence have been pointing to a predominant action on excitatory transmission, and much less is known regarding ADO modulation of GABA-mediated signaling. Hippocampal modulation of GABAergic efficacy by ADO involves differential action of adenosine receptors. It has been reported that although not directly affecting phasic GABAergic transmission in mature hippocampal neurons, A1Rs selectively modulate tonic inhibition that results from activation of extrasynaptic GABAAR, which involves a specific group of postsynaptic CA1 GABAergic neurons, the CCK-expressing interneurons (Rombo et al., 2016). On the other hand, A2AR activation directly enhances excitatory glutamatergic synapses to CA1 pyramidal cells and induces a presynaptic enhancement of phasic GABAergic inputs from PV-expressing neurons to other interneurons, leading to a disinhibition of pyramidal cells (Rombo et al., 2015). However, A2AR activation do not affect monosynaptic inhibitory inputs to excitatory PyNs (Rombo et al., 2015).

Our results show that ADO application had effect only in the PPR of eIPSCs but the effect in IPSC amplitude was variable and did no show a significant change (Fig. 8A-B). It is likely due to the technical difficulties of isolating specific inhibitory inputs onto PyNs, given that ADO acts in a interneuron-specific manner and by means of differential activation of adenosine receptors. It is supported with our results showing a clear effect of ADO on excitatory transmission, in which ADO application strongly decreased the glutamatergic efficacy (Fig. 8C-D). Future studies with ADO in GABAergic transmission should use selective experimental approaches to isolate the specific

interneuron population and the adenosine receptor type that could be involved. Also, more experiments will be required.

On the other results, we observed that ADO application failed to rescue the depression in GABAergic efficacy induced by the Panx1 blocker, PBN (Fig. 7). A link between Panx1channels and ADO was described by Prochnow et al., 2012. In this study, mouse lacking Panx1 (Panx1-/-) had enhanced excitability and showed persistent LTP responses (Prochnow et al., 2012). Interestingly this synaptic phenotype was rescued with application of ADO. Authors suggest that this result is due to Panx1-/- mouse having diminished synaptic ATP/ADO levels, however, this study was focused only on glutamatergic transmission. Given that study of ADO effect in GABAergic transmission requires a specific experimental approach.

It is known that Panx1 acts as an ATP release channel, which can activate several signaling pathways and modulate cellular processes such as synaptic plasticity (Fujii et al., 2004; Kato et al., 2004). We hypothesized that by blocking Panx1, less ATP is released into the synapse, thus an extracellular application of ATP, could be rescue or decreased the effect of PBN in GABAergic transmission. Nevertheless, we found that ATP (500Nm) application failed to change the PBN-mediated depression in GABAergic efficacy (Fig. 9). It has been described that studies made in brain slices that involved exogenous application of ATP, the effect observed was in most cases accompanied by responses mediated by adenosine receptors (Cunha et al., 1998; Masino et al., 2002), which is consistent with the rapid conversion of ATP to ADO by ectonucleotidases. In our experimental conditions ATP was added directly on the slice but without adenosine receptor antagonist, thus we cannot rule out ADO effect in our results.

In addition, another study reported that ATP application stimulates internalization of Panx1 to intracellular membranes (Boyce et al., 2015; Qiu et al., 2009), which has been described as negative feedback regulation to control ATP levels. It could be explaining that extracellular ATP had no effect in the presence of PBN, because PBN block Panx1 activity and extracellular ATP decrease the Panx1 levels in the cellular membrane. However, additional experiments are required to study this hypothesis.

Figure 19 shows a proposed mechanism explaining the effect of block Panx1 on the GABAergic synaptic efficacy and the signaling pathways that are involved.

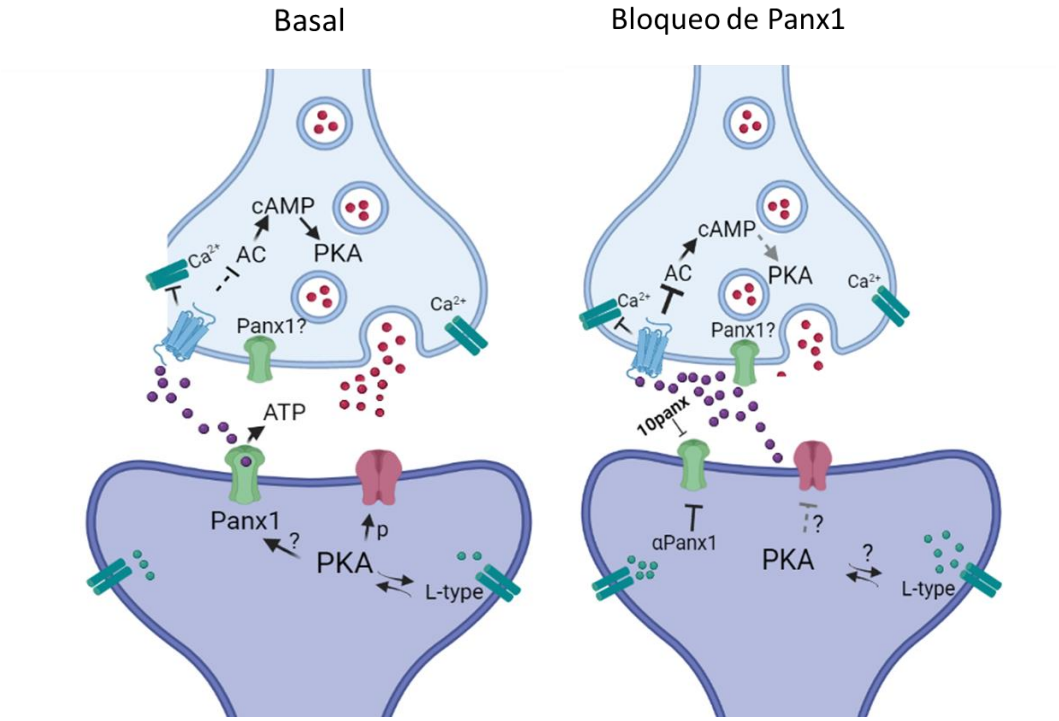

Figure 19: Proposed mechanism explaining the effect of block Panx1 in the GABAergic synaptic efficacy. Block of Panx1 channels causes a decrease in GABAergic efficacy onto CA1 PyNs in mouse hippocampus that involved a decrease of probability of GABA release and the amplitude of eIPSCs. The proposed mechanism indicates that Panx1 by facilitating the transport of eCBs into the cells contribute to maintain eCB levels. When Panx1 is blocked, an increase calcium-dependent in eCBs levels is produced. Next, eCBs activate CB1R, which leads to a decrease in GABA release probability that involved presynaptic PKA. At postsynaptic level PKA and calcium entry through of L-type channels are required. It is possible that an increase of postsynaptic calcium contributes to releasing eCBs and activates PKA, which could phosphorylate GABAR and/or Panx1 channels to modulate its activity.

This work revealed novel functions of Panx1 channels in inhibitory synaptic plasticity of hippocampal network, supporting an important role of Panx1 in the control of excitatory-inhibitory balance, brain plasticity, cognitive processes, and behavioral performance.

IX. Conclusions

Our present results suggest that neuronal Panx1 is an important modulator of hippocampal GABA synaptic transmission. We reported that blocking Panx1channels causes a decrease in GABAergic efficacy onto CA1 PyNs in mouse hippocampus. This form of synaptic depression involved a decrease GABA release probability and the amplitude of eIPSCs, which indicates a pre- and postsynaptic locus of expression.

The cellular mechanism by which the block of Panx1 induced these changes required: *i*) the increase of postsynaptic Ca^{2+}, which required the L-type VGCCs activation, *ii*) CB1 receptor activation, *iii*) differential PKA activity at both presynaptic and postsynaptic sites and *iv*) μ-opiod receptors signaling.

Together these results of the present study uncovered for the first time that Panx1 can regulate the GABAergic transmission, which may have important implications in the transfer and storage of synaptic information as well as in the mechanisms of neural plasticity and cognition.

XI. Annexes

Supplementary figures

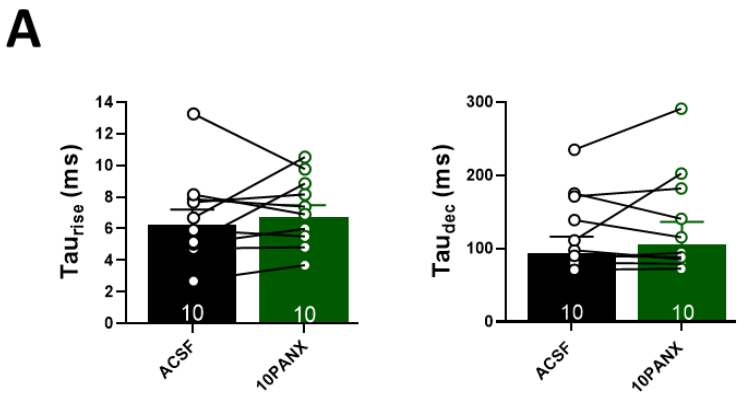

Figure S1 (related to Fig. 3): A) Mean of Tau rise (left) and Tau decay (right) analyses from eIPSCs before and after 10panx application. Data are performed as mean ± SEM . *p<0.05. Number of recorded cells is indicated within bars.

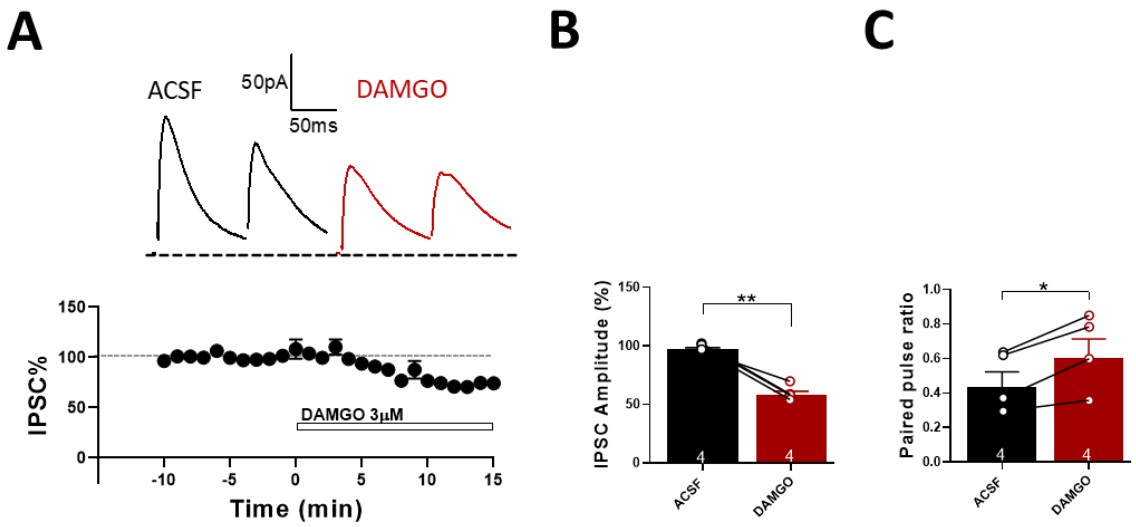

Figure S2 (related to Fig. 10): µ-opioid receptor activation decreases GABA release onto pyramidal neurons of mouse hippocampus. A) Representative samples traces from evoked IPSCs and PPR for each condition (top). Temporal course showing changes in the amplitude of eIPSC (%) before and after DAMGO (3µM) application (bottom). **B)** DAMGO application had no effects in the eIPSCs amplitude onto PyNs compared with basal condition. **C)** Bath application of DAMGO caused a significant increase of the PPR value compared with control condition in PyNs of mouse hippocampus. Data are performed as mean ± SEM . *p<0.05. Number of recorded cells is indicated within bars.

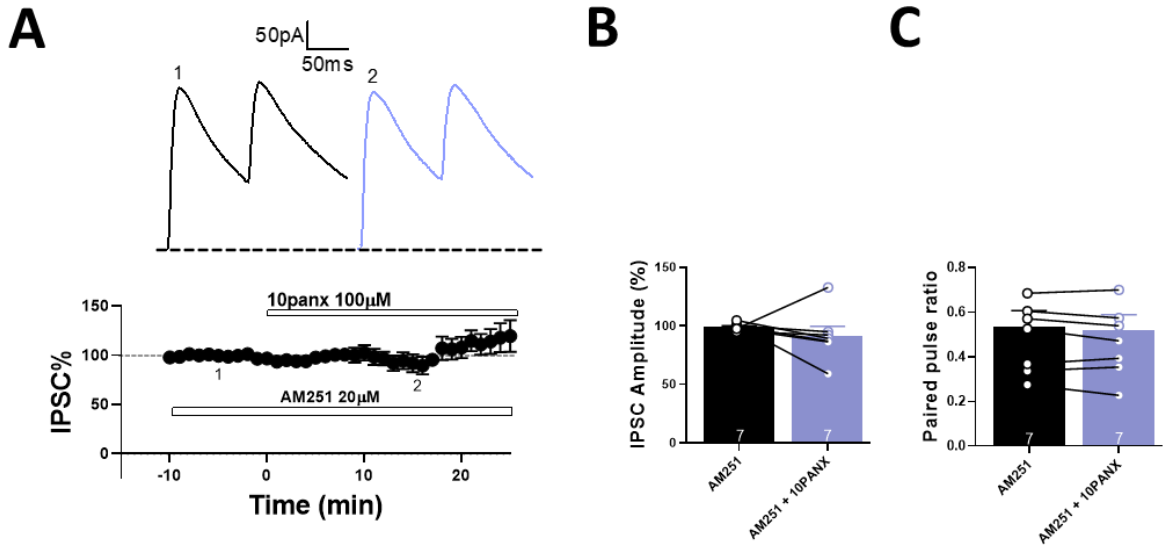

Figure S3 (related to Fig. 11): 10panx failed to decrease GABAergic efficacy in the presence of AM251. **A)** Representative samples traces from evoked IPSCs and PPR for each condition (top). Temporal course showing IPSC% before and after 10panx (100µM) application in the presence of AM51 (20µM)(bottom). **B)** In pretreated slice with AM251, bath application of 10panx had no effects in the eIPSCs amplitude onto PyNs. **C)** 10panx failed to change PPR in the presence of AM251 (20µM). Data are performed as mean ± SEM . *p<0.05. Number of recorded cells is indicated within bars.

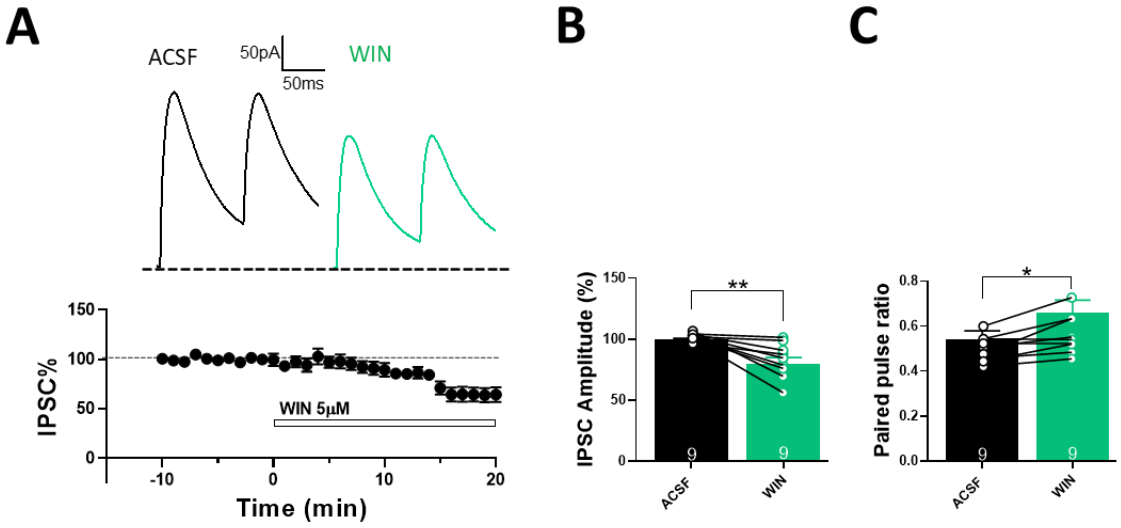

Figure S4 (related to Fig. 11): CB1R activation induces a decrease of GABA transmission onto pyramidal neurons of mouse hippocampus. A) Representative samples traces from evoked IPSCs and PPR for each condition (top). Temporal course showing IPSC% before and after WIN addition (bottom). **B)** WIN (5µM) application caused a significant decrease in the eIPSCs amplitude onto PyNs compared with basal condition. **C)** Bath application of WIN caused a significant increase of the PPR value compared with control condition. Data are performed as mean ± SEM . *p<0.05. Number of recorded cells is indicated within bars.

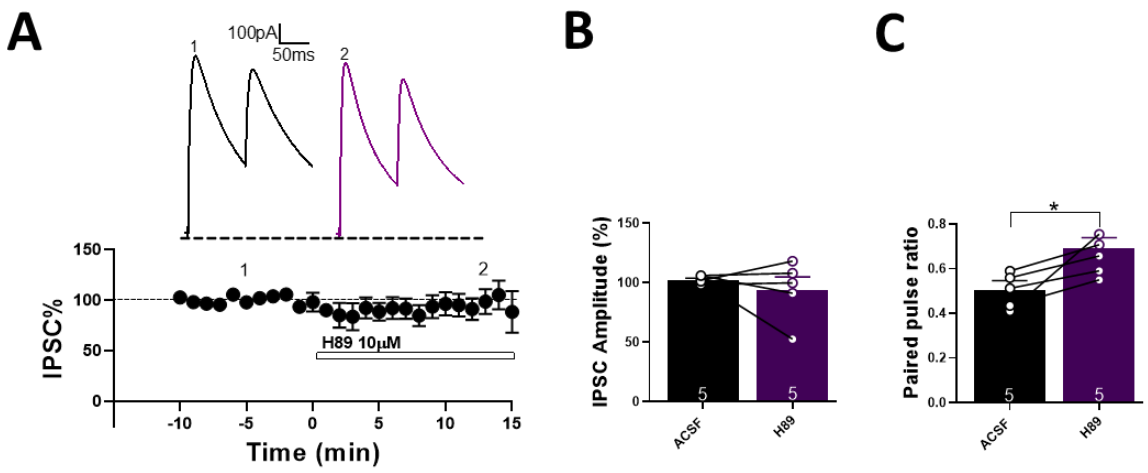

Figure S5 (related to Fig. 12): Block of PKA induces a decrease in probability of GABA release onto pyramidal neurons of mouse hippocampus. A) Representative samples traces from evoked IPSCs and PPR for each condition (top). Temporal course showing IPSC% before and after H89 addition (bottom). **B)** H89 (10µM) application had no effect in the eIPSCs amplitude onto PyNs compared with basal condition. **C)** Bath application of H89 caused a significant increase of the PPR value compared with control condition. Data are performed as mean ± SEM . *p<0.05. Number of recorded cells is indicated within bars.

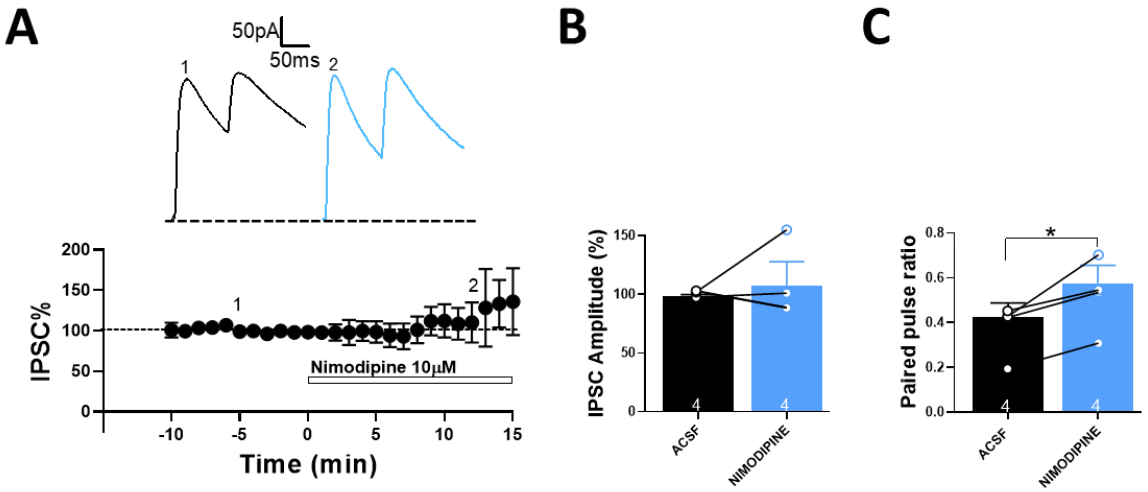

Figure S6 (related to Fig. 14): Block of L-type VGCC induces a decrease in probability of GABA release onto pyramidal neurons of mouse hippocampus. A) Representative samples traces from evoked IPSCs and PPR for each condition (top). Temporal course showing IPSC% before and after Nimodipine addition (bottom). **B)** Nimodipine (10µM) application had no effect in the eIPSCs amplitude onto PyNs compared with basal condition. **C)** Bath application of Nimodipine caused a significant increase of the PPR value compared with control condition. Data are performed as mean ± SEM . *p<0.05. Number of recorded cells is indicated within bars.

XI. References

Abraham, W. C., Bliss, T. V., & Goddard, G. V. (1985). Heterosynaptic changes accompany long term but not short-term potentiation of the perforant path in the anaesthetized rat. The Journal of Physiology, 363(1), 335–349.

Al-Hayani, A., Wease, K. N., Ross, R. A., Pertwee, R. G., & Davies, S. N. (2001). The endogenous cannabinoid anandamide activates vanilloid receptors in the rat hippocampal slice. Neuropharmacology, 41(8), 1000–1005.

Alger, B. E. (1991). Gating of GABAergic inhibition in hippocampal pyramidal cells. Annals of the New York Academy of Sciences. 627, 249—263.

Andersen, P., Morris, R., Amaral, D., O'Keefe, J., Bliss, D., & Bliss, T. (Eds.). (2007). The hippocampus book. Oxford University Press.

Anselmi, F., Hernandez, V. H., Crispino, G., Seydel, A., Ortolano, S., Roper, S. D., Kessaris, N., Richardson, W., Rickheit, G., Filippov, M. A., Monyer, H., & Mammano, F. (2008). ATP release through connexin hemichannels and gap junction transfer of second messengers propagate Ca2+ signals across the inner ear. Proceedings of the National Academy of Sciences, 105(48), 18770–18775.

Ardiles, A. O., Flores-Muñoz, C., Toro-Ayala, G., Cárdenas, A. M., Palacios, A. G., Muñoz, P., Fuenzalida, M., Saez, J. C., & Martinez, A. D. (2014). Pannexin 1 regulates bidirectional hippocampal synaptic plasticity in adult mouse. Frontiers in Cellular Neuroscience, 8.

Armstrong, C., & Soltesz, I. (2012). Basket cell dichotomy in microcircuit function: Basket cells as dichotomous microcircuit modulators. The Journal of Physiology, 590(4), 683–694.

Bao, L., Locovei, S., & Dahl, G. (2004). Pannexin membrane channels are mechanosensitive conduits for ATP. FEBS Letters, 572(1–3), 65–68.

Bazargani, N., & Attwell, D. (2016). Astrocyte calcium signaling: The third wave. Nature Neuroscience, 19(2), 182–189.

Berger, T. W., Rinaldi, P. C., Weisz, D. J., & Thompson, R. F. (1983). Single-unit analysis of different hippocampal cell types during classical conditioning of rabbit nictitating membrane response. Journal of Neurophysiology, 50(5), 1197–1219.

Bezaire, M. J., & Soltesz, I. (2013). Quantitative assessment of CA1 local circuits: Knowledge base for interneuron-pyramidal cell connectivity: Quantitative Assessment Of Ca1 Local Circuits. Hippocampus, 23(9), 751–785.

Bialecki, J., Werner, A., Weilinger, N. L., Tucker, C. M., Vecchiarelli, H. A., Egaña, J., Mendizabal-Zubiaga, J., Grandes, P., Hill, M. N., & Thompson, R. J. (2020). Suppression of Presynaptic Glutamate Release by Postsynaptic Metabotropic NMDA Receptor Signalling to Pannexin-1. The Journal of Neuroscience, 40(4), 729–742.

Billaud, M., Chiu, Y.-H., Lohman, A. W., Parpaite, T., Butcher, J. T., Mutchler, S. M., DeLalio, L. J., Artamonov, M. V., Sandilos, J. K., Best, A. K., Somlyo, A. V., Thompson, R. J., Le, T. H., Ravichandran, K. S., Bayliss, D. A., & Isakson, B. E. (2015). A molecular signature in the pannexin1 intracellular loop confers channel activation by the α1 adrenoreceptor in smooth muscle cells. Science Signaling, 8(364).

Bliss, T. V. P., & Lømo, T. (1973). Long-lasting potentiation of synaptic transmission in the dentate area of the anaesthetized rabbit following stimulation of the perforant path. The Journal of Physiology, 232(2), 331–356.

Blitz, DM., Foster, KA., Regehr, WG., (2004). Short-term synaptic plasticity: a comparison of two synapses. Nat Rev Neurosci. 5(8):630-40.

Boassa, D., Nguyen, P., Hu, J., Ellisman, M. H., & Sosinsky, G. E. (2015). Pannexin2 oligomers localize in the membranes of endosomal vesicles in mammalian cells while Pannexin1 channels traffic to the plasma membrane. Frontiers in Cellular Neuroscience, 8.

Bourne, J. N., & Harris, K. M. (2011). Coordination of size and number of excitatory and inhibitory synapses results in a balanced structural plasticity along mature hippocampal CA1 dendrites during LTP. Hippocampus, 21(4), 354–373.

Brock, J., Thomazeau, A., Watanabe, A., Ying Li, S., Sjostrom., P. (2020). A Practical Guide to Using CV Analysis for Determining the Locus of Synaptic Plasticity. Frontiers in Synaptic Neuroscience, 12(11), 1-16.

Bruzzone, R., Hormuzdi, S. G., Barbe, M. T., Herb, A., & Monyer, H. (2003). Pannexins, a family of gap junction proteins expressed in brain. Proceedings of the National Academy of Sciences, 100(23), 13644–13649.

Buchanan, K. A., & Mellor, J. (2010). The activity requirements for spike timing-dependent plasticity in the hippocampus. Frontiers in Synaptic Neuroscience, 2.

Canteras, N. S., & Swanson, L. W. (1992). Projections of the ventral subiculum to the amygdala, septum, and hypothalamus: A PHAL anterograde tract-tracing study in the rat. The Journal of Comparative Neurology, 324(2), 180–194.

Capogna, M., Gahwiler, B., & Thompson, S. (1995). Presynaptic enhancement of inhibitory synaptic transmission by protein kinases A and C in the rat hippocampus in vitro. The Journal of Neuroscience, 15(2), 1249–1260.

Castillo, P. E. (2012). Presynaptic LTP and LTD of Excitatory and Inhibitory Synapses. Cold Spring Harbor Perspectives in Biology, 4(2), a005728–a005728.

Castillo, P. E., Chiu, C. Q., & Carroll, R. C. (2011). Long-term plasticity at inhibitory synapses. Current Opinion in Neurobiology, 21(2), 328–338.

Catterall, W., & Few, A. (2008). Calcium channel regulation and presynaptic plasticity. Neuron, 59, 882–901.

Chekeni, F., Elliot, M., Sandilos, J., Walk, S., Kinchen, J., Lazarowski, E., Armstrong, A., Penuela, S., Laird, D., Salvesen, G., Isakson, B., Bayliss, D., & Ravichandran, K. (2010). Pannexin 1 channels mediate 'find-me' signal release and membrane permeability during apoptosis. Nature, 467, 863–867.

Chevaleyre, V., & Castillo, P. E. (2003). Heterosynaptic LTD of Hippocampal GABAergic Synapses: A Novel Role of Endocannabinoids in Regulating Excitability. Neuron, 38, 461–472.

Chevaleyre, V., Heifets, B. D., Kaeser, P. S., Südhof, T. C., & Castillo, E. (2008). Endocannabinoid-mediated long-term plasticity requires cAMP/PKA signaling and RIM1. Neuron, 54(5), 801-812.

Chevaleyre, V., Takahashi, K., & Castillo, P. (2006). Endocannabinoid-Mediated Synaptic Plasticity in the CNS. Annu. Rev. Neurosci., 29, 37–76.

Citri, A., & Malenka, R. C. (2008). Synaptic Plasticity: Multiple Forms, Functions, and Mechanisms. Neuropsychopharmacology, 33(1), 18–41.

Cohen, G. A., Doze, V. A., & Madison, D. V. (1992). Opioid inhibition of GABA release from presynaptic terminals of rat hippocampal interneurons. Neuron, 9(2), 325–335.

Collingridge, G. L., Peineau, S., Howland, J. G., & Wang, Y. T. (2010). Long-term depression in the CNS. Nature Reviews Neuroscience, 11(7), 459–473.

Csicsvari, J., Hirase, H., Czurkó, A., Mamiya, A., & Buzsáki, G. (1999). Oscillatory Coupling of Hippocampal Pyramidal Cells and Interneurons in the Behaving Rat. The Journal of Neuroscience, 19(1), 274–287.

Dahl, G. (2018). The Pannexin1 membrane channel: Distinct conformations and functions. FEBS Letters, 592(19), 3201–3209.

Dawe, GB., Musgaard, M., Andrews, ED., Daniels, BA., Aurousseau, MR., Biggin, PC., Bowie D. (2013). Defining the structural relationship between kainate-receptor deactivation and desensitization. Nat Struct Mol Biol. 20(9):1054-61.

Debanne, D., Guerineau, N., Gahwiler, B. H. & Thompson, S. M. (1996). Paired-pulse facilitation and depression at unitary synapses in rat hippocampus: quantal fluctuation affects subsequent release. Journal of Physiology. 491, 163—176.

De Jong, A. P., & Verhage, M. (2009). Presynaptic signal transduction pathways that modulate synaptic transmission. Current Opinion in Neurobiology, 19(3), 245–253.

Dermietzel, R., Traub, O., Hwang, T. K., Beyer, E., Bennett, M. V., Spray, D. C., & Willecke, K. (1989). Differential expression of three gap junction proteins in developing and mature brain tissues. Proceedings of the National Academy of Sciences, 86(24), 10148–10152.

Devane, W., Hanus, L., Breuer, A., Pertwee, R., Stevenson, L., Griffin, G., Gibson, D., Mandelbaum, A., Etinger, A., & Mechoulam, R. (1992). Isolation and Structure of a Brain Constituent That Binds to the Cannabinoid Receptor. Science, 258, 1946–1949.

Dias, R. B., Rombo, D. M., Ribeiro, J. A., Henley, J. M., & Sebastião, A. M. (2013). Adenosine: Setting the stage for plasticity. Trends in Neurosciences, 36(4), 248–257.

Dossi, E., Blauwblomme, T., Moulard, J., Chever, O., Vasile, F., Guinard, E., Le Bert, M., Couillin, I., Pallud, J., Capelle, L., Huberfeld, G., & Rouach, N. (2018). Pannexin-1 channels contribute to seizure generation in human epileptic brain tissue and in a mouse model of epilepsy. Science Translational Medicine, 10(443).

Dudek, S. M., & Bear, M. F. (1992). Homosynaptic long-term depression in area CAl of hippocampus and effects of N-methyl-D-aspartate receptor blockade. 5.

Faber, D. S., and Korn, H. (1991). Applicability of the coefficient of variationmethod for analyzing synaptic plasticity. Biophys. J. 60, 1288–1294.

Fanselow, M. S., & Dong, H.-W. (2010). Are the Dorsal and Ventral Hippocampus Functionally Distinct Structures? Neuron, 65(1), 7–19.

Flores, C. E., & Mendez, P. (2014). Shaping inhibition: Activity dependent structural plasticity of GABAergic synapses. Frontiers in Cellular Neuroscience, 8.

Foster, KA., Kreitzer, AC., Regehr,. WG. (2002). Interaction of postsynaptic receptor saturation with presynaptic mechanisms produces a reliable synapse. Neuron. 36(6):1115-26.

Fritschy, J.-M., & Panzanelli, P. (2014). GABA A receptors and plasticity of inhibitory neurotransmission in the central nervous system. European Journal of Neuroscience, 39(11), 1845–1865.

Froemke, R. C. (2015). Plasticity of Cortical Excitatory-Inhibitory Balance. Annual Review of Neuroscience, 38(1), 195–219.

Fykse, E., Li, C., & Sudhof, T. (1995). Phosphorylation of rabphilin-3A by Ca2+/calmodulin- and cAMP-dependent protein kinases in vitro. The Journal of Neuroscience, 15(3), 2385–2395.

Gabrieli, J. D. E., Brewer, J. B., Desmond, J. E., & Glover, G. H. (1997). Separate Neural Bases of Two Fundamental Memory Processes in the Human Medial Temporal Lobe. Science, 276(5310), 264–266.

Gajardo, I., Salazar, C. S., Lopez-Espíndola, D., Estay, C., Flores-Muñoz, C., Elgueta, C., Gonzalez-Jamett, A. M., Martínez, A. D., Muñoz, P., & Ardiles, Á. O. (2018). Lack of Pannexin 1 Alters Synaptic GluN2 Subunit Composition and Spatial Reversal Learning in Mouse. Frontiers in Molecular Neuroscience, 11, 114.

Hanstein, R., Hanani, M., Scemes, E., & Spray, D. C. (2016). Glial pannexin1 contributes to tactile hypersensitivity in a mouse model of orofacial pain. Scientific Reports, 6(1), 38266.

Hardingham, G. E., Chawla, S., Cruzalegui, F. H., & Bading, H. (1999). Control of Recruitment and Transcription-Activating Function of CBP Determines Gene Regulation by NMDA Receptors and L-Type Calcium Channels. Neuron, 22(4), 789–798.

Henke, K., Buck, A., Weber, B., & Wieser, H. G. (1997). Human hippocampus establishes associations in memory. Hippocampus, 7(3), 249–256.

Henke, P. G. (1990). Hippocampal pathway to the amygdala and stress ulcer development. Brain Research Bulletin, 25(5), 691–695.

Hirling, H., & Scheller, R. (1996). Phosphorylation of synaptic vesicle proteins: Modulation of the a SNAP interaction with the core complex. Proceedings of the National Academy of Sciences, 93, 11945–11949.

Holz, R & Fisher, S. (2012) . Synaptic Transmission and Cellular Signaling: An overview. Basic Neurochemistry. El servier. 12, 235-257.

Iglesias, R., Dahl, G., Qiu, F., Spray, D. C., & Scemes, E. (2009). Pannexin 1: The Molecular Substrate of Astrocyte "Hemichannels." Journal of Neuroscience, 29(21), 7092–7097.

Impey, S., Mark, M., Villacres, E. C., Poser, S., Chavkin, C., & Storm, D. R. (1996). Induction of CRE-Mediated Gene Expression by Stimuli That Generate Long-Lasting LTP in Area CA1 of the Hippocampus. Neuron, 16(5), 973–982.

Irving, A. J., Coutts, A. A., Harvey, J., Rae, M. G., Mackie, K., Bewick, G. S., & Pertwee, R. G. (2000). Functional expression of cell surface cannabinoid CB1 receptors on presynaptic inhibitory terminals in cultured rat hippocampal neurons. Neuroscience, 98(2), 253–262.

Jeong, H.-J., Jang, I.-S., Nabekura, J., & Akaike, N. (2003). Adenosine A 1 Receptor-Mediated Presynaptic Inhibition of GABAergic Transmission in Immature Rat Hippocampal CA1 Neurons. Journal of Neurophysiology, 89(3), 1214–1222.

Jiang, L., Sun, S., Nedergaard, M., Kang, J. (2000). Paired-pulse modulation at individual GABAergic synapses in rat hippocampus. J Physiol. 1;523 Pt 2(Pt 2):425-39.

Kato, F., Kawamura, M., Shigetomi, E., Tanaka, J., & Inoue, K. (2004). ATP- and Adenosine-Mediated Signaling in the Central Nervous System: Synaptic Purinoceptors: the Stage for ATP to Play Its "Dual-Role." Journal of Pharmacological Sciences, 94(2), 107–111.

Katona, I., Sperlágh, B., Sík, A., Käfalvi, A., Vizi, E. S., Mackie, K., & Freund, T. F. (1999). Presynaptically Located CB1 Cannabinoid Receptors Regulate GABA Release from Axon Terminals of Specific Hippocampal Interneurons. The Journal of Neuroscience, 19(11).

Kim, J., & Alger, B. E. (2010). Reduction in endocannabinoid tone is a homeostatic mechanism for specific inhibitory synapses. Nature Neuroscience, 13(5), 592–600.

Kittler, J. T., & Moss, S. J. (2003). Modulation of GABAA receptor activity by phosphorylation and receptor trafficking: Implications for the efficacy of synaptic inhibition. Current Opinion in Neurobiology, 13(3), 341–347.

Klausberger, T. (2005). Complementary Roles of Cholecystokinin- and Parvalbumin-Expressing GABAergic Neurons in Hippocampal Network Oscillations. Journal of Neuroscience, 25(42), 9782–9793.

Kuczewski, N., Langlois, A., Fiorentino, H., Bonnet, S., Diabira, D., Nadine, F., Porcher, C., & Gaiarsa, J. (2008). Spontaneous glutamatergic activity induces a BDNF-dependent potentiation of GABAergic synapses in the newborn rat hippocampus. J Physiol, 586(21), 5119–5128.

Lalo, U., Palygin, O., Verkhratsky, A., Grant, S. G. N., & Pankratov, Y. (2016). ATP from synaptic terminals and astrocytes regulates NMDA receptors and synaptic plasticity through PSD-95 multi-protein complex. Scientific Reports, 6(1), 33609.

Lambert, N. A., & Teyler, T. J. (1991). Adenosine depresses excitatory but not fast inhibitory synaptic transmission in area CA1 of the rat hippocampus. Neuroscience Letters, 122(1), 50–52.

Le Vasseur, M., Chen, V., Huang, ., Vogl, W., & Naus, C. (2019). Pannexin 2 Localizes at ER-Mitochondria Contact Sites. Cancers, 11(343), 1–19.

López, X., Escamilla, R., Fernández, P., Duarte, Y., González-Nilo, F., Palacios-Prado, N., Martinez, AD., Sáez, JC. (2020). Stretch-Induced Activation of Pannexin 1 Channels Can Be Prevented by PKA-Dependent Phosphorylation. Int J Mol Sci. 21(23):9180.

Luk, T., Jin, W., Zvonok, A., Lu, D., Lin, X.-Z., Chavkin, C., Makriyannis, A., & Mackie, K. (2004). Identification of a potent and highly efficacious, yet slowly desensitizing CB1 cannabinoid receptor agonist: An efficacious, slowly desensitizing CB1 agonist. British Journal of Pharmacology, 142(3), 495–500.

Luscher, C., & Malenka, R. C. (2012). NMDA Receptor-Dependent Long-Term Potentiation and Long-Term Depression (LTP/LTD). Cold Spring Harbor Perspectives in Biology, 4(6), a005710–a005710.

Lynch, M. A. (2004). Long-Term Potentiation and Memory. Physiol Rev, 84, 50.

Ma, W., Compan, V., Zheng, W., Martin, E., North, R. A., Verkhratsky, A., & Surprenant, A. (2012). Pannexin 1 forms an anion-selective channel. Pflügers Archiv - European Journal of Physiology, 463(4), 585–592.

Marsden, K. C., Beattie, J. B., Friedenthal, J., & Carroll, R. C. (2007). NMDA Receptor Activation Potentiates Inhibitory Transmission through GABA Receptor-Associated Protein-Dependent Exocytosis of GABAA Receptors. Journal of Neuroscience, 27(52), 14326–14337.

Marsden, K., Shemesh, A., Bayer, U., & Carroll, R. (2010). Selective translocation of Ca2+/calmodulin protein kinase IIα (CaMKIIα) to inhibitory synapses. Proceedings of the National Academy of Sciences, 107(47), 20559–20564.

McCullumsmith, R. E., Clinton, S. M., & Meador-Woodruff, J. H. (2004). Schizophrenia as a Disorder of Neuroplasticity. In International Review of Neurobiology (Vol. 59, pp. 19–45). Elsevier.

McDonald, B. J., Amato, A., Connolly, C. N., Benke, D., Moss, S. J., & Smart, T. G. (1998). Adjacent phosphorylation sites on GABAA receptor β subunits determine regulation by cAMP-dependent protein kinase. Nature Neuroscience, 1(1), 23–28.

Mederos, S., Hernández-Vivanco, A., Ramírez-Franco, J., Martín-Fernández, M., Navarrete, M., Yang, A., Boyden, E. S., & Perea, G. (2019). Melanopsin for precise optogenetic activation of astrocyte-neuron networks. Glia, 67(5), 915–934.

Menegon, A., Bonanomi, D., Albertinazzi, C., Lotti, F., Ferrari, G., Kao, H.-T., Benfenati, F., Baldelli, P., & Valtorta, F. (2006). Protein Kinase A-Mediated Synapsin I Phosphorylation Is a Central Modulator of Ca2+-Dependent Synaptic Activity. Journal of Neuroscience, 26(45), 11670–11681.

Moreau, A. W., & Kullmann, D. M. (2013). NMDA receptor-dependent function and plasticity in inhibitory circuits. Neuropharmacology, 74, 23–31.

Moser, E., Moser, M., & Andersen, P. (1993). Spatial learning impairment parallels the magnitude of dorsal hippocampal lesions, but is hardly present following ventral lesions. The Journal of Neuroscience, 13(9), 3916–3925.

Nanou, E., Lee, A., & Catterall, W. A. (2018). Control of Excitation/Inhibition Balance in a Hippocampal Circuit by Calcium Sensor Protein Regulation of Presynaptic Calcium Channels. The Journal of Neuroscience, 38(18), 4430–4440.

Neves, G., Cooke, S. F., & Bliss, T. V. P. (2008). Synaptic plasticity, memory and the hippocampus: A neural network approach to causality. Nature Reviews Neuroscience, 9(1), 65–75.

Nguyen, P., & Woo, N. (2003). Regulation of hippocampal synaptic plasticity by cyclic AMP-dependent protein kinases. Progress in Neurobiology, 71, 401–437.

Ni, M., He, J.-G., Zhou, H.-Y., Lu, X.-J., Hu, Y.-L., Mao, L., Wang, F., Chen, J.-G., & Hu, Z.-L. (2018). Pannexin-1 channel dysfunction in the medial prefrontal cortex mediates depressive-like behaviors induced by chronic social defeat stress and administration of mefloquine in mouse. Neuropharmacology, 137, 256–267.

Nusser, Z., Hájos, N., Somogyi, P., & Mody, I. (1998). Increased number of synaptic GABAA receptors underlies potentiation at hippocampal inhibitory synapses. Nature, 395(6698), 172–177.

Ohno-Shosaku, T., Maejima, T., & Kano, M. (2001). Endogenous Cannabinoids Mediate Retrograde Signals from Depolarized Postsynaptic Neurons to Presynaptic Terminals. Neuron, 29, 729–738.

Otmakhov, N., Shirke, A. M., and Malinow, R. (1993). Measuring the impact of probabilistic transmission on neuronal output. Neuron. 10, 1101–1111.

Pan, H.-C., Chou, Y.-C., & Sun, S. H. (2015). P2X 7 R-mediated Ca 2+ -independent D -serine release via pannexin-1 of the P2X 7 R-pannexin-1 complex in astrocytes: P2X 7 R Mediates D -Serine Release of Astrocytes. Glia, 63(5), 877–893.

Panchin Y., Kelmanson I., Matz M., Lukyanov S., & Usman. N. (2000). A ubiquitous family of putative gap junction molecules. Current Biology, 10(13), 1–2.

Panda, S., Nayak, S. K., Campo, B., Walker, J. R., Hogenesch, J. B., & Jegla, T. (2005). Illumination of the Melanopsin Signaling Pathway. Science, 307(5709), 600–604.

Pelegrin, P., & Surprenant, A. (2006). Pannexin-1 mediates large pore formation and interleukin-1b release by the ATP-gated P2X7 receptor. The EMBO Journal, 25, 5071–5082.

Pelkey, K. A., Chittajallu, R., Craig, M. T., Tricoire, L., Wester, J. C., & McBain, C. J. (2017). Hippocampal GABAergic Inhibitory Interneurons. Physiological Reviews, 97(4), 1619–1747.

Penuela, S., Gehi, R., & Laird, D. W. (2013). The biochemistry and function of pannexin channels. Biochimica et Biophysica Acta (BBA) - Biomembranes, 1828(1), 15–22.

Pereda, A. E. (2014). Electrical synapses and their functional interactions with chemical synapses. Nature Reviews Neuroscience, 15(4), 250–263.

Pizzarelli, R., Griguoli, M., Zacchi, P., Petrini, E. M., Barberis, A., Cattaneo, A., & Cherubini, E. (2020). Tuning GABAergic Inhibition: Gephyrin Molecular Organization and Functions. Neuroscience, 439, 125–136.

Prochnow, N., Abdulazim, A., Kurtenbach, S., Wildförster, V., Dvoriantchikova, G., Hanske, J., Petrasch-Parwez, E., Shestopalov, V. I., Dermietzel, R., Manahan-Vaughan, D., & Zoidl, G. (2012). Pannexin1 Stabilizes Synaptic Plasticity and Is Needed for Learning. PLoS ONE, 7(12), e51767.

Purves, D. (Ed.). (2004). Neuroscience (3rd ed). Sinauer Associates, Publishers. Ray, A., Zoidl, G., Weickert, S., Wahle, P., & Dermietzel, R. (2005). Site-specific and developmental expression of pannexin1 in the mouse nervous system. European Journal of Neuroscience, 21(12), 3277–3290.

Raymond, C., & Redman, S. (2006). Spatial segregation of neuronal calcium signals encodes different forms of LTP in rat hippocampus. J Physiol, 570(1), 97–111.

Regehr, W. G., Carey, M. R., & Best, A. R. (2009). Activity-Dependent Regulation of Synapses by Retrograde Messengers. Neuron, 63(2), 154–170.

Rombo, D. M., Dias, R. B., Duarte, S. T., Ribeiro, J. A., Lamsa, K. P., & Sebastião, A. M. (2016). Adenosine A 1 Receptor Suppresses Tonic GABA A Receptor Currents in Hippocampal Pyramidal Cells and in a Defined Subpopulation of Interneurons. Cerebral Cortex, 26(3), 1081–1095.

Rombo, D. M., Newton, K., Nissen, W., Badurek, S., Horn, J. M., Minichiello, L., Jefferys, J. G. R., Sebastiao, A. M., & Lamsa, K. P. (2015). Synaptic mechanisms of adenosine A 2A receptor-mediated hyperexcitability in the hippocampus. Hippocampus, 25(5), 566–580.

Rozov, A. V., Valiullina, F. F., & Bolshakov, A. P. (2017). Mechanisms of long-term plasticity of hippocampal GABAergic synapses. Biochemistry (Moscow), 82(3), 257–263.

Rubin, R., Abbott, L. F., & Sompolinsky, H. (2017). Balanced excitation and inhibition are required for high-capacity, noise-robust neuronal selectivity. Proceedings of the National Academy of Sciences, 114(44), E9366–E9375.

Santiago, M., Veliskova, J., Patel, N., Lutz, S., Caille, D., Charollais, A., Meda, P., & Scemes, E. (2011). Targeting Pannexin1 Improves Seizure Outcome. PLoS ONE, 6(9), 1–9.

Shao, C., Chen, P., Chen, Q., Zhao, M., Zhang, W.-N., & Yang, K. (2020). Mu opioid receptors inhibit GABA release from parvalbumin interneuron terminals onto CA1 pyramidal cells. Biochemical and Biophysical Research Communications, 522(4), 1059–1062.

Sherwood, M. W., Arizono, M., Hisatsune, C., Bannai, H., Ebisui, E., Sherwood, J. L., Panatier, A., Oliet, S. H. R., & Mikoshiba, K. (2017). Astrocytic IP 3 Rs: Contribution to Ca 2+ signalling and hippocampal LTP: Astrocytic IP 3 Rs: Ca 2+ Signalling and LTP. Glia, 65(3), 502–513.

Silverman, W. R., de Rivero Vaccari, J. P., Locovei, S., Qiu, F., Carlsson, S. K., Scemes, E., Keane, R. W., & Dahl, G. (2009). The Pannexin 1 Channel Activates the Inflammasome in Neurons and Astrocytes. Journal of Biological Chemistry, 284(27), 18143–18151.

Sohal, V. S., & Rubenstein, J. L. R. (2019). Excitation-inhibition balance as a framework for investigating mechanisms in neuropsychiatric disorders. Molecular Psychiatry, 24(9), 1248–1257.

Srinivasan, R., Huang, B. S., Venugopal, S., Johnston, A. D., Chai, H., Zeng, H., Golshani, P., & Khakh, B. S. (2015). Ca2+ signaling in astrocytes from Ip3r2−/− mouse in brain slices and during startle responses in vivo. Nature Neuroscience, 18(5), 708–717.

Staubli, U., & Lynch, G. (1990). Stable depression of potentiated synaptic responses in the hippocampus with 1–5 Hz stimulation. Brain Research, 513(1), 113–118.

Stella, N., Schweitzer, P., & Piomelli, D. (1997). A second endogenous cannabinoid that modulates long-term potentiation. Nature, 388(6644), 773–778.

Strange, B. A., Witter, M. P., Lein, E. S., & Moser, E. I. (2014). Functional organization of the hippocampal longitudinal axis. Nature Reviews Neuroscience, 15(10), 655–669.

Svoboda, K. R., & Lupica, C. R. (1998). Opioid Inhibition of Hippocampal Interneurons via Modulation of Potassium and Hyperpolarization-Activated Cation (I h) Currents. The Journal of Neuroscience, 18(18), 7084–7098.

Thanawala, M., Regehr, W. (2013). Presynaptic calcium influx controls neurotransmitter release in part by regulating the effective size of the readily releasable pool. The Journal of Neuroscience.13;33(11):4625-33.

Thompson, R. J., Jackson, M. F., Olah, M. E., Rungta, R. L., Hines, D. J., Beazely, M. A., MacDonald, J. F., & MacVicar, B. A. (2008). Activation of Pannexin-1 Hemichannels Augments Aberrant Bursting in the Hippocampus. Science, 322(5907), 1555–1559.

Trudeau, L.-E., Emery, D. G., & Haydon, P. G. (1996). Direct Modulation of the Secretory Machinery Underlies PKA-Dependent Synaptic Facilitation in Hippocampal Neurons. Neuron, 17(4), 789–797.

Udakis, M., Pedrosa, V., Chamberlain, S. E. L., Clopath, C., & Mellor, J. R. (2020). Interneuron-specific plasticity at parvalbumin and somatostatin inhibitory synapses onto CA1 pyramidal neurons shapes hippocampal output. Nature Communications, 11(1), 4395.

Varma, N., Carlson, G. C., Ledent, C., & Alger, B. E. (2001). Metabotropic Glutamate Receptors Drive the Endocannabinoid System in Hippocampus. The Journal of Neuroscience, 21(24), RC188–RC188.

Vogt, A., Hormuzdi, S. G., & Monyer, H. (2005). Pannexin1 and Pannexin2 expression in the developing and mature rat brain. Molecular Brain Research, 141(1), 113–120.

Weilinger, N. L., Lohman, A. W., Rakai, B. D., Ma, E. M. M., Bialecki, J., Maslieieva, V., Rilea, T., Bandet, M. V., Ikuta, N. T., Scott, L., Colicos, M. A., Teskey, G. C., Winship, I. R., & Thompson, R. J. (2016). Metabotropic NMDA receptor signaling couples Src family kinases to pannexin-1 during excitotoxicity. Nature Neuroscience, 19(3), 432–442.

Weilinger, N. L., Tang, P. L., & Thompson, R. J. (2012). Anoxia-Induced NMDA Receptor Activation Opens Pannexin Channels via Src Family Kinases. Journal of Neuroscience, 32(36), 12579–12588.

Westenbroek, R., Ahlijanian, M., & Catterall, W. (1990). Clustering of L-type Ca2+ channels at the base of major dendrites in hippocampal pyramidal neurons. Nature, 347, 281–284.

Wicki-Stordeur, L. E., & Swayne, L. (2013). Panx1 regulates neural stem and progenitor cell behaviours associated with cytoskeletal dynamics and interacts with multiple cytoskeletal elements. Cell Communication and Signaling, 11(1), 62.

Wilcox, K. S. & Dichter, M. A. (1994). Paired pulse depression in cultured hippocampal neurons is due to a presynaptic mechanism independent of GABAB autoreceptor activation. Journal of Neuroscience. 14, 1775—1788.

Wilson, R. I., & Nicoll, R. A. (2001). Endogenous cannabinoids mediate retrograde signalling at hippocampal synapses. Nature, 410(6828), 588–592.

Wimpey, T. L., & Chavkin, C. (1991). Opioids activate both an inward rectifier and a novel voltage-gated potassium conductance in the hippocampal formation. Neuron, 6(2), 281–289.

Yeung, A. K., Patil, C. S., & Jackson, M. F. (2020). Pannexin-1 in the CNS: Emerging concepts in health and disease. Journal of Neurochemistry, 154(5), 468–485.

Ylinen, A., Soltész, I., Bragin, A., Penttonen, M., Sik, A., & Buzsáki, G. (1995). Intracellular correlates of hippocampal theta rhythm in identified pyramidal cells, granule cells, and basket cells. Hippocampus, 5(1), 78–90.

Yoon, K., & Rothman, S. (1991). Adenosine inhibits excitatory but not inhibitory synaptic transmission in the hippocampus. The Journal of Neuroscience, 11(5), 1375–1380.

Zhou, S., & Yu, Y. (2018). Synaptic E-I Balance Underlies Efficient Neural Coding. Frontiers in Neuroscience, 12, 46.

Zoidl, G., Petrasch-Parwez, E., Ray, A., Meier, C., Bunse, S., Habbes, H.-W., Dahl, G., & Dermietzel, R. (2007). Localization of the pannexin1 protein at postsynaptic sites in the cerebral cortex and hippocampus. Neuroscience, 146(1), 9–16.